INFLUENCE OF LITHOGENIC ENERGY ON SUBGLACIAL MICROBIAL COMMUNITY COMPOSITION

by

Eric Corwin Dunham

A dissertation submitted in partial fulfillment
of the requirements for the degree

of

Doctor of Philosophy

in

Microbiology

MONTANA STATE UNIVERSITY
Bozeman, Montana

July 2021

ACKNOWLEDGEMENTS

Thank you, first of all, to Dr. Eric Boyd, whose commitment to excellence in all things set the tone for my graduate studies and whose confidence and investment in me made this work possible. Thanks to all members of the Geoboydology Lab, past and present, and especially to Dan, Max, Melody, Saroj, Libby, Erik, Devon, Maria, Lisa, Mason, Rachel, and Alexis for your camaraderie, expertise, and friendship. Thank you to Drs. Dan Colman, John Dore, and Seth Walk for your support of my research and service on my graduate committee. And special thanks to Ileana Yates-Johnson, who is wonderful to work with and indispensable to our department.

My scientific career could not have left the ground without the early support of Dr. Frank Rosenzweig and Carla Boulianne-Larsen at University of Montana or Drs. Hideki Ebihara, Logan Banadyga, Heinz Feldmann, and Thomas Hoenen at Rocky Mountain Laboratories. Thank you all for your patient and careful mentorship in all aspects of scientific work and career advancement. Thanks as well to our wonderful collaborators Jaimi Butler and Dr. Bonnie Baxter and their students at the Great Salt Lake Institute, Westminster College.

Thank you from the bottom of my heart to Libby, Mom and Dad, Michael, and the Fones and Moebus families. Your love and encouragement carried me through both highs and lows, and I couldn't have done this without you. And to our puppy Mica, whose record was mixed, but whose love is unconditional and whose attitude is relentlessly positive.

Finally, this work was made possible by support from the NASA Exobiology and Evolutionary Biology program, an NSF Graduate Research Fellowship, and the Dr. John Jutila Fellowship, for whose support I would also like to thank the Jutila family and MSU's Department of Microbiology and Immunology.

TABLE OF CONTENTS

TABLE OF CONTENTS CONTINUED

TABLE OF CONTENTS CONTINUED

LIST OF TABLES

Table Page

LIST OF TABLES CONTINUED

Table Page

LIST OF FIGURES

Figure Page

LIST OF FIGURES CONTINUED

ABSTRACT

Chemosynthesis, the generation of biomass using chemical energy, supported life on early Earth and continues to sustain contemporary light-independent ecosystems. The mechanisms of nutrient release from the geosphere are critical to understanding the present and historical distribution and diversity of life. Glaciers release such nutrients through comminution of bedrock, continuously resurfacing reactive minerals that can be colonized and exploited by chemosynthetic microorganisms. Bedrock mineralogy influences the nutrients available in these environments, but little is known about which nutrients are most important or how they affect microbial community composition, particularly in catchments overlying igneous bedrock like basalt. Iron and silicate minerals, common in basalt, readily generate both reductants such as H_2 and oxidants such as Fe(III) through interactions with water. Abundant H_2 in meltwaters of the basalt-based Icelandic glacier Kötlujökull (KJ) were found to support sediment microbial communities better adapted to use H_2 in chemosynthetic metabolism than those found beneath the carbonate-based Robertson Glacier (RG), Canada. KJ communities exhibited shorter lag-times and faster rates of net H_2 oxidation and dark carbon dioxide (CO_2) fixation than those from RG. A KJ sediment enrichment culture provided with H_2, CO_2, and Fe(III) produced a chemolithoautotrophic population related to *Rhodoferax ferrireducens*, which was also detected using molecular techniques in sediments from Kaldalónsjökull (Kal), another basalt-based Icelandic glacier. The abundance and composition of microbial communities that colonized defined minerals incubated for 12 months in Kal meltwater streams were examined by extracting DNA and sequencing PCR-amplifiable 16S rRNA genes. DNA quantities and the composition of 16S rRNA genes recovered from Kal sediments were most similar to those recovered from incubated Fe(III)-bearing minerals hematite and magnetite, with putative Fe(III) reducers dominating all three communities. These findings point to the importance of bedrock mineral composition in influencing the supplies of nutrients like H_2 and Fe(III) that, in turn, influence the diversity, abundance, and activity of microbial communities in subglacial environments. They further indicate the potential for subglacial habitats to serve as refugia for microbial communities in the absence of sunlight, such as during Snowball Earth episodes, or on icy planets without photosynthetic life.

CHAPTER ONE

GENERAL INTRODUCTION

Climate and Global Glaciation

Glaciers and ice sheets cover 10% of the surface of the Earth today and are thought to have covered a much larger portion in Earth's geological past [1-3]. Since at least the Huronian glaciation of ~2.3 Gya [4] and potentially the Pongolan glaciation of ~2.9 Gya [5], so-called "Icehouse Earth" states have periodically covered much of the continental landmass with ice. The causal factors in transitions to and from Icehouse Earth states are poorly constrained, although fluctuations in atmospheric levels of the greenhouse gases carbon dioxide (CO_2) and methane (CH_4) are thought to have been particularly important. High concentrations of greenhouse gases have been invoked to explain a warm climate through much of the Archean eon, when the luminosity of the sun is thought to have been only 70-80% of its current level [6]. In turn, the consumption of these greenhouse gases through mineral weathering, sequestration, and biological activity is thought to be the proximal cause responsible for tipping the global climate into Icehouse states.

The drawdown of atmospheric greenhouse gases is multifactorial and complex, with both biologically mediated and abiotic processes playing major roles. The equilibrium concentration of CO_2 in the atmosphere is tightly linked with the transformations of silicate and carbonate rocks. **Equations 1-2** describe the consumption of atmospheric CO_2 during weathering and subsequent sedimentation of silicate and carbonate rocks, respectively, and the release of CO_2 during metamorphism and magmatism after burial [7].

$$CO_2 + CaSiO_3 \rightarrow CaCO_3 + SiO_2 \quad (1)$$

Here, $CaSiO_3$ represents generalized high temperature calcium silicates, SiO_2 represents sedimentary silicates, and $CaCO_3$ represents generalized carbonates. **Equation 2** describes the weathering of carbonate minerals (e.g., calcite and dolomite) and their precipitation (reverse of Equation 2) in marine environments.

$$CO_2 + CaCO_3 + H_2O \rightarrow Ca^{2+} + 2HCO3^- \quad (2)$$

Together, these reactions describe the tight link between the geosphere, atmosphere, hydrosphere, and biosphere that is the carbonate-silicate biogeochemical cycle. The balance of the rates of the forward and reverse reactions creates an equilibrium level of atmospheric CO_2 that can change over geologic time as the processes of weathering and metamorphism-magmatism increase or decrease in rate. These rates can be influenced by such factors as the areal exposure of continental silicates, the intensity of the hydrological cycle, and tectonic activity.

Importantly, strong evidence indicates that, starting at least as early as the Huronian Glaciation of 2.7-2.5 Gya, biological processes have also played a key role in the climatic tipping points between Icehouse Earth states. The major biogeochemical transition co-occurring with the Huronian Glaciation is the rise of atmospheric O_2, driven by the evolution of oxygenic photosynthesis and the propagation of those organisms carrying out the process. The relationship between atmospheric CO_2 and O_2 after the evolution of oxygenic photosynthesis can be described by **Equation 3**, which describes photosynthetic carbon fixation in the forward direction and aerobic heterotrophy in the reverse.

$$CO_2 + H_2O \rightarrow CH_2O + O_2 \quad (3)$$

When burial of organic matter in the deep oceans outpaces aerobic respiration, the reaction is driven forward, and atmospheric oxygen levels increase. It is thought that progressive oxidation of the atmosphere allowed for the oxidation (or resulted in a decreased production) of CH_4 that maintained a warm climate [3]. This, in turn, allowed for the Earth to enter what is known as the Paleoproterozoic Snowball Earth episode that was marked by the Huronian glaciations. This is perhaps the first incident of global climatic change to be strongly correlated to biological activity.

The onset of the Huronian glaciation, driven largely by oxygenic photosynthesis and geosphere-biosphere feedbacks involving the oxygen, carbon, and calcium-silicate cycles, highlights an important implication of Snowball Earth periods for biology. In particular, given that a substantial portion of the biosphere has been supported by photosynthetically fixed carbon since the evolution of oxygenic photosynthesis [8], the exclusion by ice cover of light energy from vast portions of the Earth's surface during Snowball Earth periods presents a problem for the sustainment of such a biosphere. A potential mechanism for the preservation of the biosphere through periods of global ice cover and decreased photosynthetic production was uncovered by early discoveries of microbial life beneath extant glaciers [9-11] and ice sheets [12-14]. These findings give credence to the idea that critical genes and metabolic pathways could be sustained in microbial populations living beneath ice, either through consumption of relict or buried organic carbon or by generation of endogenous organic carbon through chemolithotrophic primary production [15]. Genes and metabolic pathways associated with photosynthesis could have been sustained by phototrophic life living on the surface of ice [16]. Further work on the subglacial biosphere showed that microbially-mediated redox reactions that sustain sub-ice

biospheres also contribute to chemical weathering of bedrock [9, 17-20]. Indeed, it has been suggested that microbial activity may play a major role in the carbonate-silicate biogeochemical cycle that influences atmospheric carbon levels and, thus, global climate [21-26]. This is due to the ability for microbes to generate acidity, which can weather carbonate and silicate bedrock [27].

Geomicrobiology of Glacial Systems

Although the presence of viable bacteria in snow and ice had been established by early in the 20th century [28, 29], interest languished for the next few decades. A resurgence of interest in the microbiology of glaciers and ice sheets began with the pioneering work of Abyzov et al. in Antarctica, with several studies documenting the viability of microbes entrapped for millennia in ice cores at depths of up to 2,405 m [12, 14, 30]. Further studies documented viable bacteria in Antarctic ice core samples at depths of 3,600 m [13, 31] and glacial ice samples of global distribution and ages ranging from five to 20,000 years [32, 33]. Interest in the basal ice environment picked up after Sharp et al. in 1999 documented apparently dividing cells and, in simple sediment incubation experiments, putatively microbially-mediated sulfide oxidation at Glacier de Tsanfleuron and Haut Glacier d'Arolla, Switzerland [9]. Skidmore et al. in 2000 documented microbial respiration under near *in situ* conditions in subglacial sediment enrichments from John Evans Glacier, Canada, using ^{14}C-labelled acetate [10]. This study also documented drawdown of nitrate (NO_3^-) and sulfate (SO_4^{2-}) over the course of the incubations, demonstrating the potential for chemotrophic metabolism in these systems. Further enrichment efforts recovered aerobic and anaerobic bacterial populations from "brown silty" ice at the base of an ice core from the Greenland Ice Sheet that had been frozen for over 100,000 years [34, 35].

Studies in the following years accumulated evidence for microbial activity in subglacial environments from around the world. Wadham et al. used meltwater isotopic signatures to show that microbial sulfate reduction must be occurring beneath Finsterwalderbreen, Svalbard, and posited the subglacial biosphere might be supported by chemoautotrophy [36]. Similarly, Foght et al. enriched chemolithotrophic organisms, including iron-reducing and nitrate-reducing populations and a nitrogen fixing population, from Fox and Franz Josef Glaciers in the Southern Alps of New Zealand [11]. Waters from Blood Falls, a saline discharge of Taylor Glacier in Antarctica, were likewise used to culture heterotrophic bacteria and measure biological incorporation of ^{3}H-thymidine and ^{3}H-leucine [37]. Later studies used RNA data to demonstrate that microbial populations were active *in situ* beneath Robertson Glacier, Canada [18] and Russell Glacier, Greenland [38].

As evidence accumulated for the existence and activity of microbial populations in subglacial environments, parallel studies interrogated their potential to influence chemical weathering. Tranter et al. proposed microbially-mediated oxidation of organic carbon and sulfide minerals beneath Haut Glacier d'Arolla, Switzerland, on the basis of excess carbonate and sulfate concentrations in meltwaters [39]. Skidmore et al. expanded upon the theme by correlating the meltwater aqueous geochemistries of John Evans Glacier, Ellesmere Island, Canada, and Bench Glacier, Alaska, with the metabolic capabilities of their respective subglacial microbial communities as inferred by 16S rRNA gene sequence relatedness to cultured taxa [20]. At Midtre Lovénbreen, Svalbard, nitrogen and oxygen isotope ratios were used to infer microbial nitrogen cycling and sulfide oxidation [40, 41]. Further analysis of data collected at Finsterwalderbreen allowed Wadham et al. to posit that microbial activity accounts for up to

65% of total meltwater solute flux [42]. Geochemical and isotopic data yielded similar results in a study of the Tuva Glacier basin in Antarctica [43]. In the first study to directly link inferred microbial metabolism to colonization of specific redox-active mineral surfaces, Mitchell et al. incubated sterilized mineral samples in the outflow of Robertson Glacier and examined the 16S rRNA gene sequences of the microbial communities that colonized them after incubation for seven months in situ [44].

Understanding microbially mediated subglacial weathering, its potential influence on global climate, and the ability for microbial life to be sustained through Snowball Earth states requires an understanding of the distribution, composition, and function of microbial communities in contemporary glacial and ice sheet ecosystems. A primary control, as mentioned above, is the availability of organic carbon. Relict organic carbon may be present in the subglacial environment when glaciers override previously productive environments [22, 26]. Alternatively, allochthonous organic carbon can wash into the subglacial environment from supraglacial sources through crevasses and moulins [45]. Stibal et al. showed that differing organic carbon substrates support subglacial microbial communities of differing composition [46]. Finally, it has been shown in several glacial systems that chemolithotrophic primary production can provide autochthonous organic carbon, allowing for the development of microbial ecosystems founded on chemical energy released from redox reactions involving minerals or mineral-sourced nutrients [15, 47, 48]. These results indicate that availability of oxidants and reductants to fuel chemolithotrophic primary production is an additional constraint on the habitability of sub-ice environments.

The availability of oxygen in subglacial channels and sediments has been shown to depend on sub-ice temperature and hydrological regimes [49]. Several studies have found evidence of widespread anoxia at glacier beds, with concomitant evidence for the metabolism of geologically derived energy sources [17, 36, 42, 50, 51]. Despite this, few early studies examined the relationship between the availability of various lithogenic energy sources and the composition of the microbial communities found in subglacial environments. This relationship began to be researched in detail in a series of studies at Robertson Glacier beginning in 2010.

Robertson Glacier, in the Canadian Rockies, is underlain by limestone and shale containing pyrite (FeS_2), which is common in sedimentary rocks. FeS_2 oxidation has been implicated as the dominant weathering process beneath many glaciers [17, 20, 36, 39], and has been shown to be important in supporting microbial metabolism in these systems [15, 44, 48]. Microbial FeS_2 oxidation was shown to support populations of autotrophic *Sideroxydans* at Robertson Glacier [15, 18]. Further, the FeS_2 oxidation products thiosulfate and Fe(III) are themselves redox active compounds that support the metabolic needs of *Thiobacillus*, an autotrophic thiosulfate oxidizer [48], and *Rhodoferax*, a chemotrophic iron reducer [44], in Robertson Glacier sediments. The presence and abundance of FeS_2 in subglacial bedrock and sediments has thus been proposed to be a primary control on the composition of microbial communities in these environments [44].

Evidence in support of this hypothesis comes from incubation experiments in which iron, carbonate, and/or silicate-bearing minerals (calcite, quartz, hematite, magnetite, olivine) were incubated in proglacial meltwaters for seven months to assess the compositions of the microbial communities that colonized the mineral surfaces [44]. The community associated with the

carbonate and shale subglacial sediments of the catchment was most similar to that colonizing incubated FeS_2 at the end of the experiment. Further emphasizing the importance of FeS_2 in supplying the substrates of microbial energy metabolism in this system, the iron-bearing minerals FeS_2, hematite, and ferrihydrite yielded more extractable DNA (used as a proxy for biomass in this study) than silicate minerals or calcite, which are not redox active. These results present a strong case that FeS_2 serves as a key control on microbial community composition and function in glacial sediments derived from carbonate or shale.

But glaciers and ice sheets exist in catchments with diverse bedrock chemistry. Granitic and gneissic bedrock are overlain by glaciers in a variety of environments, including in the European Alps [52] and Antarctica [53]. Similarly, basalt-based glaciers can be found in Washington, USA, and Iceland, among other locations. These systems can be broadly classified as silicate-based, and far less is known about the nutrients that support microbial metabolism in their subglacial and proglacial sediments, with most information coming from studies of Switzerland's granite-based Damma Glacier [52, 54, 55]. The focus of this work is on extending the evidence that lithogenic energy sources shape microbial community composition in subglacial sediments to other silicate-based glacial systems. A major thrust in this effort revolves around the interactions between minerals in silicate and basalt-based bedrock and water, which can generate H_2, a potent reductant that can support a variety of microbial metabolisms [56, 57].

H_2 is locally abundant in a variety of microenvironments inhabited by chemolithotrophic microbial communities including hot springs [58] and the deep subsurface [59], among others. It has been put forward as a major component of some of the earliest energy-yielding metabolic reactions along with carbon dioxide (CO_2) in pathways similar to those used by modern

methanogens and acetogens [60] and is even proposed to have played a key role in the transition from an abiotic to a biotic world [61]. The ability to metabolize H_2 is encoded in ~30% of microbial genomes [62], including those that inhabit modern rock-hosted ecosystems [58, 63, 64], such as sub-ice environments [56, 57]. H_2 can be generated abiotically through a variety of mechanisms that will be explored in depth in Chapter 2. Briefly, these include radiolysis of water [59], reduction of water by ferrous iron minerals [65], and the reaction of water with silica radicals generated by mechanical shearing of silicate minerals [66]. The activities of several classes of microbial enzymes can also produce hydrogen that can then be utilized for metabolism [62].

Microbial redox reactions also depend heavily on iron in many rock-hosted ecosystems. As will be discussed in Chapter 3, iron minerals such as pyroxene, olivine, magnetite, and hematite, are abundant in basaltic terrains especially and, due to the multiple valence states of iron in these minerals, can serve alternatively as electron donors and/or acceptors. Potential iron oxidizers have been identified in glacial sediments from Robertson Glacier [18], as noted above, as well as Bench Glacier in Alaska [20] and subglacial Lake Vostok [67]. Iron reducers, meanwhile, have been documented in numerous glacial settings including the Greenland [50] and West Antarctic Ice Sheets [68], and both polar and alpine glaciers worldwide (e.g., [11, 69-71]) and are proposed in this work to play a major role in structuring microbial communities in glaciated basaltic terrains.

Overarching Goals

This work seeks to develop a new understanding of the relationship between bedrock mineralogy and the distribution and function of microbial populations that derive energy from redox reactions involving mineral-sourced nutrients in glacial environments. Overlying ice and sediments exclude photosynthesis and allow for the study of microbial life supported by chemical sources of energy under conditions that may have been widespread during Snowball Earth periods in the geologic past [72] and might exist on other planetary bodies in our solar system and beyond [73, 74]. Thus, the primary focus of this work is on glacial systems overlying igneous rock without substantial relict organic carbon, although comparisons are drawn to a glacial system overlying carbonate rock that has substantial relict organic carbon. Glacial environments in Iceland provides an abundance of such systems whose bedrock differs in age, composition, and the extent that it has been weathered.

In Chapter 2, I compare the availability of H_2 in meltwaters from Kötlujökull, a basalt-hosted glacier in Iceland, to that in meltwaters from Robertson Glacier, a carbonate-hosted glacier in Canada whose geochemistry and microbial ecology has been well documented [15, 18, 23, 44, 48, 75]. I or my colleagues collected sediments generated by glacial comminution from near the terminus of each glacier and examined the activities and identities of hydrogenotrophic and autotrophic members of their respective microbial communities. I hypothesized that, with more available abiotic mechanisms for H_2 generation, the concentration of H_2 in meltwaters emanating from the basalt-hosted Icelandic glacier would be elevated relative to those from the carbonate-based Canadian glacier. This result was confirmed by gas chromatography of dissolved gases sampled from each meltwater stream. By comparing the rates of microbial H_2

oxidation in microcosms inoculated with proglacial sediments and amended with H_2 and various potential oxidants, I showed that the community associated with Kötlujökull sediments was adapted to utilize H_2 more quickly and more robustly than the corresponding Robertson sediment community. I further demonstrated using ^{14}C labelled bicarbonate that hydrogenotrophic members of the Kötlujökull community are able to couple the oxidation of H_2 to autotrophic growth and that this activity was stimulated by the addition of Fe(III) minerals.

Chapter 3 describes work undertaken to evaluate the hypothesis that community composition in the sediments of Kaldalónsjökull, another basalt-based glacier in northwest Iceland, is influenced by the abundance of Fe(III) minerals. To test this hypothesis, I analyzed 16S rRNA gene data from proglacial sediments from two meltwater streams, both draining Kaldalónsjökull. I compare this sediment-derived data to that derived from defined mineral substrates (hematite, magnetite, pyrite, olivine, and quartz) incubated for 12 months in the two outlets in order to assess the influence of mineralogy on the composition of the microbial communities that colonized the incubated mineral surfaces and the native sediments. The results of this study suggest that the supply of Fe(III) in meltwaters and sediments exerts a strong influence on the assembly of the subglacial microbial communities at Kaldalónsjökull.

The conclusions drawn in Chapters 2 and 3 are synthesized and further discussed in Chapter 4. In drawing comparisons between basalt-based and carbonate-based glacial systems and between basalt-based microenvironments of different ages and weathering histories, I pursued several research questions unified in their focus on addressing the overarching hypothesis that bedrock mineralogy influences the availability of chemical energy in the form of redox disequilibrium in lithogenic nutrients and thus the distribution of microbial populations

supported by chemolithotrophic metabolisms. The major findings of each study are examined through the lens of habitability, with discussion focused on the influence of geological context in supporting potential microbial communities and on the potential for their scientific observation. Lastly, I cover potential future research directions in the vein of exploring habitability via geobiological approaches.

Importantly, while my thesis work is focused on glacial geomicrobiology, I also co-authored several other papers and book chapters during my time as a graduate student. For context, I list those below:

Dunham, E.C., E.M. Fones, Y. Fang, M. Lindsay, C. Steuer, N. Fox, M. Willis, A. Walsh, D. Colman, B. Baxter, D. Lageson, D. Mogk, A.L. Rupke, H. Xu, and E. Boyd, *An Ecological Perspective on Dolomite Formation in Great Salt Lake, Utah.* Frontiers in Earth Science, 2020. **8**.

Lindsay, M.R., **E.C. Dunham**, and E.S. Boyd, *Microbialites of Great Salt Lake,* in *Great Salt Lake Biology: A Terminal Lake in a Time of Change*, B.K. Baxter and J.K. Butler, Editors. 2020, Springer International Publishing: Cham. p. 87-118.

Payne, D., **E.C. Dunham**, E. Mohr, I. Miller, A. Arnold, R. Erickson, E.M. Fones, M.R. Lindsay, D.R. Colman, and E.S. Boyd, *Geologic legacy spanning >90 years explains unique Yellowstone hot spring geochemistry and biodiversity.* Environmental Microbiology, 2019. **21**(11): p. 4180-4195.

Poudel, S., **E.C. Dunham**, M.R. Lindsay, M.J. Amenabar, E.M. Fones, D.R. Colman, and E.S. Boyd, *Origin and Evolution of Flavin-Based Electron Bifurcating Enzymes.* Frontiers in Microbiology, 2018. **9**.

References

1. Hoffman, P.F., et al., *A Neoproterozoic Snowball Earth.* Science, 1998. **281**(5381): p. 1342-1346.

2. Hoffman, P.F. and D.P. Schrag, *The snowball Earth hypothesis: testing the limits of global change.* Terra Nova, 2002. **14**(3): p. 129-155.

3. Kasting, J.F. and S. Ono, *Palaeoclimates: the first two billion years.* Philosophical Transactions of the Royal Society B: Biological Sciences, 2006. **361**(1470): p. 917-929.

4. Tang, H. and Y. Chen, *Global glaciations and atmospheric change at ca. 2.3 Ga.* Geoscience Frontiers, 2013. **4**(5): p. 583-596.

5. Young, G.M., et al., *Earth's Oldest Reported Glaciation: Physical and Chemical Evidence From the Archean Mozaan Group (~2.9 Ga) of South Africa.* The Journal of Geology, 1998. **106**(5): p. 523-538.

6. Sagan, C. and G. Mullen, *Earth and Mars: Evolution of Atmospheres and Surface Temperatures.* Science, 1972. **177**(4043): p. 52-56.

7. Berner, R.A., A.C. Lasaga, and R.M. Garrels, *The carbonate-silicate geochemical cycle and its effect on atmospheric carbon dioxide over the past 100 million years.* American Journal of Science, 1983. **283:7**.

8. Des Marais, D.J., *When did photosynthesis emerge on Earth?* Science, 2000. **289**(5485): p. 1703-1705.

9. Sharp, M., et al., *Widespread bacterial populations at glacier beds and their relationship to rock weathering and carbon cycling.* Geology, 1999. **27**(2): p. 107-110.

10. Skidmore, M.L., J.M. Foght, and M.J. Sharp, *Microbial Life beneath a High Arctic Glacier.* Applied and Environmental Microbiology, 2000. **66**(8): p. 3214-3220.

11. Foght, J., et al., *Culturable Bacteria in Subglacial Sediments and Ice from Two Southern Hemisphere Glaciers.* Microbial Ecology, 2004. **47**(4): p. 329-340.

12. Abyzov, S.S., *Microorganisms in the Antarctic ice.* Antarctic Microbiology, 1993. **1**(1): p. 265-296.

13. Priscu, J.C., et al., *Geomicrobiology of Subglacial Ice Above Lake Vostok, Antarctica.* Science, 1999. **286**(5447): p. 2141-2144.

14. Abyzov, S.S., et al. *Long-term conservation of viable microorganisms in the ice sheet of Central Antarctica*. in *Instruments, Methods, and Missions for Astrobiology*. 1998. International Society for Optics and Photonics.

15. Boyd, E.S., et al., *Chemolithotrophic primary production in a subglacial ecosystem.* Applied and Environmental Microbiology, 2014. **80**(19): p. 6146-53.

16. Corsetti, F.A., A.N. Olcott, and C. Bakermans, *The biotic response to Neoproterozoic snowball Earth.* Palaeogeography, Palaeoclimatology, Palaeoecology, 2006. **232**(2): p. 114-130.

17. Bottrell, S.H. and M. Tranter, *Sulphide oxidation under partially anoxic conditions at the bed of the Haut Glacier d'Arolla, Switzerland.* Hydrological Processes, 2002. **16**(12): p. 2363-2368.

18. Hamilton, T.L., et al., *Molecular evidence for an active endogenous microbiome beneath glacial ice.* The ISME Journal, 2013. **7**(7): p. 1402-12.

19. Montross, S.N., et al., *A microbial driver of chemical weathering in glaciated systems.* Geology, 2013. **41**(2): p. 215-218.

20. Skidmore, M., et al., *Comparison of Microbial Community Compositions of Two Subglacial Environments Reveals a Possible Role for Microbes in Chemical Weathering Processes.* Applied and Environmental Microbiology, 2005. **71**(11): p. 6986-6997.

21. Wadham, J.L., et al., *Potential methane reservoirs beneath Antarctica.* Nature, 2012. **488**(7413): p. 633-637.

22. Stibal, M., et al., *Methanogenic potential of Arctic and Antarctic subglacial environments with contrasting organic carbon sources.* Global Change Biology, 2012. **18**(11): p. 3332-3345.

23. Boyd, E.S., et al., *Methanogenesis in subglacial sediments.* Environmental Microbiology Reports, 2010. **2**(5): p. 685-692.

24. Christner, B.C., G.G. Montross, and J.C. Priscu, *Dissolved gases in frozen basal water from the NGRIP borehole: implications for biogeochemical processes beneath the Greenland Ice Sheet.* Polar Biology, 2012. **35**(11): p. 1735-1741.

25. Michaud, A.B., et al., *Microbial oxidation as a methane sink beneath the West Antarctic Ice Sheet.* Nature Geoscience, 2017. **10**(8): p. 582-586.

26. Wadham, J.L., et al., *Subglacial methanogenesis: A potential climatic amplifier?* Global Biogeochemical Cycles, 2008. **22**(2).

27. Bennett, P.C., et al., *Silicates, Silicate Weathering, and Microbial Ecology.* Geomicrobiology Journal, 2001. **18**(1): p. 3-19.

28. McLean, A.L., *Bacteria of Ice and Snow in Antarctica.* Nature, 1918. **102**(2550): p. 35-39.

29. Darling, C.A. and P.A. Siple, *Bacteria of Antarctica.* Journal of Bacteriology, 1941. **42**(1): p. 83-98.

30. Abyzov, S., N. Bobin, and B. Dudriashov, *Quantitative registration of microorganisms at microbiological studies of the Antarctic glaciers.* Izvestiya Akademii nauk SSSR. Seriya Biologicheskaya, 1982.

31. Karl, D.M., et al., *Microorganisms in the Accreted Ice of Lake Vostok, Antarctica.* Science, 1999. **286**(5447): p. 2144-2147.

32. Dancer, S., P. Shears, and D. Platt, *Isolation and characterization of coliforms from glacial ice and water in Canada's High Arctic.* Journal of Applied Microbiology, 1997. **82**(5): p. 597-609.

33. Christner, B.C., et al., *Recovery and Identification of Viable Bacteria Immured in Glacial Ice.* Icarus, 2000. **144**(2): p. 479-485.

34. Sheridan, P.P., V.I. Miteva, and J.E. Brenchley, *Phylogenetic Analysis of Anaerobic Psychrophilic Enrichment Cultures Obtained from a Greenland Glacier Ice Core.* Applied and Environmental Microbiology, 2003. **69**(4): p. 2153-2160.

35. Miteva, V.I., P.P. Sheridan, and J.E. Brenchley, *Phylogenetic and Physiological Diversity of Microorganisms Isolated from a Deep Greenland Glacier Ice Core.* Applied and Environmental Microbiology, 2004. **70**(1): p. 202-213.

36. Wadham, J.L., et al., *Stable isotope evidence for microbial sulphate reduction at the bed of a polythermal high Arctic glacier.* Earth and Planetary Science Letters, 2004. **219**(3): p. 341-355.

37. Mikucki, J.A., et al., *Geomicrobiology of Blood Falls: An Iron-Rich Saline Discharge at the Terminus of the Taylor Glacier, Antarctica.* Aquatic Geochemistry, 2004. **10**(3): p. 199-220.

38. Dieser, M., et al., *Molecular and biogeochemical evidence for methane cycling beneath the western margin of the Greenland Ice Sheet.* The ISME Journal, 2014. **8**(11): p. 2305-2316.

39. Tranter, M., et al., *Geochemical weathering at the bed of Haut Glacier d'Arolla, Switzerland—a new model.* Hydrological Processes, 2002. **16**(5): p. 959-993.

40. Wynn, P.M., A. Hodson, and T. Heaton, *Chemical and Isotopic Switching within the Subglacial Environment of a High Arctic Glacier.* Biogeochemistry, 2006. **78**(2): p. 173-193.

41. Wynn, P.M., et al., *Nitrate production beneath a High Arctic glacier, Svalbard.* Chemical Geology, 2007. **244**(1): p. 88-102.

42. Wadham, J.L., et al., *Hydro-biogeochemical coupling beneath a large polythermal Arctic glacier: Implications for subice sheet biogeochemistry.* Journal of Geophysical Research: Earth Surface, 2010. **115**(F4).

43. Hodson, A., et al., *Chemical weathering and solute export by meltwater in a maritime Antarctic glacier basin.* Biogeochemistry, 2010. **98**(1-3): p. 9-27.

44. Mitchell, A.C., et al., *Influence of bedrock mineral composition on microbial diversity in a subglacial environment.* Geology, 2013. **41**(8): p. 855-858.

45. Irvine-Fynn, T.D., et al., *Polythermal glacier hydrology: a review.* Reviews of Geophysics, 2011. **49**(4).

46. Stibal, M., et al., *Prokaryotic diversity in sediments beneath two polar glaciers with contrasting organic carbon substrates.* Extremophiles, 2012. **16**(2): p. 255-265.

47. Christner, B.C., et al., *A microbial ecosystem beneath the West Antarctic ice sheet.* Nature, 2014. **512**(7514): p. 310-313.

48. Harrold, Z.R., et al., *Aerobic and Anaerobic Thiosulfate Oxidation by a Cold-Adapted, Subglacial Chemoautotroph.* Applied and Environmental Microbiology, 2016. **82**(5): p. 1486-1495.

49. Tranter, M., M. Skidmore, and J. Wadham, *Hydrological controls on microbial communities in subglacial environments.* Hydrological Processes, 2005. **19**(4): p. 995-998.

50. Yde, J.C., et al., *Basal ice microbiology at the margin of the Greenland ice sheet.* Annals of Glaciology, 2010. **51**(56): p. 71-79.

51. Sheik, C.S., et al., *Microbial communities of the Lemon Creek Glacier show subtle structural variation yet stable phylogenetic composition over space and time.* Frontiers in Microbiology, 2015. **6**.

52. Frey, B., et al., *Weathering-Associated Bacteria from the Damma Glacier Forefield: Physiological Capabilities and Impact on Granite Dissolution.* Applied and Environmental Microbiology, 2010. **76**(14): p. 4788-4796.

53. Cottle, J.M. and A.F. Cooper, *Geology, geochemistry, and geochronology of an A-type granite in the Mulock Glacier area, southern Victoria Land, Antarctica.* New Zealand Journal of Geology and Geophysics, 2006. **49**(2): p. 191-202.

54. Wongfun, N., et al., *Weathering of Granite from the Damma Glacier Area: The Contribution of Cyanogenic Bacteria.* Geomicrobiology Journal, 2014. **31**(2): p. 93-100.

55. Lapanje, A., et al., *Pattern of elemental release during the granite dissolution can be changed by aerobic heterotrophic bacterial strains isolated from Damma Glacier (central Alps) deglaciated granite sand.* Microbial Ecology, 2012. **63**(4): p. 865-882.

56. Telling, J., et al., *Rock comminution as a source of hydrogen for subglacial ecosystems.* Nature Geoscience, 2015. **8**(12).

57. Macdonald, M.L., et al., *Glacial Erosion Liberates Lithologic Energy Sources for Microbes and Acidity for Chemical Weathering Beneath Glaciers and Ice Sheets.* Frontiers in Earth Science, 2018. **6**.

58. Spear, J.R., et al., *Hydrogen and bioenergetics in the Yellowstone geothermal ecosystem.* Proceedings of the National Academy of Sciences of the United States of America, 2005. **102**(7): p. 2555-2560.

59. Lin, L.-H., et al., *Radiolytic H_2 in continental crust: Nuclear power for deep subsurface microbial communities.* Geochemistry, Geophysics, Geosystems, 2005. **6**(7).

60. Martin, W.F., *Hydrogen, metals, bifurcating electrons, and proton gradients: the early evolution of biological energy conservation.* FEBS Letters, 2012. **586**(5): p. 485-493.

61. Wächtershäuser, G., *Evolution of the first metabolic cycles.* Proceedings of the National Academy of Sciences of the United States of America, 1990. **87**(1): p. 200-204.

62. Peters, J.W., et al., *[FeFe]- and [NiFe]-hydrogenase diversity, mechanism, and maturation.* Biochimica et Biophysica Acta (BBA) - Molecular Cell Research, 2015. **1853**(6): p. 1350-1369.

63. Lindsay, M.R., et al., *Probing the geological source and biological fate of hydrogen in Yellowstone hot springs.* Environmental Microbiology, 2019. **21**(10): p. 3816-3830.

64. Nealson, K.H., F. Inagaki, and K. Takai, *Hydrogen-driven subsurface lithoautotrophic microbial ecosystems (SLiMEs): do they exist and why should we care?* Trends in Microbiology, 2005. **13**(9): p. 405-410.

65. Stevens, T.O. and J.P. McKinley, *Abiotic controls on H_2 production from basalt-water reactions and implications for aquifer biogeochemistry.* Environmental Science & Technology, 2000. **34**(5): p. 826-831.

66. Kita, I., S. Matsuo, and H. Wakita, *H_2 generation by reaction between H_2O and crushed rock: An experimental study on H_2 degassing from the active fault zone.* Journal of Geophysical Research: Solid Earth, 1982. **87**(B13): p. 10789-10795.

67. Christner, B.C., et al., *Limnological conditions in subglacial Lake Vostok, Antarctica.* Limnology and Oceanography, 2006. **51**(6): p. 2485-2501.

68. Lanoil, B., et al., *Bacteria beneath the West Antarctic Ice Sheet.* Environmental Microbiology, 2009. **11**(3): p. 609-615.

69. Bhatia, M., M. Sharp, and J. Foght, *Distinct bacterial communities exist beneath a high Arctic polythermal glacier.* Applied and Environmental Microbiology, 2006. **72**(9): p. 5838-5845.

70. Cheng, S.M. and J.M. Foght, *Cultivation-independent and -dependent characterization of Bacteria resident beneath John Evans Glacier.* FEMS Microbiology Ecology, 2007. **59**(2): p. 318-330.

71. Nixon, S.L., et al., *Viable cold-tolerant iron-reducing microorganisms in geographically diverse subglacial environments.* Biogeosciences, 2017. **14**(6): p. 1445-1455.

72. Hoffman, P.F., et al., *Snowball Earth climate dynamics and Cryogenian geology-geobiology.* Science Advances, 2017. **3**(11): p. e1600983.

73. Vance, S.D., K.P. Hand, and R.T. Pappalardo, *Geophysical controls of chemical disequilibria in Europa.* Geophysical Research Letters, 2016. **43**(10): p. 4871-4879.

74. Hsu, H.-W., et al., *Ongoing hydrothermal activities within Enceladus.* Nature, 2015. **519**(7542): p. 207-210.

75. Boyd, E.S., et al., *Diversity, Abundance, and Potential Activity of Nitrifying and Nitrate-Reducing Microbial Assemblages in a Subglacial Ecosystem.* Applied and Environmental Microbiology, 2011. **77**(14): p. 4778-4787.

CHAPTER TWO

LITHOGENIC HYDROGEN SUPPORTS MICROBIAL PRIMARY PRODUCTION IN SUBGLACIAL AND PROGLACIAL ENVIRONMENTS

Contributions of Authors and Co-Authors

Manuscript in Chapter 2

Author: Eric C. Dunham

Contributions: Designed research, performed fieldwork and laboratory research, analyzed data, and co-wrote the manuscript.

Co-Author: John E. Dore

Contributions: Analyzed H_2 oxidation and CO_2 fixation data.

Co-Author: Mark L. Skidmore

Contributions: Performed fieldwork and contributed equipment for field- and laboratory-based work.

Author: Eric E. Roden

Contributions: Analyzed Fe(III) reduction and microbial growth data.

Author: Eric S. Boyd

Contributions: Designed research, analyzed data, and co-wrote the manuscript.

Manuscript Information

Eric C. Dunham, John E. Dore, Mark L. Skidmore, Eric E. Roden, and Eric S. Boyd

Proceedings of the National Academy of Sciences of the United States of America

Status of Manuscript:
____ Prepared for submission to a peer-reviewed journal
____ Officially submitted to a peer-reviewed journal
____ Accepted by a peer-reviewed journal
__X__ Published in a peer-reviewed journal

National Academy of Sciences of the United States of America
Published 12 January 2021, Volume 118, Issue 2
https://doi.org/10.1073/pnas.2007051117

Abstract

Life in environments devoid of photosynthesis, such as on early Earth or in contemporary dark subsurface ecosystems, is supported by chemical energy. How, when, and where chemical nutrients released from the geosphere fuel chemosynthetic biospheres is fundamental to understanding the distribution and diversity of life, both today and in the geologic past. Hydrogen (H_2) is a potent reductant that can be generated when water interacts with reactive components of mineral surfaces such as silicate radicals and ferrous iron. Such reactive mineral surfaces are continually generated by physical comminution of bedrock by glaciers. Here we show that dissolved H_2 concentrations in meltwaters from an iron and silicate mineral-rich basaltic glacial catchment were an order of magnitude higher than those from a carbonate-dominated catchment. Consistent with higher H_2 abundance, sediment microbial communities from the basaltic catchment exhibited significantly shorter lag times and faster rates of net H_2 oxidation and dark carbon dioxide (CO_2) fixation than those from the carbonate catchment, indicating adaptation to use H_2 as a reductant in basaltic catchments. An enrichment culture of basaltic sediments provided with H_2, CO_2, and ferric iron produced a chemolithoautotrophic population related to *Rhodoferax ferrireducens* with a metabolism previously thought to be restricted to (hyper)thermophiles and acidophiles. These findings point to the importance of physical and chemical weathering processes in generating nutrients that support chemosynthetic primary production. Further, they show that differences in bedrock mineral composition can influence the supplies of nutrients like H_2 and, in turn, the diversity, abundance, and activity of microbial inhabitants.

Significance

In the absence of light, biomass production is driven by chemical energy through microbial chemosynthesis. H_2, a potent reductant capable of supporting chemosynthesis, is readily generated by reactions between iron and silicate minerals and water. Here, we show that lithogenic H_2 produced by glacial comminution of iron- and silica-rich basaltic bedrock supports microbial chemosynthesis. Lithogenic production of H_2 in cold, dark subglacial environments and its use to generate chemosynthetic biomass suggests the potential for subglacial habitats to serve as refugia for microbial communities in the absence of sunlight, such as during Snowball Earth episodes or on icy planets where photosynthesis may not yet have evolved or where light is restricted.

Introduction

Sub- and proglacial environments host abundant, diverse, and active microbiomes supported by combinations of nutrients derived from relict organic matter, minerals, and the interaction of water and minerals [9, 10, 18, 76, 77]. In catchments containing abundant sedimentary carbonates and shales, the biological oxidation of pyrite (FeS_2) has been suggested to be a primary control on the composition of subglacial sediment microbiomes [44, 48, 77], likely due to its potential role in supplying reductant to drive primary production [15]. Far less is known of the nutrients that support communities inhabiting sub- and proglacial systems overlaying silicate (e.g., granite, gneiss, basalt) bedrock. This is a major knowledge gap considering that silicate-based glaciers are prevalent habitat types on Earth both today and in the

geological past [9, 19] and potentially on other icy planetary bodies such as Saturn's moon Enceladus [74].

Hydrogen (H_2) is a common metabolic substrate in many rock-hosted ecosystems [58, 59, 63, 64], including subglacial environments [56, 57]. H_2 can be generated abiotically through the reduction of water by ferrous iron minerals [65, 78], the radiolysis of water [59], or the activity of one of several classes of microbial enzymes [62, 79]. In addition, H_2 can be produced through silica radical-based mechanisms [66], which have recently been suggested to be of importance in generating H_2 in cold (~0°C), dark subglacial ecosystems [56, 57, 80]. In this process, mechanical shearing of silicates is proposed to generate surface radicals that, when exposed to water, produce H_2 through reactions 1 and 2:

$$Si^{\bullet} + H_2O \rightarrow SiOH + H^{\bullet} \quad (1)$$

$$H^{\bullet} + H^{\bullet} \rightarrow H_2 \quad (2)$$

Moreover, this mechanism may help to explain why abundant members of microbial communities in various subglacial ecosystems appear to be dependent on H_2 as an electron donor in the absence of evidence for other known biotic or abiotic pathways for H_2 production [18, 23, 25, 56, 81, 82].

H_2 may be expected to be an even more important electron donor supporting primary production in mafic (basaltic) sub- and proglacial systems when compared to those underlain by felsic (granitic) or carbonate bedrock. In addition to containing abundant silicates, basalts are typically enriched in iron (8-13% by weight, [83]). The iron in basalts has been linked to production of H_2 from water in subsurface ecosystems in the Columbia River (CR) basin, Washington, USA [65]. For example, in laboratory experiments containing anoxic water

buffered at pH 6.0, H_2 production from crushed CR basalt was 4.1 and 5.5 nmol g^{-1} day^{-1} at 30°C and 60°C, respectively. When water-rock reactions were buffered at pH 7.0, rates decreased to 2.4 and 2.9 nmol H_2 g^{-1} day^{-1} at 30°C and 60°C, respectively. Assuming Arrhenius kinetics, an extrapolation of these rates to temperatures relevant to glacial meltwaters (~0°C) yields anticipated H_2 production rates of 2.8 and 2.0 nmol g^{-1} day^{-1} at pH 6.0 and 7.0, respectively. These rates are similar to those (~5 nmol H_2 g^{-1} day^{-1}) obtained in crushing experiments using a variety of silicate minerals incubated at 0°C [56, 57]. Thus, glaciers overriding basaltic bedrock might be expected to generate H_2 via either the silica radical- or iron-based mechanisms—or both—which may in turn support more abundant and active hydrogenotrophic communities than those in carbonate-hosted subglacial systems.

Here, we examine the role of H_2 in supporting microbial communities in proglacial and subglacial sediments collected from contrasting basaltic and carbonate/shale catchments: Kötlujökull, Iceland (KJ), and Robertson Glacier, Alberta, Canada (RG), respectively. These sediments, collected beneath or near the terminus of each glacier, represent recently exposed subglacial material generated by glacial comminution. Further, the microbial communities they host are likely seeded by and highly reflective of those existing in the subglacial environments of their host catchments, as has been reported previously [44, 76]. We hypothesized that H_2 would be elevated in meltwaters and/or sediment porewaters from the former when compared to the latter. In turn, we hypothesized that the abundance and activity of hydrogenotrophic autotrophs would be higher in the basaltic system due to selection for such organisms during the assembly of those communities. Our results are discussed in consideration of the role of bedrock type in supporting H_2-dependent primary production in diverse sub- and proglacial sediment habitats in

contemporary and past environments on Earth and in subglacial habitats on extraterrestrial icy planetary bodies such as Enceladus.

Materials and Methods

Field Site Descriptions

Kötlujökull (63°36’N, 18°52’W) drains the southeast flank of Mýrdalsjökull, a temperate ice cap in southern Iceland atop Katla volcano, and is the largest outlet on its east side. As of 1997, the glacier ranged in elevation from 1200 to 220 m over a length of 15 km, with its terminal ice front stretching nearly 12 km on a flat outwash plain known as Mýrdalssandur [84]. The bedrock beneath KJ consists primarily of Upper Pleistocene-aged hyaloclastites, pillow lava, and associated basaltic sediments [85]. The iron and silica content of the basaltic and rhyolitic rock in the Katla volcanic system range from ~4 to 17% and 46 to 74% by weight, respectively [86].

Robertson Glacier (50°44’N, 115°20’W) drains the northern flank of the Haig Icefield in Peter Lougheed Provincial Park, Kananaskis Country, Alberta, Canada. The bedrock in this catchment is of Upper-Devonian-age and consists of impure limestones, dolostones, and dolomitic limestones with interbeds of shale, siltstone, and sandstone [87, 88]. Sediments from RG consist of 25 to 56% carbonate with the balance potassium feldspar (20-49%), quartz (18-25%), muscovite (0.5-3%), and pyrite (0-1%) [89]. As of 2011 the glacier spanned an elevational gradient of 2,900 to 2,370 m with a length of approximately 2 km, terminating on a flat till plain.

Sample Collection and Field-Based Analyses

At KJ, dangerously high water levels on 11 October 2016 dictated that water and sediments be collected from the Múlakvisl meltwater stream at a proglacial location (63° 32.099' N, 18° 50.421' W) approximately 1 km downstream from the glacier terminus. Saturated sediments were collected from the stream bank using a flame-sterilized stainless-steel spoon and were placed into sterile 500 mL jars. Sediments were frozen on site with dry ice and maintained at -20°C during transport to and storage at Montana State University. Saturated sediments from RG were collected from an ice cave at the terminus of the glacier on 14 September 2009, as reported previously [15] and are subglacial in nature given the sampling location beneath the glacier. At both sample locations, the surface layer (1 cm) of sediments were removed before samples were collected and preserved for analyses.

Electrical conductivity (EC) and pH were measured using a SevenGo Duo pro pH/Ion/Conductivity probe (Mettler Toledo, Columbus, OH). Meltwaters were collected with a syringe and were immediately transferred to clean glass serum vials, stoppered and crimp sealed, then subjected to dissolved oxygen and alkalinity titrations within five hours of sampling. Samples were allowed to equilibrate to ambient temperature in sealed vials prior to taking measurements. Dissolved oxygen was measured using a Mettler Toledo OptiOx probe. Total alkalinity was determined using a Hach digital titrator to titrate samples with 1.6N sulfuric acid to an endpoint pH of 4.5. The pH was monitored using a SevenGo Duo pro pH/Ion/Cond probe.

Total sulfide was determined using the methylene blue reduction method [90]. KJ meltwater was filtered through a 0.2 μm nylon membrane button filter directly into assay reagents in the field. Assay tubes were then wrapped in aluminum foil and subjected to

absorbance analyses at the lab within 1 week of collection using a Genesys 10S Vis spectrophotometer (Thermo Scientific, Waltham, MA) and a wavelength of 670 nm. Samples for determining concentrations of dissolved gases other than sulfide (H_2, CH_4, and CO_2) were collected using a modified bubble-strip method, as described previously [91]. Briefly, a 60 mL Luer-lock syringe was filled with 20 ml N_2 gas. Twenty milliliters of KJ meltwater were then introduced into the syringe followed by vigorous shaking for 1 min to allow for gas equilibration. The gas bubbles were then transferred to glass vials containing a saturated sodium chloride solution for storage until analysis by gas chromatography, as previously described [92].

Total Organic Carbon (TOC) and Total Nitrogen (TN) Determinations

KJ and RG sediment samples were dried overnight at 80°C, then hand milled in an acid-washed (overnight in 10% HNO_3) porcelain mortar and pestle and sieved to 63 μm. Triplicate subsamples were acidified with 2N HCl in silver foil cups until acid addition did not induce bubbling during a two hour incubation. Acidified subsamples were then washed twice with diH_2O and dried for 24 hours at 80°C after each wash. Triplicate acidified (Ag foil-wrapped) and triplicate unacidified samples were then wrapped in tin foil and analyzed on a Costech ECS 4010 (Costech Analytical Technologies Inc., Valencia, CA) equipped for carbon and nitrogen analyses using a combustion temperature of 980°C, a reducing oven temperature of 650°C, a GC oven temperature of 65°C, and a 4m length GC column. External acetanilide standards were used to create C and N calibration curves. Total organic carbon was determined as the difference between total carbon in unacidified and acidified samples.

Most Probable Number (MPN) Assay Preparation

MPN assays were conducted to determine the abundance of cultivatable cells associated with RG and KJ glacial sediments capable of coupling H_2 oxidation to autotrophic growth. Clean, acid-washed (overnight with 5% HNO_3) 24-mL serum vials were filled with 9 mL M9 minimal medium [93] with the following modifications: the concentration of $MgSO_4$ was reduced to 200 µM and carbon sources were omitted. Medium was deoxygenated by purging with 0.2 µm nylon filter-sterilized nitrogen (N_2) gas passed over heated (210°C) and H_2-reduced copper shavings. The headspace of vials was flushed with H_2 for 5 minutes and then CO_2 was added to achieve a final headspace mixing ratio of 80% H_2 and 20% CO_2. Oxidants, including Na_2SO_4, the ferric iron-containing minerals hematite and ferrihydrite, and $NaNO_3$ were prepared in sterile anoxic M9 salts medium and added to a final concentration of 1 mM. Hematite particles (<5 µm) were purchased from Sigma-Aldrich. Ferrihydrite was synthesized as previously described [94]. For aerobic MPNs, 16 mL (at ambient pressure) filter-sterilized air was added to each vial via syringe. Anoxic and filter-sterilized Wolfe's vitamins and SL-10 trace elements solutions [93] were added to each bottle to final dilutions of 1 mL L^{-1}.

Glacial sediments were thawed overnight at 4°C and 5 g of thawed sediment (wet weight) were added to 27 mL of autoclaved and cooled M9 salts to generate a ~1:10 vol:vol sediment slurry. Vials were sealed and deoxygenated as described above and were kept on ice during all manipulations. Serial 1:10 dilutions of this slurry (initial dilution factor 10^1) were made in sterile, anoxic M9 medium out to a sediment dilution factor of 10^7. Finally, MPN series were inoculated in triplicate by transfer of 1 mL of the appropriate sediment dilution to each experimental vial. Three abiotic control vials were prepared for each condition. These were autoclaved for 30 min

at 121°C, incubated for 24 h at 4°C to allow for germination of spores, and re-autoclaved. All vials were incubated at 4°C.

MPN Assessment Using DNA Evidence

Following six months of incubation, MPN vials were qualitatively judged to be positive or negative for growth by measuring the amount of extractable DNA in each microcosm. Two mL of culture was removed from each MPN assay microcosm and was concentrated by centrifugation (14 000 x *g*, 15 min., 4°C). Pellets were overlain with 400 µL CTAB buffer and 200 µL of a 500 mg L^{-1} molecular grade skim milk solution (Hardy Diagnostics, Santa Maria, CA) and DNA was then extracted following the CTAB S protocol [95]. DNA was resuspended in 50 µL molecular grade H_2O and the concentration was determined with the Qubit dsDNA HS Assay kit and fluorometer (Molecular Probes, Eugene, OR).

Microcosms were determined to be positive for growth if >2 ng DNA was recovered from a 2 mL culture sample. This amount of DNA was empirically determined to be associated with the growth of cells in MPN vials based on recovery of ≤1 ng mL^{-1} in autoclave killed controls. Microcosms were assayed until all three microcosms in two sequential serial dilutions had been judged negative. Then the pattern of positive and negative growth across three serial dilutions, along with the sediment dilution factors associated with those microcosms, was used to estimate the MPN of cells capable of growth under the provided enrichment conditions present in each gram of proglacial sediment inoculum. Selection of three appropriate serial dilutions, proper accounting for sediment dilution factor, and the tables used in estimating MPN are described in the FDA Bacteriological Analytical Manual [96].

MPN Assessment Using Metabolic Evidence

Metabolic activity assays were used in parallel with DNA extractions to generate MPN estimates correlated with the use of experimentally supplied oxidants. In microcosms with CO_2 only, acetate and methane were measured. Sulfide was assayed in microcosms amended with sulfate. Ferrous iron was measured in hematite- and ferrihydrite-amended microcosms and nitrite was assayed in microcosms amended with nitrate. Microcosms were judged to be positive if the concentration of the assayed metabolite was three standard deviations higher than its average concentration in three killed controls. MPN was then estimated from the pattern of positive and negative microcosms as described above.

Production of acetate was determined using a 1 mL culture sample via ion chromatography using a Metrohm 930 Compact IC Flex ion chromatograph (Metrohm, Herisau, Switzerland) equipped with a 25 mm Metrosep A Supp 5 anion column and 930 Compact IC Flex 1 conductivity detector. Column oven temperature was set to 40°C. A 3.2 mM Na_2CO_3 plus 1 mM $NaHCO_3$ solution was used as eluent at a flow rate of 0.7 mL min^{-1}. The lower limit of acetate detection, as determined by standard curves, was 2.4 μM. Production of methane was determined from a 1 mL headspace sample via gas chromatograph as described previously [92]. Production of sulfide was determined from a 0.75 mL culture sample using the methylene blue reduction method [90]. Production of soluble or particulate ferrous iron was determined in a 0.5 mL culture sample using the ferrozine method [97]. To prevent oxidation, samples were immediately acidified by addition of HCl to a final concentration of 0.5 M. Production of nitrite was determined in a 1 mL culture sample using a Griess assay modified as described previously [98].

MPN (Meta)genome Sequencing

Total genomic DNA from select MPN microcosms was subjected to Illumina library preparation and paired-end sequencing (2 × 150 bp) with the NovaSeq platform at the Genomics Core Facility at the University of Wisconsin-Madison. Sequences were assembled, binned, and annotated as previously described ([99]; detailed in SI Appendix). Manual BLASTp searches were conducted to search for specific proteins involved in CO_2 fixation pathways, dissimilatory sulfate reduction, dissimilatory nitrate reduction, putative ferric iron reduction pathways, and reversible H_2 oxidation (i.e., [NiFe]- and [FeFe]-hydrogenases). BLAST searches were conducted using bait sequences specific to the subunits harboring the active site as well as requisite accessory subunits of each protein complex of interest. Matches with an E-value $<1x10^{-6}$, >30% amino acid homology, and covering >60% of the length of the BLASTp bait sequence were considered positive hits. Hits were further screened based on the presence of amino acid residues unique to select functional genes, e.g. the conserved cysteinyl residues demarcating [NiFe]-hydrogenases from membrane bound oxidoreductases (Mbx, Nuo) [100]. Putative [NiFe]- and [FeFe]-hydrogenases were confirmed and classified using the HydDB tool [101]. The assembled metagenomic data are available under the NCBI BioProject ID PRJNA622799.

H_2 Oxidation Assays

H_2 oxidation assays were conducted in acid-washed 160 mL serum vials prepared as described above for MPN assays. Vials were filled with artificial Skálm Pore Water (SPW) medium (for KJ sediment samples) or artificial RG Pore Water (RGPW) medium (for RG sediment samples) made in milliQ H_2O. The composition of SPW was derived from a previous geochemical analysis of the Skálm river, an outlet of KJ to the north of Múlakvisl [102]. The

composition of this medium is as follows: SiO_2 (500 µM), NaCl (500 µM), KCl (25 µM), $CaCl_2$ (250 µM), and $MgCl_2$ (150 µM). The pH of the medium was adjusted to 6.8 with 1M NaOH. RGPW medium composition was derived from geochemical analysis of RG outflow waters and has been described previously [75]. Serum bottles were filled with 60 mL of SPW or RGPW medium for uninoculated controls or 48 mL for heat-killed sediment controls and experimental vials. Vials containing medium were autoclaved and then cooled to 4°C. Twenty g sediment (wet weight) was added to each vial except for uninoculated controls, followed immediately by stoppering and deoxygenation with N_2 on ice as described above. Assays to measure rates of H_2 transformation under aerobic conditions were not subjected to deoxygenation. Heat-killed sediment controls were autoclaved twice after inoculation as described above.

Twenty-five mL of headspace gas was removed from each microcosm and replaced with filter-sterilized CO_2 to achieve a final headspace mixing ratio of 20%. Oxidant solutions (prepared in sterile anoxic SPW or RGPW medium using salts described above) were added to microcosms to achieve a final concentration of 1 mM. The uninoculated and heat-killed controls had the same headspace and medium composition as the CO_2-amended rate assays, with extra medium added to uninoculated microcosms to account for the lack of sediment. Finally, H_2 was added to a final headspace mixing ratio of 500 ppmv (approximately 1.7 µmol H_2 per microcosm). Vials were incubated at 4°C upside-down to minimize potential H_2 diffusion through stoppers.

The headspace mixing ratio of H_2 was monitored over time via gas chromatography. For subsampling, 1 mL ultrapure N_2 gas was added to microcosm headspace and mixed well. One mL of the mixed headspace was then removed and diluted 1:4 with ultrapure N_2. Gases were

allowed to equilibrate and the concentration of H_2 was determined as previously described [92]. Gas phase concentrations were converted to dissolved aqueous phase concentrations according to Henry's law, as previously described [58]. Total microcosm H_2 content was calculated as the sum of headspace and aqueous phase H_2. The maximum rate of net H_2 oxidation was calculated by applying linear regressions to subsets of each data series, as indicated in **SI Appendix Tables 2.3/S1** and **2.4/S2**. The inverse of the slope of each regression, as presented in **SI Appendix Table 2.5/S3**, was taken to be the rate of net H_2 oxidation. Following termination of the incubation, microcosms were assayed for concentrations of total ferrous iron (soluble and particulate), acetate, and methane, as described above.

CO_2 Fixation Assays

Rates of CO_2 fixation were determined using previously described methods [15]. Briefly, acid-washed 160 mL serum vials were filled with 55 mL SPW or RGPW medium and autoclaved before inoculation with 10 g wet weight of KJ or RG sediments, respectively. After inoculation, microcosms were amended with oxidant solutions/suspensions to achieve a final concentration of 1 mM, as described above. Inoculated microcosms were purged with N_2 gas as described above. The headspace of microcosms was then flushed with filter-sterilized H_2 gas. For oxic microcosms, 33 mL each of filter-sterilized air and CO_2 were added to the headspace and mixed before 66 mL mixed gas was removed, leaving 100 mL headspace comprising 60% H_2, 20% air, and 20% CO_2. In all other microcosms, 25 mL filter-sterilized CO_2 was added and mixed before 25 mL mixed gas was removed, for final headspace composition of 80% H_2 and 20% CO_2. Heat-killed controls were prepared by double-autoclaving as described above. Assays were initiated by the addition of 5 μCi $NaH^{14}CO_3$.

The amount of ^{14}C incorporated into biomass was determined by uniformly resuspending sediments and removing a 1 mL subsample aseptically using an N_2 purged and sterile syringe and needle. Subsamples were acidified to pH <2 by addition of 12N HCl, vortexed, and allowed to vent in a fume hood for 1 hr to volatilize and off-gas unreacted $NaH^{14}CO_3$. Samples were then spun down for 10 min at 17 000 x *g* and supernatant was removed. Pellets were washed three times by adding 1 mL 0.1 M HCl, vortexing, and spinning down as described above. Finally, washed pellets were resuspended in 1 mL milliQ water, transferred to scintillation vials, and mixed with 10 mL CytoScint scintillation cocktail (MP Biomedicals, Irvine, CA). The radioactivity associated with each sample was then quantified with a Tri-Carb 2900TR liquid scintillation counter (PerkinElmer, Waltham, MA).

A standard curve was constructed to account for quenching of photons by sediments suspended in the scintillation cocktail. Microcosms not spiked with ^{14}C were prepared as described above and sub-samples were processed as described above. $NaH^{14}CO_3$ was then added in the amount of 40, 70, and 200 pCi per scintillation vial. Triplicate sub-samples were prepared at each ^{14}C activity for vials that contained sediments and those that did not, and activity was counted by liquid scintillation as described above.

To determine the amount of CO_2 fixed in each microcosm, the following calculations were used. Radioactivity measured in disintegrations per minute was converted to μCi and activity in μCi was corrected for sediment quenching using the curve described above. Carbon uptake (C_{uptake}) was calculated using equation 3 below, where DIC is the sum of inorganic carbon added to each microcosm and present in growth medium, A_{POC} is the measured activity of

sample particulate organic carbon, and A_{DIC} is the activity of the $H^{14}CO_3^-$ spike added to each microcosm.

$$C_{uptake} = \frac{DIC \times A_{POC}}{A_{DIC}} \quad (3)$$

Results were normalized to grams dry weight sediment (gdws) and the means and standard deviations of measurements on triplicate microcosms are reported. Rates of microbial carbon fixation were determined by applying linear regressions to subsets of the C_{uptake} datasets presented in **SI Appendix Tables 2.6/S4** and **2.7/S5**. The slopes of these regressions are presented in **SI Appendix Table 2.8/S6** and were taken to be the maximum rates of carbon fixation.

Inoculation and Monitoring of Transfer Cultures

MPN cultures inoculated with KJ sediments and amended with hematite were transferred at a 1:10 vol:vol ratio into fresh microcosms (70 mL serum bottles, 30 mL M9 medium prepared and amended as described above for MPN assays). Production of cells was monitored by filtering cells onto 0.22 μm black polycarbonate filters (MilliporeSigma, Burlington, MA), staining cells with SYBR Gold nucleic acid gel stain (Life Technologies, Carlsbad, CA) at a final dilution factor of 10 000, and enumeration via epifluorescence microscopy using an Evos FL microscope (Life Technologies).

Results and Discussion

Sources of H_2 in Glacial Meltwaters

The concentration of dissolved H_2 in the outflow stream of KJ, a basalt hosted glacier in southern Iceland, was 426.8 ± 248.2 nM (n=3) in October 2016 (~1 km from glacier terminus).

The variability in the H_2 measurement may be due to the highly turbulent nature of the stream flow at the time of sampling. At RG, a carbonate-hosted system in southern Alberta, Canada, the concentration of H_2 in meltwater sampled from the terminus of the glacier was 41.6 nM in October 2014 [103]. Unfortunately, the variability associated with this measurement cannot be assessed due to the lack of replicate samples. Other measured geochemical parameters are reported in **Table 2.1**.

The concentration of H_2 measured in KJ meltwaters was similar to or in excess of concentrations measured in waters typically thought of as being enriched in H_2, including high temperature volcanic influenced hot spring systems where dissolved H_2 concentrations rarely exceed 1 µM (Spear 2005; Lindsay 2019). Given that KJ drains Katla volcano, it cannot be ruled out that the H_2 detected in the meltwaters may be volcanic in origin. However, unlike KJ waters, whose low conductivities (82 µS/cm) are consistent with a meteoric origin, waters influenced by volcanic input tend to have much higher conductivities (average >1700 µS/cm [104]). This observation, combined with the ~15 km distance between the KJ sampling location and the primary vent of Katla Volcano, suggests that other sources are likely contributing H_2 to meltwaters at KJ leading to the high concentrations measured. However, without knowing the precise conduits emanating from the volcano and their proximity to KJ, a hydrothermal source for H_2 in meltwaters cannot be excluded.

Previous studies have shown that pulverization of silicate minerals followed by exposure to water can generate H_2 at temperatures ranging from ~0 to 35°C [56]. Based on the detection of silica radicals following mineral pulverization, a cataclastic mechanism of H_2 generation was proposed (i.e., reactions 1 and 2; [56]). Further, it was suggested that this cataclastic mechanism

mimics the process of glacial comminution of silicate bedrock [56] and thus could explain the unusually high H_2 concentrations detected in meltwaters from several subglacial habitats [23]. However, this study only accounted for gas that was generated upon exposure of pulverized minerals to water and thus excluded the potential for gas to be released from rock inclusions during mechanical crushing. More recent studies have shown that fluid inclusions in muddy carbonates and shales (including those sampled from RG) contain H_2 that is released during rock crushing [57] and could be responsible for the H_2 detected in RG meltwaters.

The minerology of basalts and other mafic rocks makes possible another H_2-generating mechanism: the reduction of water by ferrous silicates, as proposed for the Columbia River Basalt group of central Washington, USA [65]. This mechanism might be enhanced in subglacial systems that are actively exposing fresh iron bearing minerals (e.g., fayalite) capable of reacting with water. Importantly, like muddy carbonates and shales, fluid inclusions in basalts have also been shown to contain H_2 that is suggested to derive from iron-based reduction of water when the basalts were crystalizing at high temperature (>400°C) [105]. Thus, glacial comminution or fracturing of the host basalt bedrock could expose fresh iron and silicate minerals capable of reacting with water and producing H_2 via mechanisms described above or could release H_2 from fluid inclusions.

Regardless of the relative contributions of each of these mechanisms to the availability of H_2 in sub- and proglacial systems, Icelandic volcanic rocks, being enriched in both silica and iron [83, 86, 106] relative to carbonates/shales such as those dominating the RG catchment [89], may thus be predicted to generate more H_2 during glacial comminution. Our field data support this prediction, with an order of magnitude more dissolved H_2 measured in the meltwaters of KJ than

in those of RG. Importantly, the dissolved H_2 measured in meltwaters from both systems was higher than would be expected based on equilibration with atmospheric H_2 alone (<0.5 nM, given an atmospheric concentration of ~500 parts per billion [107]), consistent with a source for H_2 in the glacial bedrock/sediments as described above. Furthermore, H_2 at concentrations even lower than those measured in KJ or RG meltwaters has been shown to support biological H_2 oxidation in other systems [108], and H_2 oxidizing microbial populations have been recently reported in subglacial ecosystems in Antarctica [82]. Together, these observations suggest the potential for H_2 oxidation to support microbial life in both KJ and RG sediment communities.

An additional question concerns the source of oxidants capable of supporting H_2-dependent growth in subglacial habitats. The generation of H_2 due to reduction of water by either cataclastic silica radical- or ferrous iron-based reactions must achieve charge/redox balance, which should occur via an accompanying oxidation reaction. In the case of silica-radical-based reduction of water, it has been suggested that hydroxyl radicals are formed and that these can oxidize ferrous iron or sulfide in bedrock minerals, leading to formation of ferric iron or sulfate [57]. Likewise, reduction of water by ferrous iron in minerals is accompanied by iron oxidation to yield ferric iron [65, 105]. In subglacial systems, constant flow of ice and meltwater along with comminution of underlying bedrock could transport both H_2 (however produced) and oxidized minerals downstream [109] to environments with geochemical conditions that are favorable for the reverse of these reactions to occur.

Rates of Net H_2 Oxidation

To begin to assess the role of H_2 in supporting microbial life in sub- and proglacial habitats, potential rates of net H_2 oxidation were determined in microcosm assays amended with

H_2 and CO_2 with or without one of several common oxidants, including SO_4^{2-}, hematite, ferrihydrite, NO_3^-, and O_2 (**Fig. 2.1A, C**). In microcosms prepared without sediments (uninoculated) or with autoclaved sediments (heat killed), net H_2 loss was equivalent to loss due to sample removal. This indicates that rates of net H_2 oxidation exceeding those measured in abiotic controls can be ascribed to biological activity.

All microcosms exhibited an initial lag phase, defined as the time between introduction of the substrate (H_2) and its detectable consumption by microbial activity (**Fig. 2.1A**, **C**). In KJ microcosms, the lag phase lasted no more than 12 days. In contrast, the lag phase for RG sediments lasted 18 days under most conditions. While RG sediments were frozen in storage for several years between their collection in 2009 and their use as inocula here, the lag times observed in this experiment match closely with those observed in other growth experiments that used RG sediments stored for between one and five years [15, 23, 75]. Indeed, similar lag times were associated with the onset of CO_2 fixation using the same sediments collected from RG in 2009 but frozen for two years [15] versus nine years in the present study. This suggests that any deleterious effects of long-term storage on RG sediment microbiota were minimal.

It has been suggested that the duration of the lag phase can be used as a proxy for the degree of adaptation by a given microorganism (or community of microorganisms) to use a given substrate [110, 111], with shorter lag times indicative of a greater degree of adaptation. In this context, the results of the current study suggest that hydrogenotrophic members of the microbial communities inhabiting KJ sediments may be better adapted to take advantage of H_2 as an electron donor than those of RG sediments. Alternatively, hydrogenotrophs may be numerically more abundant at KJ than RG.

The most straightforward approach to addressing the likelihood of these possibilities would be to use molecular methods to determine the abundance of organisms with the genomic capacity to oxidize H_2. However, numerous attempts to extract genomic DNA from KJ sediments, including using methods specifically developed for basaltic sediments [112], failed to yield detectable (>0.5 ng DNA per gram dry weight sediment (gdws)) DNA. Moreover, extracts did not yield PCR amplicons when probed using universal 16S rRNA gene primers. This prevented application of molecular approaches to characterize endogenous sediment communities in KJ and to estimate their abundance.

To further examine the role of H_2 oxidation in supporting subglacial and proglacial sediment communities, the maximum rate of net H_2 oxidation was determined. This rate ranged from 2.9-9.3 (median = 7.6) nmol d^{-1} $gdws^{-1}$ for KJ microcosms and from 0.8-2.3 (median = 1.1) nmol d^{-1} $gdws^{-1}$ for RG microcosms (**Fig. 2.2**, **SI Appendix Table 2.5/S3**). Maximum rates of net H_2 oxidation in KJ microcosms were up to ten-fold higher than those in RG microcosms, adding further support to the hypothesis that the microbial communities associated with KJ sediments are better adapted to use H_2 as a reductant. For perspective, maximum net rates of H_2 oxidation in KJ were within an order of magnitude of those (~84 nmol H_2 d^{-1} $gdws^{-1}$) measured in Antarctic desert surface soils incubated at a slightly higher temperature (10°C; [113]).

Rates of Net CO_2 Fixation

A second set of microcosm assays was conducted to measure rates of net CO_2 fixation among members of the KJ and RG sediment communities and to gauge whether autotrophy is coupled to hydrogenotrophy in either community, in addition to the extent to which this is similarly (or not) influenced by oxidant amendment. Each microcosm contained H_2 and CO_2 (a

fraction labeled as $^{14}CO_2$) and was amended with O_2, NO_3^-, hematite, SO_4^{2-}, or was unamended (CO_2 only) (**Fig. 2.1B**, **D**). No microcosms were amended with ferrihydrite because, in H_2 oxidation assays, there was no discernable difference in activity between microcosms amended with ferrihydrite and those amended with hematite.

In heat-killed control microcosms containing sediments from KJ and RG, net uptake of $^{14}CO_2$ did not occur (**Fig. 2.1B**, **D**). In contrast, net uptake of $^{14}CO_2$ began to increase after an initial lag phase in all test microcosms. In KJ microcosms, the lag phase lasted 7 to 14 days, depending on the supplied oxidant, whereas in RG microcosms it lasted approximately 28 days regardless of oxidant. The lengths of these lag phases match closely with those measured for net H_2 oxidation in KJ microcosms, while they are roughly 1.5 times longer than those measured for net H_2 oxidation in RG microcosms. This suggests that H_2 may be the primary reductant supporting CO_2 fixation for at least part of the KJ community, while its primary role in RG may be to supplement facultatively autotrophic or mixotrophic (with respect to electron donor) microbial populations. Support for this possibility comes from the relatively high levels of total organic carbon (TOC) in RG subglacial sediments (24.8 ± 14.0 mg $gdws^{-1}$; **Table 2.1**) and their porewaters (~60 μM; [75]), a characteristic that would otherwise be expected to promote chemoheterotrophy or chemolithoheterotrophy over chemolithoautotrophy, as has been shown for other natural systems [114] and cultures [115, 116]. In contrast, the amount of TOC in KJ sediments is below the practical limit of quantitation for the instrumentation and techniques used in this study (<1.06 mg $gdws^{-1}$). Extrapolation beyond the lower quantitation limit based on the slope of the calibration curve indicates that TOC in KJ sediments is roughly two orders of magnitude lower than in RG sediments (0.38 ± 0.14 mg $gdws^{-1}$; **Table 2.1**).

The maximum rate of net CO_2 fixation ranged from 0.37-2.39 (median = 0.44) nmol C d^{-1} $gdws^{-1}$ for KJ and from 0.04-1.98 (median = 0.08) nmol C d^{-1} $gdws^{-1}$ for RG microcosms (**Fig. 2.3**, **SI Appendix Table 2.8/S6**). Rates of net CO_2 fixation were 4.8- to 12.2-fold higher in KJ microcosms than in RG microcosms for oxidants other than NO_3^-. The dramatic increase in both maximum CO_2 fixation rate and total accumulated fixed $^{14}CO_2$ in microcosms amended with NO_3^- is a notable feature of each data set, and is consistent with previous evidence indicating the potential for NO_3^- reduction in subglacial environments from a variety of catchments [11, 40], including those from RG [75]. For comparison, a previous measurement of the rate of CO_2 fixation (1.2 ± 0.7 nmol C d^{-1} $gdws^{-1}$) in unamended (no added H_2 or exogenous oxidant) microcosm assays containing RG sediments incubated over a period of 176 days [15] falls between the low rates described above and that observed in RG microcosms amended with NO_3^-, which was 1.98 ± 0.39 nmol C d^{-1} $gdws^{-1}$.

Given the extremely low nitrogen content of sediments from both catchments (KJ: <27 µg $gdws^{-1}$, RG: 212.7 ± 54.2 µg $gdws^{-1}$, **Table 2.1**) and their correspondingly high organic C:N ratios, it is possible that the addition of NO_3^- simply relieved fixed N limitation, thereby increasing the metabolic activities of all members of these communities. However, given that in RG microcosm assays H_2 oxidation commenced prior to CO_2 fixation, it is unlikely the two processes are tightly linked in the metabolism of a single microbial population. In any case, the higher rates of both H_2 oxidation and CO_2 fixation in KJ microcosms, and their matching lag times, together point to the linking of these processes in KJ sediments much more strongly than in RG sediments.

KJ and RG microcosms amended with ferrihydrite and hematite, as well as RG microcosms amended with SO_4^{2-}, exhibited maximum rates of net H_2 oxidation and CO_2 fixation that were similar to unamended (CO_2 only) controls (**Figs. 2.2** and **2.3**). This suggests that dominant primary producers are either *i*) using CO_2 as an oxidant (i.e., they are acetogens or methanogens) or *ii*) utilizing an oxidant or reductant endogenous to their source sediments in lieu of those supplied experimentally. Microcosms were therefore probed for evidence of these two possibilities. Neither acetate nor CH_4 were detected in the medium or headspace of any of the microcosm assays. Similarly, no microcosm medium contained dissolved sulfide, even when SO_4^{2-} had been added. Ferrous iron was detected in microcosms amended with ferrihydrite (KJ mean ± standard deviation: 22.7 ± 9.0 μM, RG: 74.8 ± 62.3 μM), hematite (KJ: 40.7 ± 7.6 μM, RG: 20.3 ± 5.1 μM), SO_4^{2-} (KJ: 33.2 ± 5.4 μM, RG: 39.5 ± 27.9 μM), and CO_2 only (KJ: 20.9 ± 2.9 μM, RG: 8.7 ± 4.4 μM), but was also present in KJ heat killed control microcosms (13.2 ± 0.9 μM), which might be expected given the Fe(II) content of the iron rich basaltic sediments at KJ. NO_2^-, an intermediate in the reduction of NO_3^-, was present in NO_3^- amended microcosms from both catchments (KJ: 131.4 ± 8.5 μM, RG: 5.8 ± 2.7 μM), suggesting that NO_3^- may stimulate both hydrogen oxidation and CO_2 fixation in both systems.

Abundance of Hydrogenotrophs and Oxidant Coupling

To further investigate the abundance of hydrogenotrophs and the oxidants that couple with H_2 oxidation in KJ and RG sediment populations, a most probable number (MPN) cultivation approach was undertaken (**Fig. 2.4**). Microcosm assays containing M9 minimal medium, with H_2 as the sole added reductant and CO_2 as the sole added carbon source, were amended with O_2, NO_3^-, ferrihydrite, hematite, SO_4^{2-} or were not amended (CO_2 only).

Surprisingly, there were between two- and ninety-fold more cultivatable hydrogenotrophs in RG sediments than in those from KJ. This observation is consistent with the higher amounts of DNA recovered from RG sediments (7.4 ng $gdws^{-1}$) when compared to KJ sediments (<0.5 ng $gdws^{-1}$). To the extent that cultivation and DNA extraction/recovery bias was minimized in these experiments, these data suggest that the faster onset and higher rates of microbial H_2 oxidation and CO_2 fixation activity observed in KJ sediment microcosms described above are unlikely to result from a greater *in situ* abundance of hydrogenotrophic cells. Rather, they suggest that the community inhabiting KJ sediments is assembled to include populations better adapted to efficiently utilize available nutrients such as H_2, which is at a concentration in KJ meltwaters that is nearly an order of magnitude greater than observed in RG meltwaters.

A related possibility is that the apparent abundance of hydrogenotrophs at RG reflects populations that are mixotrophic and/or can facultatively oxidize H_2. Evidence in support of this possibility comes from physiological and genomic studies of the dominant primary producer in RG sediments, *Thiobacillus* sp. RG5 [15]. This strain is supported primarily by products (e.g., thiosulfate) of abiotic FeS_2 oxidation, but its genome also encodes a group 1 [NiFe]-hydrogenase [48] that is predicted to function in H_2 oxidation [62]. While growth experiments aimed at evaluating H_2 transformation were not conducted with *Thiobacillus* sp. RG5, they have been conducted with a close relative, *Thiobacillus denitrifications*. *T. denitrificans* also encodes a group 1 [NiFe]-hydrogenase but was shown to be unable to use H_2 as sole electron donor when growing autotrophically via NO_3^- reduction [117]. This suggests the possibility for mixotrophic energy metabolism as it relates to H_2, as has been shown for other organisms [115, 116].

MPNs were evaluated by quantifying DNA and reduced products from supplied oxidants. When MPNs were estimated using total extractable DNA, the abundance of hydrogenotrophs in both KJ and RG sediments differed by less than an order of magnitude among experimental conditions (supplied oxidants) (**Fig. 2.4A**). KJ sediment MPNs estimated by total extractable DNA were not substantially different from those estimated by the detection of Fe^{2+} for ferrihydrite and hematite amended microcosms, nor were DNA-based MPN estimates different than those based on detection of NO_2^- for NO_3^- amended KJ and RG microcosms (**Fig. 2.4B**). However, MPNs estimated based on the detection of products of the reduction of SO_4^{2-} and CO_2 did substantially differ from those based on total extractable DNA (**Fig. 2.4A, B**). Given that sediments from both RG and KJ are known to contain iron oxides (**SI Appendix Fig. 2.6/S1**; [118, 119]), it is possible that sulfide generated from SO_4^{2-} reduction was oxidized by Fe(III) in a cryptic cycle similar to what has been described for other freshwater sediment ecosystems [120]. However, the similar numbers of hydrogenotrophs in the SO_4^{2-} (also containing CO_2) and CO_2 only conditions, combined with the absence of detectable methane or acetate in MPN and microcosm assays, indicate instead that the microbial populations enriched under the CO_2 only and SO_4^{2-} amended conditions (for both KJ and RG sediments) likely possess mixotrophic metabolisms in which H_2 oxidation is not necessarily coupled to autotrophy. As such, these cells may have been supported by remnant organic carbon in sediments used to inoculate the MPN enrichment series.

The observation of similar MPN estimates derived from DNA extraction and Fe^{2+} detection in hematite- and ferrihydrite-amended KJ sediments (**Fig. 2.4**), combined with evidence for both net H_2 oxidation and CO_2 fixation in hematite- and ferrihydrite-amended KJ

microcosms (**Figs. 2.1**, **2.2**, and **2.3**), point to potential coupling of H_2 oxidation, iron reduction, and CO_2 fixation in KJ sediments. To further investigate this possibility, microcosms containing M9 minimal growth medium amended with H_2, CO_2, and hematite were inoculated with MPN cultures exhibiting both microbial growth and iron reduction. Due to the dilution of glacial sediment during preparation of MPN cultures and their subsequent transfer into M9 medium, the transfer of endogenous oxidants and organic carbon to these cultures was presumed to be negligible (transfer cultures estimated to contain 0.6 µg TOC mL^{-1} after ~600 fold vol:vol dilution of sediments). Continued growth of a single morphotype was observed and this growth was associated with the production of Fe^{2+} (**Fig. 2.5**). Given that CO_2 was the only provided carbon source and H_2 the only provided reductant, these observations point to this population coupling H_2 oxidation with the reduction of hematite to fuel autotrophic growth. While H_2 oxidizing, chemolithoautotrophic Fe(III) reducers are known to occur in high temperature environments [121, 122] and have recently been identified in low pH, moderate temperature environments [123], to our knowledge such organisms have not previously been identified in low temperature environments of circumneutral pH.

MPN (Meta)genomic Sequence Analysis

Nutrient amendments that promoted both H_2 oxidation and CO_2 fixation were targeted to identify the population(s) responsible for the observed activities and to probe mechanisms of H_2 oxidation in these taxa. These amendments included NO_3^-, hematite, ferrihydrite, SO_4^{2-}, and CO_2 alone for KJ sediments and NO_3^- for RG sediments. MPN cultures grown with each of these amendments were subjected to DNA extraction and metagenomic sequencing. The composition of each sequenced MPN community is shown in **Table 2.2**, while the completeness and

contamination of each recovered metagenome assembled genome (MAG) is presented in **SI Appendix Table 2.9/S7**.

Sequencing of genomic DNA from KJ MPN assays amended with H_2/CO_2 only and with $H_2/CO_2/SO_4^{2-}$ yielded the same three MAGs. The most abundant MAG in the H_2/CO_2 only and the $H_2/CO_2/SO_4^{2-}$ amended MPNs (93% and 89% of total reads, respectively) exhibited close affiliation (92% identity at the amino acid level of the RNA polymerase β subunit (RpoB) for both bins) with *Glaciimonas*, a metabolically flexible genus common to glacial ecosystems (e.g., [124-126]). Both *Glaciimonas* MAGs encode homologs of [NiFe]-hydrogenases and ribulose-1,5-bisphosphate carboxylase/oxygenase (RuBisCO), consistent with an ability to grow autotrophically using H_2 as an electron donor. However, despite being 99% similar at the level of RpoB sequence identity, the two MAGs differed in the complements of encoded [NiFe]-hydrogenases. Both *Glaciimonas* MAGs encode homologs of group 2b H_2 sensing [NiFe]-hydrogenases that regulate transcription and maturation of oxidative [NiFe]-hydrogenases [62, 127]. In addition to the group 2b homolog, the *Glaciimonas* MAG from the $H_2/CO_2/SO_4^{2-}$ amended microcosm encodes a group 1d oxidative [NiFe]-hydrogenase and the MAG from the H_2/CO_2 amended microcosm encodes a bidirectional group 3d [NiFe]-hydrogenase. The presence of both an H_2 sensing and an oxidative [NiFe]-hydrogenase points to adaptation to efficiently utilize H_2 when it is available while potentially minimizing costs associated with *de novo* protein and co-factor biosynthesis. However, the presence of a bidirectional hydrogenase in the H_2/CO_2 *Glaciimonas* MAG, rather than an oxidative hydrogenase as found in the $H_2/CO_2/SO_4^{2-}$ MAG, casts doubt on the reliance of this population on H_2 as its sole source of electrons during growth and could be further evidence of mixotrophic or facultatively autotrophic metabolism. Homologs

of the dissimilatory bisulfite reductase, a gene required for reduction of SO_4^{2-}, were not detected in either *Glaciimonas* MAG, consistent with the absence of detectable sulfide in KJ MPN and activity assay microcosms amended with SO_4^{2-}.

Sequencing of DNA extracted from hematite- and ferrihydrite-amended KJ MPNs failed. However, a single transfer of the H_2/CO_2/hematite amended MPN into fresh medium grew (**Fig. 2.5**) and this culture was subjected to DNA extraction and (meta)genomic sequencing. Both the hematite KJ MPN transfer culture and NO_3^- amended KJ MPN culture comprised a dominant MAG that was closely related (94% RpoB sequence identity) to *Rhodoferax ferrireducens*, a genus that is commonly identified in subglacial habitats [11, 128] including RG [18, 44]. Interestingly, like one of the *Glaciimonas* MAGs, the *Rhodoferax* MAG encoded homologs of a group 2b H_2 sensing [NiFe]-hydrogenase and a group 1d uptake [NiFe] hydrogenase, again pointing to adaptation to effectively respond to H_2 availability and use it as a component of energy metabolism. The MAG also encoded RuBisCO and dissimilatory nitrate reductase (NarGHJI), consistent with the stimulation of H_2 oxidation and CO_2 fixation by amendment with NO_3^-. Importantly, *Rhodoferax ferrireducens* strains have been shown to be metabolically flexible, displaying growth phenotypes as diverse as photoheterotrophy, aerobic heterotrophy, and fermentation [129]. To our knowledge, however, H_2 dependent chemolithoautotrophic growth has not so far been observed in this genus.

Despite evidence for iron reduction in KJ MPN assays, activity assays, and transfer cultures containing *Rhodoferax*, we were unable to identify genes encoding the porin cytochrome complexes that have been implicated in Fe(III) reduction in other bacteria. Notably, both the Pcc system used by *Geobacter* and several other metal-reducing organisms [130, 131] and the Mtr

system that plays a similar role in *Shewanella* [132, 133] were absent from the *Rhodoferax* MAGs, despite each being estimated to be 99% complete. Shi et al. [132] previously reported the discovery of homologs of MtrABC and accessory proteins encoded in the genome of *R. ferrireducens* using a BLAST-based approach. However, a BLASTp analysis of amino acid sequences of MtrABC in *Shewanella oneidensis* against the genome of *R. ferrireducens* only revealed a homolog of the MtrA subunit (*e* value <1E-70). No homologs of MtrABC were detected in the KJ-derived *Rhodoferax* MAGs. Importantly, dissimilatory iron reduction has been demonstrated in *R. ferrireducens* [134] despite this lack of evidence for the presence of known Fe(III) reduction pathways in its genome or in the KJ-derived *Rhodoferax* MAGs.

The only nutrient that stimulated both net H_2 oxidation and CO_2 fixation at RG was NO_3^- (**Fig. 2.1C, D**). For this reason, only the NO_3^- amended RG MPN was subjected to metagenomic sequencing and analysis. Two MAGs were identified in this MPN and were both affiliated with *Polaromonas* strains. While both MAGs encoded homologs of RuBisCO and dissimilatory nitrate reductase (NarGHJI), neither encoded homologs of [FeFe]- or [NiFe]-hydrogenases or proteins involved in their maturation. Thus, it is not clear how these organisms were growing in MPN assays unless they were using an endogenous reductant, such as organic carbon, FeS_2, or products derived from FeS_2 oxidation. Importantly, a transfer of this MPN into the same medium did not yield growth, consistent with the use of an endogenous reductant in the MPN assays.

Conclusions

Both silicate- and iron-bearing minerals can generate H_2 through cataclastic radical and reductive mechanisms in the presence of water. These minerals are chemically altered in the process, however, thereby preventing sustained reactivity unless those minerals are re-surfaced.

Glacial comminution is one mechanism of generating fresh mineral surfaces capable of reacting with water on a continual basis. Thus, subglacial environments have the potential to provide continuous sources of chemical energy, in the form of disequilibrium between H_2 and oxidized minerals, that can support chemolithotrophic microbial primary production in subglacial and downstream proglacial environments.

Meltwaters from KJ, which overlays a basaltic catchment, had an order of magnitude more dissolved H_2 than those from RG, which sits in a carbonate catchment. The sediment community at KJ exhibited shorter lag times and significantly faster rates of H_2 oxidation and CO_2 fixation than those measured for the RG sediment community. Metabolic activity assays and MPN experiments show that at least two populations of autotrophic hydrogenotrophs inhabit KJ sediments: one metabolically flexible mixotroph (*Glaciimonas* sp.) and one that can, at a minimum, utilize H_2, CO_2, and Fe(III) or NO_3^- (*Rhodoferax* sp.). In RG sediments, however, differing lag times between H_2 oxidation and CO_2 fixation experiments suggest that the two processes are not tightly coupled. A potential explanation for this comes from a prior study that showed the dominant primary producer in RG sediments depended primarily on FeS_2 or derivatives of its oxidation (i.e., thiosulfate) as reductants [15, 48]. Thus, H_2 oxidation in RG sediment populations may be attributable to a mixotrophic or chemolithoheterotrophic metabolism, as has been recently demonstrated in other taxa [115, 116].

(Meta)genomic sequencing of the most dilute MPN assays from KJ identified a relative of the NO_3^-- and Fe(III)-reducing *Rhodoferax* and a novel population of *Glaciimonas* as the dominant H_2 oxidizing autotrophs and/or mixotrophs in this system. Transfers of the *Rhodoferax* MPN culture into fresh medium further demonstrated the ability of this population to grow

autotrophically using the H_2/Fe(III) redox couple. This represents the only report to date of chemolithoautotrophic, H_2 dependent iron reduction in a non-hyperthermophilic or acidophilic organism, and experiments to further characterize this bacterium are underway.

Collectively, these results indicate that differences in bedrock mineral composition likely influence supplies of lithogenic H_2 and oxidants and that these, in turn, influence the diversity, abundance, and activity of H_2-dependent autotrophs in sub- and proglacial habitats. More broadly, they further underscore the importance of physical and chemical weathering processes in releasing nutrients capable of sustaining microbial primary production in these habitats, corroborating recent evidence that such communities could be supported by chemolithotrophic primary production, independent of photosynthetically fixed carbon [15]. This finding has important implications for the survival of terrestrial life through Snowball Earth periods of globally-extensive glaciation [1, 135] and for the possibility of discovering life on other icy planetary bodies [136]. Indeed, the recent discovery of H_2 gas in plumes of material erupting from the icy crust of Enceladus [137] points to active rock-water interactions occurring beneath the ice surface and implies a subsurface geochemical system with potentially important parallels to that of KJ and other glaciers in basaltic terrains.

Acknowledgements

This work was supported by a grant (NNX16AJ64G) from the NASA Exobiology and Evolutionary Biology program to M.L.S. and E.S.B. E.C.D. was supported by an NSF Graduate Research Fellowship.

References

1. Hoffman, P.F., et al., *A Neoproterozoic Snowball Earth.* Science, 1998. **281**(5381): p. 1342-1346.

9. Sharp, M., et al., *Widespread bacterial populations at glacier beds and their relationship to rock weathering and carbon cycling.* Geology, 1999. **27**(2): p. 107-110.

10. Skidmore, M.L., J.M. Foght, and M.J. Sharp, *Microbial Life beneath a High Arctic Glacier.* Applied and Environmental Microbiology, 2000. **66**(8): p. 3214-3220.

11. Foght, J., et al., *Culturable Bacteria in Subglacial Sediments and Ice from Two Southern Hemisphere Glaciers.* Microbial Ecology, 2004. **47**(4): p. 329-340.

15. Boyd, E.S., et al., *Chemolithotrophic primary production in a subglacial ecosystem.* Applied and Environmental Microbiology, 2014. **80**(19): p. 6146-53.

18. Hamilton, T.L., et al., *Molecular evidence for an active endogenous microbiome beneath glacial ice.* The ISME Journal, 2013. **7**(7): p. 1402-12.

19. Montross, S.N., et al., *A microbial driver of chemical weathering in glaciated systems.* Geology, 2013. **41**(2): p. 215-218.

23. Boyd, E.S., et al., *Methanogenesis in subglacial sediments.* Environmental Microbiology Reports, 2010. **2**(5): p. 685-692.

25. Michaud, A.B., et al., *Microbial oxidation as a methane sink beneath the West Antarctic Ice Sheet.* Nature Geoscience, 2017. **10**(8): p. 582-586.

40. Wynn, P.M., A. Hodson, and T. Heaton, *Chemical and Isotopic Switching within the Subglacial Environment of a High Arctic Glacier.* Biogeochemistry, 2006. **78**(2): p. 173-193.

44. Mitchell, A.C., et al., *Influence of bedrock mineral composition on microbial diversity in a subglacial environment.* Geology, 2013. **41**(8): p. 855-858.

48. Harrold, Z.R., et al., *Aerobic and Anaerobic Thiosulfate Oxidation by a Cold-Adapted, Subglacial Chemoautotroph.* Applied and Environmental Microbiology, 2016. **82**(5): p. 1486-1495.

56. Telling, J., et al., *Rock comminution as a source of hydrogen for subglacial ecosystems.* Nature Geoscience, 2015. **8**(12).

57. Macdonald, M.L., et al., *Glacial Erosion Liberates Lithologic Energy Sources for Microbes and Acidity for Chemical Weathering Beneath Glaciers and Ice Sheets.* Frontiers in Earth Science, 2018. **6**.

58. Spear, J.R., et al., *Hydrogen and bioenergetics in the Yellowstone geothermal ecosystem.* Proceedings of the National Academy of Sciences of the United States of America, 2005. **102**(7): p. 2555-2560.

59. Lin, L.-H., et al., *Radiolytic H_2 in continental crust: Nuclear power for deep subsurface microbial communities.* Geochemistry, Geophysics, Geosystems, 2005. **6**(7).

62. Peters, J.W., et al., *[FeFe]- and [NiFe]-hydrogenase diversity, mechanism, and maturation.* Biochimica et Biophysica Acta (BBA) - Molecular Cell Research, 2015. **1853**(6): p. 1350-1369.

63. Lindsay, M.R., et al., *Probing the geological source and biological fate of hydrogen in Yellowstone hot springs.* Environmental Microbiology, 2019. **21**(10): p. 3816-3830.

64. Nealson, K.H., F. Inagaki, and K. Takai, *Hydrogen-driven subsurface lithoautotrophic microbial ecosystems (SLiMEs): do they exist and why should we care?* Trends in Microbiology, 2005. **13**(9): p. 405-410.

65. Stevens, T.O. and J.P. McKinley, *Abiotic controls on H_2 production from basalt-water reactions and implications for aquifer biogeochemistry.* Environmental Science & Technology, 2000. **34**(5): p. 826-831.

66. Kita, I., S. Matsuo, and H. Wakita, *H_2 generation by reaction between H_2O and crushed rock: An experimental study on H_2 degassing from the active fault zone.* Journal of Geophysical Research: Solid Earth, 1982. **87**(B13): p. 10789-10795.

74. Hsu, H.-W., et al., *Ongoing hydrothermal activities within Enceladus.* Nature, 2015. **519**(7542): p. 207-210.

75. Boyd, E.S., et al., *Diversity, Abundance, and Potential Activity of Nitrifying and Nitrate-Reducing Microbial Assemblages in a Subglacial Ecosystem.* Applied and Environmental Microbiology, 2011. **77**(14): p. 4778-4787.

76. Cameron, K.A., et al., *Meltwater export of prokaryotic cells from the Greenland ice sheet.* Environmental Microbiology, 2017. **19**(2): p. 524-534.

77. Hindshaw, R.S., et al., *Influence of glaciation on mechanisms of mineral weathering in two high Arctic catchments.* Chem. Geol., 2016. **420**: p. 37-50.

78. Kelley, D.S., et al., *A Serpentinite-Hosted Ecosystem: The Lost City Hydrothermal Field.* Science, 2005. **307**(5714): p. 1428.

79. Boyd, E.S., et al., *[FeFe]-hydrogenase in Yellowstone National Park: evidence for dispersal limitation and phylogenetic niche conservatism.* The ISME Journal, 2010. **4**(12): p. 1485.

80. Parkes, R.J., et al., *Rock-crushing derived hydrogen directly supports a methanogenic community: significance for the deep biosphere.* Environmental Microbiology Reports, 2019. **11**(2): p. 165-172.

81. Ma, H., et al., *Ex Situ Culturing Experiments Revealed Psychrophilic Hydrogentrophic Methanogenesis Being the Potential Dominant Methane-Producing Pathway in Subglacial Sediment in Larsemann Hills, Antarctic.* Frontiers in Microbiology, 2018. **9**.

82. Yang, Z., et al., *H_2 Metabolism revealed by metagenomic analysis of subglacial sediment from East Antarctica.* Journal of Microbiology, 2019. **57**(12): p. 1095-1104.

83. Gale, A., et al., *The mean composition of ocean ridge basalts.* Geochemistry, Geophysics, Geosystems, 2013. **14**(3): p. 489-518.

84. Kruger, J., *Development of minor outwash fans at Kötlujökull, Iceland.* Quaternary Science Reviews, 1997. **16**(7): p. 649-659.

85. Jóhannesson, H., *Geological Map of Iceland. Bedrock Geology*. 2014, Icelandic Institute of Natural History: Reykjavík.

86. Lacasse, C., et al., *Bimodal volcanism at the Katla subglacial caldera, Iceland: insight into the geochemistry and petrogenesis of rhyolitic magmas.* Bulletin of Volcanology, 2006. **69**(4): p. 373.

87. McMechan, M.E., *Geology of Peter Lougheed Provincial Park, Rocky Mountain Front Ranges, Alberta*. 1988: Geological Survey of Canada.

88. Sharp, M., R.A. Creaser, and M. Skidmore, *Strontium isotope composition of runoff from a glaciated carbonate terrain.* Geochimica et Cosmochimica Acta, 2002. **66**(4): p. 595-614.

89. Griggs, R.K., *Characterization of Subglaical Till from Robertson Glacier, Alberta, Canada: Implications for Biogeochemical Weathering*, in *Department of Earth Sciences*. 2013, Montana State University: Bozeman, Montana.

90. Fogo, J.K. and M. Popowsky, *Spectrophotometric Determination of Hydrogen Sulfide - Methylene Blue Method.* Analytical Chemistry, 1949. **21**(6): p. 732-734.

91. Chapelle, F.H., et al., *Practical Considerations for Measuring Hydrogen Concentrations in Groundwater.* Environmental Science & Technology, 1997. **31**(10): p. 2873-2877.

92. Lindsay, M.R., et al., *Subsurface processes influence oxidant availability and chemoautotrophic hydrogen metabolism in Yellowstone hot springs.* Geobiology, 2018. **16**(6): p. 674-692.

93. Atlas, R.M., in *Handbook of Microbiological Media*. 2004, ASM Press: Washington, D.C. p. 981.

94. Straub, K.L., A. Kappler, and B. Schink, *Enrichment and isolation of ferric-iron- and humic-acid-reducing bacteria.* Methods in Enzymology, 2005. **397**: p. 58-77.

95. Mitchell, K.R. and C.D. Takacs-Vesbach, *A comparison of methods for total community DNA preservation and extraction from various thermal environments.* Journal of Industrial Microbiology and Biotechnology, 2008. **35**(10): p. 1139-47.

96. Blodgett, R. *Appendix 2: Most Probable Number from Serial Dilutions*. Bacterial Analytical Manual 2010 [cited 2017 14 July]; 8th:[Available from: https://www.fda.gov/food/foodscienceresearch/laboratorymethods/ucm109656.htm.

97. Viollier, E., et al., *The ferrozine method revisited: Fe(II)/Fe(III) determination in natural waters.* Applied Geochemistry, 2000. **15**(6): p. 785-790.

98. Strickland, J.D.H. and T.R. Parsons, *A Practical Handbook of Seawater Analysis*, J.C. Stevenson, Editor. 1972, Fisheries Research Board of Canada: Ottawa. p. 77-80.

99. Payne, D., et al., *Geologic legacy spanning >90 years explains unique Yellowstone hot spring geochemistry and biodiversity.* Environmental Microbiology, 2019. **21**(11): p. 4180-4195.

100. Schut, G.J., et al., *The role of geochemistry and energetics in the evolution of modern respiratory complexes from a proton-reducing ancestor.* Biochimica et Biophysica Acta (BBA) - Bioenergetics, 2016. **1857**(7): p. 958-970.

101. Søndergaard, D., C.N.S. Pedersen, and C. Greening, *HydDB: A web tool for hydrogenase classification and analysis.* Scientific Reports, 2016. **6**(1): p. 34212.

102. Jones, M.T., et al., *Monitoring of jökulhlaups and element fluxes in proglacial Icelandic rivers using osmotic samplers.* Journal of Volcanology and Geothermal Research, 2015. **291**: p. 112-124.

103. Canovas, P.A., *Energy Transfer Between the Geosphere and Biosphere*. 2016, Arizona State University: United States -- Arizona. p. 433.

104. Amenabar, M.J., M.R. Urschel, and E.S. Boyd, *Metabolic and taxonomic diversification in continental magmatic hydrothermal systems.* Microbial Evolution Under Extreme Conditions. Berlin: De Gruyter, 2015.

105. Klein, F., N.G. Grozeva, and J.S. Seewald, *Abiotic methane synthesis and serpentinization in olivine-hosted fluid inclusions.* Proceedings of the National Academy of Sciences of the United States of America, 2019. **116**(36): p. 17666-17672.

106. Bas, M.J.L. and A.L. Streckeisen, *The IUGS systematics of igneous rocks.* Journal of the Geological Society, 1991. **148**(5): p. 825-833.

107. Novelli, P.C., et al., *Molecular hydrogen in the troposphere: Global distribution and budget.* Journal of Geophysical Research. Atmospheres, 1999. **104**(D23): p. 30427-30444.

108. Greening, C., et al., *Persistence of the dominant soil phylum Acidobacteria by trace gas scavenging.* Proceedings of the National Academy of Sciences of the United States of America, 2015. **112**(33): p. 10497-10502.

109. Tranter, M., *Sediment and Solute Transport in Glacial Meltwater Streams,* in *Encyclopedia of Hydrological Sciences*. 2006.

110. Wiggins, B.A., S.H. Jones, and M. Alexander, *Explanations for the acclimation period preceding the mineralization of organic chemicals in aquatic environments.* Applied and Environmental Microbiology, 1987. **53**(4): p. 791-796.

111. Aamand, J., et al., *Microbial adaptation to degradation of hydrocarbons in polluted and unpolluted groundwater.* Journal of Contaminant Hydrology, 1989. **4**(4): p. 299-312.

112. Wang, H. and K.J. Edwards, *Bacterial and Archaeal DNA Extracted from Inoculated Experiments: Implication for the Optimization of DNA Extraction from Deep-Sea Basalts.* Geomicrobiology Journal, 2009. **26**(7): p. 463-469.

113. Ji, M., et al., *Atmospheric trace gases support primary production in Antarctic desert surface soil.* Nature, 2017. **552**(7685): p. 400.

114. Urschel, M.R., et al., *Substrate preference, uptake kinetics and bioenergetics in a facultatively autotrophic, thermoacidophilic crenarchaeote.* FEMS Microbiology Ecology, 2016. **92**(5).

115. Amenabar, M.J., et al., *Electron acceptor availability alters carbon and energy metabolism in a thermoacidophile.* Environmental Microbiology, 2018. **20**(7): p. 2523-2537.

116. Carere, C.R., et al., *Mixotrophy drives niche expansion of verrucomicrobial methanotrophs.* The ISME Journal, 2017. **11**(11): p. 2599-2610.

117. Beller, H.R., et al., *The Genome Sequence of the Obligately Chemolithoautotrophic, Facultatively Anaerobic Bacterium Thiobacillus denitrificans.* Journal of Bacteriology, 2006. **188**(4): p. 1473-1488.

118. Jónasson, K., *Silicic volcanism in Iceland: Composition and distribution within the active volcanic zones.* Journal of Geodynamics, 2007. **43**(1): p. 101-117.

119. Robson, G.R., *The volcanic geology of Vestur–Skaftarfellssýsla Iceland*. 1956, Durham University.

120. Hansel, C.M., et al., *Dominance of sulfur-fueled iron oxide reduction in low-sulfate freshwater sediments.* The ISME Journal, 2015. **9**(11): p. 2400-2412.

121. Kashefi, K., et al., *Geoglobus ahangari gen. nov., sp. nov., a novel hyperthermophilic archaeon capable of oxidizing organic acids and growing autotrophically on hydrogen with Fe(III) serving as the sole electron acceptor.* International Journal of Systematic and Evolutionary Microbiology,, 2002. **52**(3): p. 719-728.

122. Kashefi, K., et al., *Use of Fe(III) as an Electron Acceptor To Recover Previously Uncultured Hyperthermophiles: Isolation and Characterization of Geothermobacterium ferrireducens gen. nov., sp. nov.* Applied and Environmental Microbiology, 2002. **68**(4): p. 1735-1742.

123. Norris, P.R., et al., *Acidithiobacillus ferrianus sp. nov.: an ancestral extremely acidophilic and facultatively anaerobic chemolithoautotroph.* Extremophiles, 2020. **24**(2): p. 329-337.

124. Margesin, R., et al., *Glaciimonas frigoris sp. nov., a psychrophilic bacterium isolated from ancient Siberian permafrost sediment, and emended description of the genus Glaciimonas.* International Journal of Systematic and Evolutionary Microbiology, 2016. **66**(2): p. 744-748.

125. Frasson, D., et al., *Glaciimonas alpina sp. nov. isolated from alpine glaciers and reclassification of Glaciimonas immobilis Cr9-12 as the type strain of Glaciimonas alpina sp. nov.* International Journal of Systematic and Evolutionary Microbiology, 2015. **65**(Pt 6): p. 1779-1785.

126. Zhang, D.-C., et al., *Glaciimonas immobilis gen. nov., sp. nov., a member of the family Oxalobacteraceae isolated from alpine glacier cryoconite.* International Journal of Systematic and Evolutionary Microbiology, 2011. **61**(9): p. 2186-2190.

127. Lenz, O., et al., *The hydrogen-sensing apparatus in Ralstonia eutropha.* Journal of Molecular Microbiology and Biotechnology, 2002. **4**(3): p. 255-262.

128. Darcy, J.L., et al., *Global Distribution of Polaromonas Phylotypes - Evidence for a Highly Successful Dispersal Capacity.* PLOS ONE, 2011. **6**(8): p. e23742.

129. Hiraishi, A. and J.F. Imhoff, *Rhodoferax*, in *Bergey's Manual of Systematics of Archaea and Bacteria*. 2015. p. 1-11.

130. Liu, Y., et al., *A trans-outer membrane porin-cytochrome protein complex for extracellular electron transfer by Geobacter sulfurreducens PCA.* Environmental Microbiology Reports, 2014. **6**(6): p. 776-785.

131. Shi, L., J.K. Fredrickson, and J.M. Zachara, *Genomic analyses of bacterial porin-cytochrome gene clusters.* Frontiers in Microbiology, 2014. **5**.

132. Shi, L., et al., *Mtr extracellular electron-transfer pathways in Fe(III)-reducing or Fe(II)-oxidizing bacteria: a genomic perspective.* Biochemical Society Transactions, 2012. **40**(6): p. 1261-1267.

133. White, G.F., et al., *Rapid electron exchange between surface-exposed bacterial cytochromes and Fe(III) minerals.* Proceedings of the National Academy of Sciences of the United States of America, 2013. **110**(16): p. 6346-6351.

134. Finneran, K.T., C.V. Johnsen, and D.R. Lovley, *Rhodoferax ferrireducens sp. nov., a psychrotolerant, facultatively anaerobic bacterium that oxidizes acetate with the reduction of Fe(III).* International Journal of Systematic and Evolutionary Microbiology, 2003. **53**(3): p. 669-673.

135. Hotaling, S., E. Hood, and T.L. Hamilton, *Microbial ecology of mountain glacier ecosystems: biodiversity, ecological connections and implications of a warming climate: Microbial ecology of mountain glaciers.* Environmental Microbiology, 2017. **19**(8): p. 2935-2948.

136. Garcia-Lopez, E. and C. Cid, *Glaciers and Ice Sheets As Analog Environments of Potentially Habitable Icy Worlds.* Frontiers in Microbiology, 2017. **8**.

137. Waite, J.H., et al., *Cassini finds molecular hydrogen in the Enceladus plume: Evidence for hydrothermal processes.* Science, 2017. **356**(6334): p. 155-159.

Tables

Table 2.1. Geochemical measurements for glacial meltwaters and sediments from Kötlujökull, Iceland and Robertson Glacier, Alberta, Canada.

Sample Site	pH	EC (µS/cm)	DO (ppm)	Fe^{2+} (mg/l)	S^{2-} (µM)	H_2 (nM)	CH_4 (nM)	CO_2 (µM)	DIC (µM)	TOC (mg $gdws^{-1}$)	TN (µg $gdws^{-1}$)
Kötlujökull	6.8	82.1	10.3	ND	3.00	426.8 (248.2)	1.1 (0.1)	77.3 (50.2)	ND	0.38 (0.14)	BLD
Robertson	8.8*	32.5*	11.3*	0.05†	0.31†	41.6†	10.8†	ND	603‡	24.8 (14.0)	212.7 (54.2)

Standard deviations of triplicate analyses are denoted in parentheses, where available. The limit of detection for nitrogen, given the instrumentation and techniques used, was 27 µg $gdws^{-1}$. Abbreviations: EC, electrical conductivity; DO, dissolved oxygen; DIC, dissolved inorganic carbon; TOC, total organic carbon; gdws, gram dry weight sediment; TN, total nitrogen; ND, not determined; BLD, below limit of detection.

*Data from Boyd et al., 2011

†Data from Canovas, 2016

‡Data from Boyd et al., 2014

Table 2.2. Composition of communities from the most dilute most probable number (MPN) assays amended with H_2, CO_2, and (where indicated) other oxidants and containing pro- or subglacial sediments from Kötlujökull or Robertson Glacier, respectively. Community DNA was extracted and subjected to metagenomic sequencing to reveal the relative abundance of metagenome assembled genomes (MAGs) in the community, the taxonomic composition of MAGs via RNA polymerase β subunit (RpoB) homology, and the presence of protein homologs that would allow for H_2 oxidation, CO_2 fixation, and the coupling of H_2 oxidation with supplied oxidants.

Glacier	Supplied Oxidant	% Binned Populations	Taxon	RpoB Identity	Hydrogenase (subgroup)	CO_2 Fixation Marker	Terminal Reductase
Kötlujökull	CO_2	92.9	*Glaciimonas* sp. PCH181	91.9%	HupUV (2b), HoxYH (3d)	CbbSL	
		3.9	*Cellulomonas* sp. WB94	99.2%	HydA (A1)	none	
		3.3	*Phycicoccus* sp. Soil748	93.5%	HyhBGSL (3b)	none	
	SO_4^{2-}	88.5	*Glaciimonas* sp. PCH181	92.0%	HupUV (2b), HyaABC (1d)	CbbSL	
		3.5	*Phycicoccus* sp. Soil748	93.8%	HyhBGSL (3b)	none	
		4.3	*Cellulomonas* sp. WB94	99.2%	HydA (A1)	none	
	Hem.*	97.3	*Rhodoferax ferrireducens*	93.7%	HupUV (2b), HyaABC (1d)	CbbM	NarGHJI
		2.7	*Polaromonas* sp. CF318	95.6%	HupUV (2b)	none	NarGHJI
	NO_3^-	100.0	*Rhodoferax ferrireducens*	93.7%	HupUV (2b), HyaABC (1d)	CbbM	NarGHJI
Robertson	NO_3^-	96.7	*Polaromonas* sp. A23	96.9%	none	CbbSL	NarGHJI
		3.3	*Polaromonas glacialis*	98.1%	none	4-hydroxybutyryl-CoA dehydratase	NarGHJI

Abbreviations: HupUV, the small and large subunits of the group 2b sensory [NiFe]-hydrogenase (see Peters et al., 2015); HoxYH, the small and large subunits of the group 3d bidirectional [NiFe]-hydrogenase; HydA, the catalytic subunit of [FeFe]-hydrogenases; HyhBGSL, the iron-sulfur, diaphorase, small, and large subunits of the group 3b bidirectional [NiFe]-hydrogenase, respectively;

HyaABC, the small, large, and cytochrome subunits of the group 1d uptake [NiFe]-hydrogenase, respectively; CbbSL, the small and large subunits of ribulose-1,5-bisphosphate carboxylase/oxygenase involved in the Calvin Cycle, respectively; Hem., hematite; CbbM, the large subunit of the proteobacterial form II (L_2) ribulose-1,5-bisphosphate carboxylase/oxygenase; NarGHJI, the alpha, beta, molybdenum cofactor assembly chaperone, and gamma subunits of the dissimilatory nitrate reductase complex, respectively.
*The MAGs described for Kötlujökull hematite-amended MPN assays were recovered from a culture transferred into fresh medium, the growth and Fe(III) reduction activity of which is depicted in Figure 2.5.

Figures

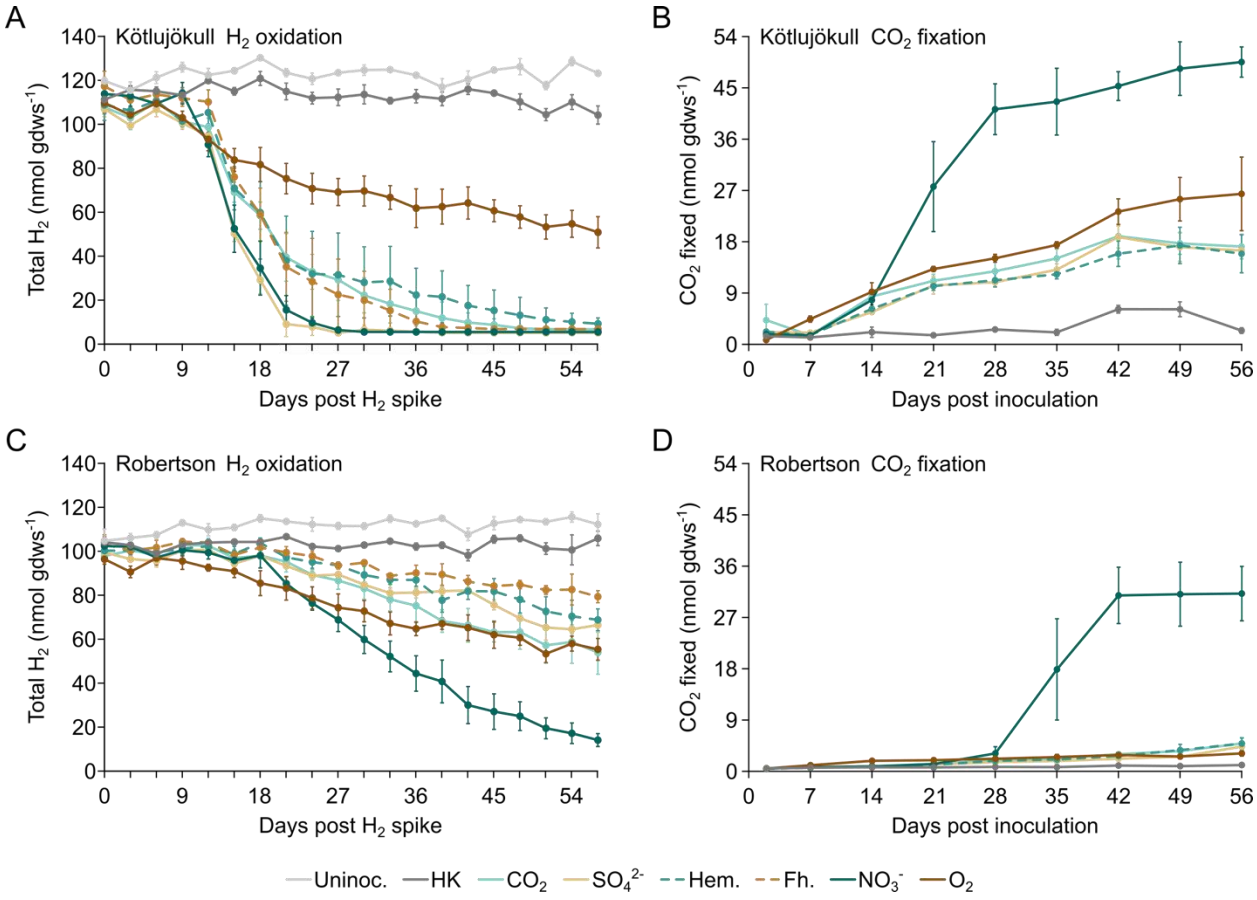

Figure 2.1. H_2 content (A, C) and carbon fixation (B, D) in microcosms inoculated with pro- or subglacial sediments from Kötlujökull (A, B) or Robertson Glacier (C, D), respectively, and incubated in the dark at 4°C. The means and standard deviations of measurements from triplicate microcosms are presented. Abbreviations: gdws, gram dry weight sediment; Uninoc., uninoculated control; HK, heat-killed control; Hem., hematite; Fh., ferrihydrite.

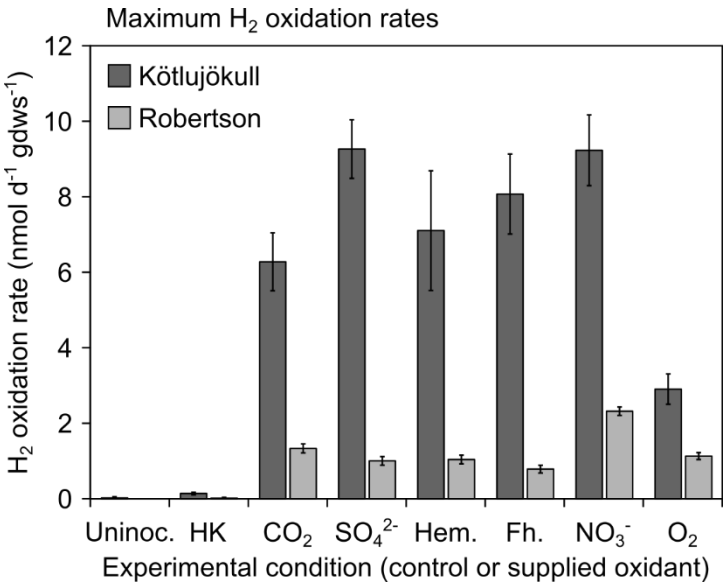

Figure 2.2. Maximum H_2 oxidation rates in microcosms containing pro- or subglacial sediments from Kötlujökull or Robertson Glacier, respectively, when incubated in the dark at 4°C. Linear regressions were applied to selected data from the sets represented in Figures 2.1A and 2.1C, and the inverse of the slope of each regression is reported. Error bars represent the standard deviation associated with the slope of each regression. Abbreviations: gdws, gram dry weight sediment; d, day; Uninoc., uninoculated control; HK, heat-killed control; Hem., hematite; Fh., ferrihydrite.

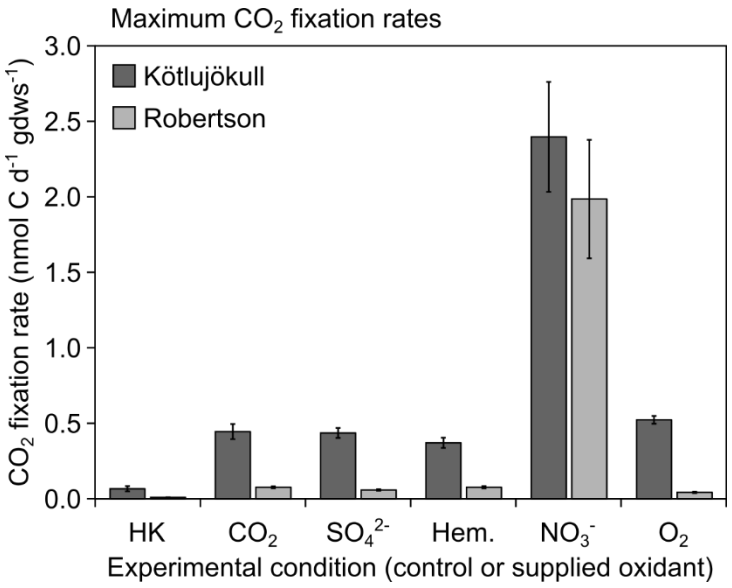

Figure 2.3. Maximum CO_2 fixation rates within microcosms containing pro- or subglacial sediments from Kötlujökull or Robertson Glacier, respectively, when incubated in the dark at 4°C. Linear regressions were applied to selected data from the sets represented in Figures 2.1B and 2.1D, and the slope of each regression is reported. Error bars represent the standard deviation associated with the slope of each regression. Abbreviations: gdws, gram dry weight sediment; d, day; HK, heat-killed control; Hem., hematite. Microcosms were not amended with ferrihydrite for this experiment given the similar rates of H_2 oxidation in ferrihydrite and hematite amended microcosms.

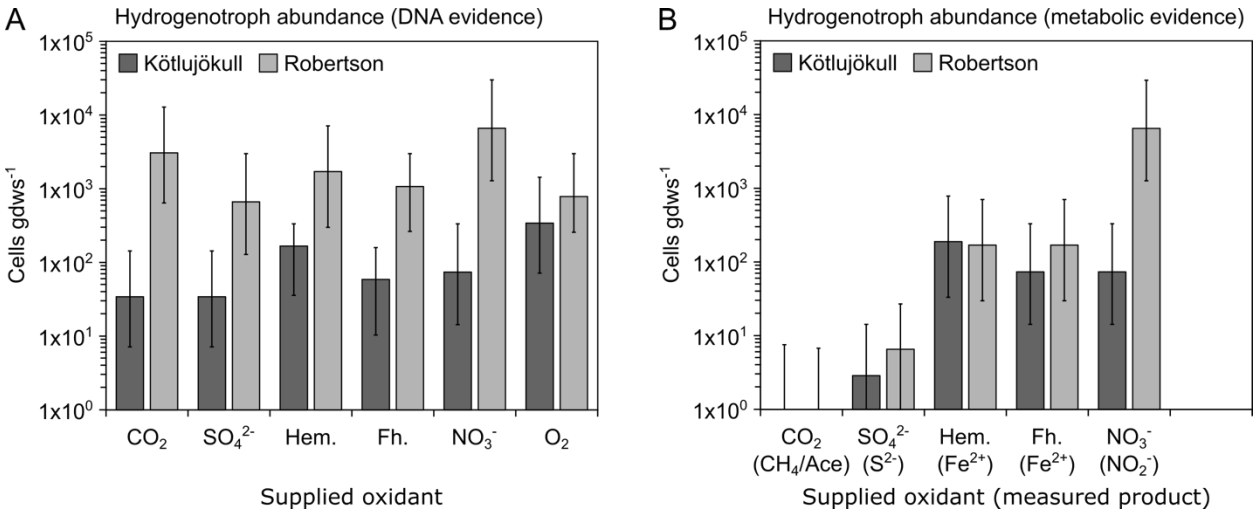

Figure 2.4. Abundance of hydrogenotrophic cells capable of autotrophic growth as determined by most probable number (MPN) assays containing dilutions of pro- or subglacial sediments from Kötlujökull or Robertson Glacier, respectively. The MPN was assessed first by quantifying total extractable DNA (**A**) and further refined by measurement of the metabolic products of CO_2, SO_4^{2-}, Fe(III), or NO_3^- reduction (methane and/or acetate, sulfide, ferrous iron, and nitrite, respectively) (**B**). Microbial growth was detected in CO_2- and SO_4^{2-}-amended microcosms without associated reduction of CO_2 or SO_4^{2-}. This observation led to the hypothesis that growth under these conditions is supported by heterotrophy. Error bars represent 95% confidence intervals. Abbreviations: gdws, gram dry weight sediment; Hem., hematite; Fh., ferrihydrite; Ace., acetate.

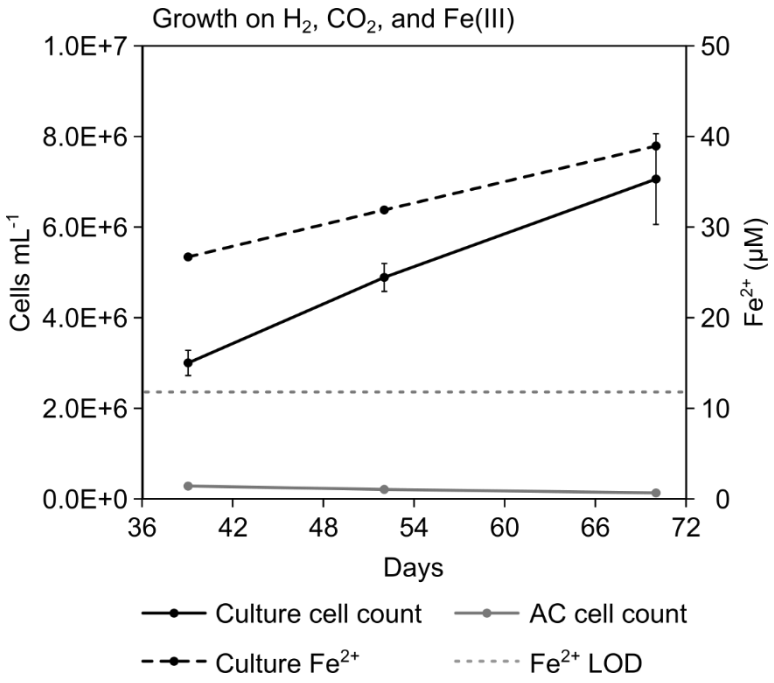

Figure 2.5. Activity and growth of a Kötlujökull most probable number (MPN) culture amended with H_2, CO_2, and hematite when transferred into fresh medium containing these components. (Meta)genomic sequencing of DNA extracted from this culture reveals a single metagenome assembled genome affiliated (94% RpoB ID) with *Rhodoferax ferrireducens*. Culture Fe^{2+} content was calculated as the concentration of Fe^{2+} measured in the biotic controls minus that measured in the abiotic controls. Error bars represent standard error of the mean. Abbreviations: AC, abiotic control; LOD, limit of detection.

Supplementary Materials and Methods

Metagenomic Sequence Assembly and Binning

Sequences received from the Genomics Core Facility at the University of Wisconsin-Madison were quality trimmed and cleaved of Illumina sequencing adapters using TrimGalore v.0.6.0 (https://github.com/FelixKrueger/TrimGalore) and Cutadapt v.1.18 [138]. The BBnorm script of the BBMap program suite (https://sourceforge.net/projects/bbmap/) was used to down-sample quality-filtered reads with a minimum depth of 5x and a target down-sampling average coverage of 100x. Down-sampled reads were assembled via MetaSPAdes (v.3.1.0) using a range of k-mer lengths and the default parameters. The metaquast function of quast v4.3 [139] was used to select and assess the final assembly (k-mer size = 121). Bowtie2 [140] was used for alignment and mapping of non-down-sampled, quality-filtered reads to the final assembly contigs. Contigs (>2.5 kbp) from were then binned into draft metagenome-assembled-genomes (MAGs) using unsupervised binning in MetaBAT v.0.26.3 [141] based on tetranucleotide frequency distribution patterns and differential sequence coverage profiles with the "verysensitive" parameter settings. CheckM v.1.0.5 [142] was used to assess the quality, completeness, and contamination of draft bins. Specifically, the completeness and contamination of each recovered bin (presented in **Table S7**) were used to determine bin quality using previously described metrics [142], according to which all recovered bins can be described as nearly complete (≥90%) draft genomes with low (≤5%) contamination. Relative abundances were calculated using the 'profile' function of CheckM.

X-ray Diffraction (XRD) Analysis

Bedrock samples from the RG proglacial area with visible concretions of oxidized iron were dried overnight at 80°C, powdered with a mortar and pestle, and passed through a 2 μm sieve. The sieved powders were analyzed by powder X-ray diffraction on a Scintag X1 diffraction system operated in the Imaging and Chemical Analysis Laboratory (ICAL) at Montana State University. Mineral phases were identified on Jade 9.0 and Scintag DMSNT software.

Supplementary Results and Discussion

X-ray Diffraction (XRD) Analysis

XRD spectrum reflection peak patterns indicated the presence of hematite in RG bedrock samples along with quartz, calcite, and pyrite (**Fig. 2.6/S1**). Thus, the visible iron oxides present in RG bedrock likely consist primarily of hematite, thought to be a product of pyrite oxidation [44].

Supplementary Tables

Table 2.3/S1. Unoxidized H_2 in triplicate microcosms containing proglacial sediments from Kötlujökull during H_2 oxidation activity assays, as presented in Figure 2.1A. Unoxidized H_2 represents the sum of H_2 in microcosm headspace and medium and H_2 removed during sampling over the course of the experiment. Linear regressions were applied to data points in bold face to determine rates of microbial H_2 oxidation as presented in Figure 2.2. Abbreviations: gdws, gram dry weight sediment; Uninoc., uninoculated control; HK, heat-killed control; Hem., hematite; Fh., ferrihydrite.

Days post	Kötlujökull unoxidized H_2 (nmol $gdws^{-1}$)							
H_2 spike	Uninoc.	HK	CO_2	SO_4^{2-}	Fe(III) (Hem.)	Fe(III) (Fh.)	NO_3^-	O_2
0	117.21	**117.04**	104.40	105.33	109.06	111.18	106.79	113.71
0	121.07	**113.85**	111.85	103.33	99.74	113.18	116.78	111.32
0	120.14	**102.27**	106.26	111.72	117.18	126.76	117.18	103.60
3	111.98	**115.68**	110.38	98.01	101.90	109.11	119.19	106.20
3	113.21	**115.39**	98.73	99.32	100.35	111.39	109.69	101.39
3	120.53	**115.29**	99.08	100.33	115.68	112.04	108.89	104.38
6	**117.76**	**116.43**	114.28	101.93	111.05	112.06	104.53	**109.80**
6	**124.47**	**112.01**	104.12	109.78	108.96	115.16	111.45	**106.67**
6	**120.79**	**115.90**	111.53	107.86	111.51	112.76	111.58	**111.55**
9	**122.65**	**108.53**	99.96	103.48	97.90	106.38	**109.03**	**107.02**
9	**128.08**	**116.84**	100.24	96.62	101.39	113.50	**112.02**	**100.81**
9	**126.37**	**113.58**	103.32	100.81	104.49	115.20	**120.67**	**100.55**
12	**117.84**	**118.91**	**92.84**	**90.13**	**102.21**	**106.90**	**85.47**	**100.23**
12	**125.06**	**119.71**	**100.30**	**98.25**	**100.53**	**117.68**	**87.83**	**87.97**
12	**123.60**	**120.15**	**102.34**	**95.16**	**112.58**	**105.28**	**98.42**	**90.63**
15	**122.04**	**115.80**	**69.13**	**48.70**	**66.87**	**70.27**	**66.76**	**90.96**
15	**125.19**	**112.35**	**63.22**	**54.90**	**60.79**	**79.01**	**40.91**	**78.33**
15	**125.05**	**116.12**	**74.60**	**46.72**	**84.52**	**78.35**	**49.47**	**81.55**
18	**129.61**	**116.78**	**59.32**	**27.79**	**61.70**	**44.63**	**51.87**	92.39
18	**130.12**	**120.49**	**50.16**	**37.37**	**32.40**	**57.31**	**24.46**	73.39
18	**130.11**	**124.56**	**65.50**	**22.06**	**85.09**	**74.48**	**27.10**	78.77
21	**120.84**	**110.31**	**47.95**	**4.94**	**41.83**	**20.62**	24.60	85.31
21	**123.21**	**114.18**	**23.80**	**17.16**	**10.54**	**27.28**	13.05	69.87
21	**125.61**	**119.62**	**46.33**	**5.01**	**61.17**	**57.25**	8.92	70.24
24	**123.58**	**108.83**	37.95	4.94	36.56	13.16	12.52	80.95
24	**120.37**	**110.87**	21.30	13.54	5.24	15.35	9.66	64.98
24	**117.45**	**115.30**	39.24	5.01	53.80	56.77	6.83	65.88
27	**121.66**	**106.79**	34.77	4.94	35.77	9.37	5.76	78.28
27	**124.56**	**113.52**	15.59	5.33	5.24	11.84	7.84	65.10
27	**123.35**	**115.85**	37.27	5.01	53.42	46.16	5.47	63.75
30	**124.26**	**108.19**	23.17	4.94	31.91	8.33	5.76	79.57
30	**127.44**	**112.85**	11.41	9.62	5.24	11.89	5.30	66.15
30	**121.56**	**119.06**	31.82	5.01	46.91	39.46	5.47	62.79
33	**125.93**	**108.27**	21.32	4.94	35.06	8.62	5.76	74.88
33	**123.94**	**111.63**	5.84	8.33	5.24	7.14	5.30	62.41
33	**124.01**	**111.64**	27.52	5.01	45.39	30.02	5.47	62.35
36	**120.81**	**111.13**	15.60	4.94	23.60	5.95	5.76	73.07
36	**122.41**	**109.59**	5.84	7.02	5.24	6.45	5.30	61.70
36	**123.00**	**116.92**	23.57	5.01	38.13	18.50	5.47	50.32
39	**118.97**	**106.96**	6.86	4.94	21.35	5.95	5.76	72.96
39	**119.78**	**112.33**	5.84	5.41	5.24	6.45	5.30	62.17
39	**111.18**	**114.79**	22.79	5.01	37.73	10.74	5.47	52.15
42	**124.71**	**112.32**	6.86	4.94	16.02	5.95	5.76	74.59
42	**120.45**	**118.40**	5.84	5.41	5.24	6.45	5.30	62.25

Days post H_2 spike	Kötlujökull unoxidized H_2 (nmol $gdws^{-1}$)							
	Uninoc.	HK	CO_2	SO_4^{2-}	Fe(III) (Hem.)	Fe(III) (Fh.)	NO_3^-	O_2
42	**115.51**	**116.50**	16.67	5.01	31.20	9.57	5.47	55.33
45	**124.09**	**115.20**	6.86	4.94	10.37	5.95	5.76	68.10
45	**124.19**	**113.08**	5.84	5.41	5.24	6.45	5.30	59.12
45	**124.94**	**113.55**	13.42	5.01	30.20	8.09	5.47	54.41
48	**121.58**	**105.58**	6.86	4.94	7.31	5.95	5.76	65.54
48	**125.55**	**114.62**	5.84	5.41	5.24	6.45	5.30	56.10
48	**130.71**	**109.90**	8.82	5.01	26.66	8.09	5.47	51.48
51	**114.65**	**100.26**	6.86	4.94	7.31	5.95	5.76	62.16
51	**119.19**	**104.85**	5.84	5.41	5.24	6.45	5.30	49.18
51	**118.39**	**107.41**	7.63	5.01	20.70	8.09	5.47	48.25
54	**126.05**	**109.92**	6.86	4.94	7.31	5.95	5.76	64.20
54	**128.08**	**105.63**	5.84	5.41	5.24	6.45	5.30	51.92
54	**131.02**	**114.07**	7.47	5.01	17.73	8.09	5.47	47.66
57	**123.00**	**99.70**	6.86	4.94	7.31	5.95	5.76	60.13
57	**122.12**	**109.75**	5.84	5.41	5.24	6.45	5.30	51.49
57	**123.75**	**102.55**	7.47	5.01	15.14	8.09	5.47	40.66

Table 2.4/S2. Unoxidized H_2 in triplicate microcosms containing subglacial sediments from Robertson Glacier during H_2 oxidation activity assays, as presented in Figure 2.1C. Unoxidized H_2 represents the sum of H_2 in microcosm headspace and medium and H_2 removed during sampling over the course of the experiment. Linear regressions were applied to data points in bold face to determine rates of microbial H_2 oxidation as presented in Figure 2.2. Empty cells in SO_4^{2-} column after day 33 represent a microcosm that was broken during handling. Abbreviations: gdws, gram dry weight sediment; Uninoc., uninoculated control; HK, heat-killed control; Hem., hematite; Fh., ferrihydrite.

Days post H_2 spike	Robertson unoxidized H_2 (nmol $gdws^{-1}$)							
	Uninoc.	HK	CO_2	SO_4^{2-}	Fe(III) (Hem.)	Fe(III) (Fh.)	NO_3^-	O_2
0	**97.07**	**107.10**	98.52	102.69	97.44	97.09	104.96	96.01
0	**109.02**	**100.90**	96.73	93.87	98.52	103.76	97.21	93.51
0	**107.59**	**103.64**	97.92	101.50	104.24	107.82	104.36	98.99
3	**106.78**	**108.17**	98.20	96.92	98.31	98.78	100.64	86.73
3	**103.06**	**97.98**	101.04	94.22	98.91	102.30	101.52	92.79
3	**107.71**	**101.46**	101.05	97.51	102.90	99.23	103.38	91.76
6	**105.20**	**101.97**	93.34	96.46	98.46	102.27	95.80	**93.45**
6	**109.22**	**98.48**	102.89	91.47	96.21	105.10	94.31	**101.00**
6	**107.10**	**95.56**	98.96	98.37	103.21	97.01	100.83	**95.67**
9	**110.66**	**102.26**	101.42	101.36	101.10	103.40	99.26	**90.45**
9	**113.99**	**103.28**	104.02	99.54	97.40	106.26	97.63	**95.68**
9	**113.52**	**102.95**	102.92	99.70	104.46	102.74	103.85	**99.84**
12	**105.64**	**103.26**	97.41	101.64	104.00	103.58	95.58	**90.16**
12	**112.23**	**103.21**	105.75	94.68	99.43	103.72	99.07	**92.81**
12	**110.80**	**104.79**	103.57	105.09	102.74	103.98	102.96	**94.03**
15	**108.93**	**104.14**	91.69	94.28	102.27	98.86	**89.60**	**87.23**
15	**112.59**	**103.14**	96.76	93.46	93.85	97.45	**97.18**	**90.38**
15	**110.19**	**104.73**	101.60	94.78	99.57	98.31	**100.14**	**94.47**
18	**113.32**	**103.95**	**95.68**	**97.58**	**106.12**	**102.56**	**91.55**	**77.12**
18	**113.66**	**105.21**	**99.61**	**98.67**	**100.60**	**101.14**	**96.45**	**88.88**
18	**117.22**	**102.88**	**98.17**	**97.02**	**104.11**	**100.70**	**105.64**	**89.91**
21	**113.44**	**106.49**	**88.26**	**92.32**	**98.19**	**96.75**	**80.87**	**77.05**
21	**112.23**	**106.57**	**97.94**	**92.58**	**95.96**	**103.06**	**88.44**	**90.34**
21	**114.26**	**106.13**	**98.99**	**94.37**	**96.87**	**97.85**	**86.02**	**81.60**
24	**107.45**	**103.57**	**85.53**	**88.91**	**96.62**	**96.00**	**75.81**	**71.12**
24	**115.07**	**101.26**	**90.41**	**85.84**	**90.68**	**96.05**	**80.11**	**82.38**
24	**113.42**	**101.05**	**91.23**	**91.22**	**97.32**	**100.81**	**72.66**	**82.27**
27	**110.37**	**101.44**	**82.41**	**89.64**	**95.15**	**95.36**	**68.32**	**65.14**
27	**113.63**	**101.74**	**84.95**	**88.81**	**91.31**	**91.71**	**75.27**	**80.32**
27	**109.93**	**99.74**	**92.22**	**89.35**	**93.71**	**92.81**	**62.39**	**77.10**
30	**109.12**	**101.91**	**76.52**	**83.21**	**92.59**	**93.87**	**64.57**	**66.50**
30	**111.45**	**102.57**	**83.13**	**85.48**	**83.35**	**94.72**	**63.83**	**79.06**
30	**113.10**	**103.30**	**89.03**	**85.18**	**91.25**	**95.24**	**50.84**	**72.24**
33	**113.59**	**104.28**	**71.88**	84.71	**89.52**	**90.10**	**58.63**	**63.45**
33	**117.02**	**105.20**	**76.76**	82.83	**83.89**	**88.33**	**55.03**	**74.68**
33	**113.06**	**103.66**	**85.22**	74.78	**87.21**	**87.42**	**42.39**	**62.91**
36	**113.79**	**100.00**	**68.03**	78.83	**90.83**	90.82	**52.76**	**60.96**
36	**112.10**	**101.99**	**70.92**		**83.60**	85.33	**46.74**	**69.19**
36	**110.86**	**103.78**	**86.25**	83.82	**85.88**	93.72	**33.39**	**63.63**
39	**115.17**	**102.70**	**63.19**	84.21	**74.73**	94.99	**42.78**	62.74
39	**116.10**	**100.65**	**65.38**		**72.57**	83.02	**51.61**	68.77
39	**113.06**	**104.25**	**75.72**	80.19	**85.36**	89.69	**27.65**	69.37
42	**107.60**	**101.24**	**57.58**	82.24	87.10	88.82	**40.69**	56.54
42	**110.93**	**97.75**	**63.96**		77.78	87.12	**29.45**	71.32
42	**103.79**	**94.94**	**77.01**	83.32	80.18	82.28	**19.71**	67.40
45	**115.73**	**104.06**	**60.51**	78.59	88.25	84.26	**36.92**	53.63
45	**113.11**	**107.69**	**58.83**		73.48	83.02	**27.48**	69.84

Days post H_2 spike	Robertson unoxidized H_2 (nmol $gdws^{-1}$)							
	Uninoc.	HK	CO_2	SO_4^{2-}	Fe(III) (Hem.)	Fe(III) (Fh.)	NO_3^-	O_2
45	**108.66**	**104.02**	**69.73**	74.18	83.05	84.70	**16.58**	62.18
48	**114.12**	**104.39**	57.97	70.72	84.76	82.04	**32.87**	57.00
48	**113.03**	**104.84**	56.63		69.15	86.39	**25.73**	65.95
48	**115.47**	**107.81**	74.89	70.21	79.87	85.58	**16.17**	58.71
51	**111.06**	**100.78**	54.21	72.31	78.12	85.04	**24.97**	50.98
51	**114.37**	**97.90**	48.33		62.50	80.96	**20.62**	59.28
51	**114.09**	**104.35**	68.77	60.71	76.89	80.62	**12.66**	49.48
54	**117.17**	**107.51**	54.95	67.71	80.49	91.52	23.07	52.29
54	**116.80**	**102.69**	48.29		61.99	74.17	17.74	61.02
54	**112.10**	**91.08**	72.61	64.00	68.39	81.58	10.66	60.31
57	**105.75**	104.39	50.21	71.30	74.16	82.90	16.63	48.49
57	**112.55**	102.39	43.13		61.11	76.02	16.25	62.05
57	**117.72**	110.11	68.13	64.57	70.66	78.60	9.33	55.26

Table 2.5/S3. Parameters of linear regressions used to determine rates of microbial H_2 oxidation as presented in Figure 2.2. Regressions were applied to data presented in bold in Tables 2.3/S1 and 2.4/S2 using the LINEST function of Microsoft Excel. The inverse of the slope of each linear regression is reported as the maximum rate of microbial H_2 oxidation, with error bar lengths corresponding to the standard deviation of that slope. Abbreviations: Uninoc., uninoculated control; HK, heat-killed control; Hem., hematite; Fh., ferrihydrite; std dev, standard deviation.

Kötlujökull	Uninoc.	HK	CO_2	SO_4^{2-}	Fe(III) (Hem.)	Fe(III) (Fh.)	NO_3^-	O_2
slope, m	-0.02	-0.14	-6.27	-9.25	-7.09	-8.06	-9.22	-2.90
std dev of slope	0.04	0.03	0.77	0.77	1.58	1.06	0.93	0.40
intercept, b	123.82	116.64	169.72	198.29	185.37	202.90	197.25	127.63
std dev of intercept	1.25	1.14	12.90	13.04	26.65	17.82	13.00	4.41
$R^2=SS_R/SS_T$	0.01	0.22	0.87	0.93	0.67	0.85	0.91	0.84
$s_{y,x}$, std dev of y	4.06	4.59	8.90	9.00	18.39	12.30	10.86	4.65
Fisher F statistic, $SS_R(n-2)/SS_E$	0.35	16.63	66.92	142.68	20.08	57.98	97.20	52.49
degrees of freedom, n-2	52	58	10	10	10	10	10	10
regression SS (SS_R); explained variation	5.77	350.31	5304.16	11547.70	6790.04	8768.89	11465.92	1136.22
errors SS (SS_E); unexplained variation	855.86	1221.77	792.62	809.35	3381.65	1512.48	1179.62	216.45
Robertson	Uninoc.	HK	CO_2	SO_4^{2-}	Fe(III) (Hem.)	Fe(III) (Fh.)	NO_3^-	O_2
slope, m	0.11	-0.01	-1.33	-1.00	-1.04	-0.78	-2.32	-1.13
std dev of slope	0.03	0.03	0.12	0.11	0.11	0.10	0.11	0.09
intercept, b	108.47	103.06	122.13	114.75	120.76	115.81	131.94	105.57
std dev of intercept	0.88	0.83	3.90	2.80	3.32	2.67	3.86	2.09
$R^2=SS_R/SS_T$	0.22	0.01	0.82	0.85	0.79	0.78	0.92	0.83
$s_{y,x}$, std dev of y	3.52	3.26	5.64	1.88	3.81	2.23	7.76	4.94
Fisher F statistic, $SS_R(n-2)/SS_E$	15.99	0.29	124.32	76.43	84.36	58.38	438.16	155.53
degrees of freedom, n-2	58	55	28	13	22	16	37	31
regression SS (SS_R); explained variation	198.17	3.07	3953.01	271.53	1224.96	290.96	26366.90	3788.58
errors SS (SS_E); unexplained variation	718.77	584.01	890.29	46.18	319.46	79.75	2226.53	755.16

Table 2.6/S4. Carbon fixed in triplicate microcosms containing proglacial sediments from Kötlujökull during CO_2 fixation activity assays, as presented in Figure 2.1B. Linear regressions were applied to data points in bold face to determine rates of microbial CO_2 fixation as presented in Figure 2.3. Abbreviations: gdws, gram dry weight sediment; HK, heat-killed control; Hem., hematite.

Days post inoculation	Kötlujökull C fixed (nmol $gdws^{-1}$)					
	HK	CO_2	SO_4^{2-}	Fe(III) (Hem.)	NO_3^-	O_2
2	**1.56**	3.80	1.56	1.99	1.57	**0.99**
2	**0.45**	7.83	2.53	2.41	1.04	**0.62**
2	**2.24**	1.06	2.33	2.15	2.62	**0.63**
7	**1.00**	**1.50**	**2.03**	**1.60**	1.31	**4.20**
7	**0.84**	**1.69**	**1.70**	**1.52**	1.79	**5.16**
7	**1.72**	**1.43**	**2.33**	**1.66**	1.48	**3.87**
14	**2.09**	**9.23**	**5.14**	**6.38**	**7.29**	**8.04**
14	**1.01**	**7.47**	**5.98**	**6.99**	**9.57**	**11.46**
14	**3.23**	**8.42**	**5.83**	**5.23**	**6.42**	**8.09**
21	**1.70**	**9.60**	**8.38**	**9.84**	**37.21**	**13.54**
21	**1.52**	**11.41**	**10.54**	**11.20**	**17.87**	**13.49**
21	**1.50**	**12.36**	**12.08**	**9.55**	**27.93**	**12.60**
28	**2.75**	**10.10**	**11.04**	**12.72**	**45.01**	**14.30**
28	**2.10**	**14.12**	**10.36**	**11.12**	**43.79**	**16.00**
28	**2.91**	**14.24**	**11.21**	**9.86**	**34.99**	**14.97**
35	**1.36**	**12.73**	**12.19**	**13.22**	50.66	**16.64**
35	**2.63**	**16.40**	**12.52**	**12.34**	40.19	**17.90**
35	**2.26**	**16.08**	**14.55**	**11.27**	36.92	**17.76**
42	**5.62**	**14.55**	**17.44**	**18.62**	46.58	**21.50**
42	**5.71**	**18.12**	**17.42**	**15.89**	47.61	**21.89**
42	**7.10**	**24.23**	**21.58**	**13.14**	41.80	**26.45**
49	**4.30**	15.38	15.43	19.19	53.20	24.05
49	**7.04**	17.66	15.11	19.99	49.98	21.66
49	**7.08**	20.06	20.59	12.86	42.01	30.71
56	**3.07**	14.21	16.96	17.54	51.18	27.46
56	**1.98**	17.96	15.07	18.87	45.80	18.01
56	**2.13**	19.27	17.38	11.21	51.65	33.73

Table 2.7/S5. Carbon fixed in triplicate microcosms containing subglacial sediments from Robertson Glacier during CO_2 fixation activity assays, as presented in Figure 2.1D. Linear regressions were applied to data points in bold face to determine rates of microbial CO_2 fixation as presented in Figure 2.3. Abbreviations: gdws, gram dry weight sediment; HK, heat-killed control; Hem., hematite.

Days post inoculation	Robertson C fixed (nmol $gdws^{-1}$)					
	HK	CO_2	SO_4^{2-}	Fe(III) (Hem.)	NO_3^-	O_2
2	**0.48**	**0.52**	**0.50**	**0.46**	0.37	**0.51**
2	**0.49**	**0.51**	**0.53**	**0.38**	0.45	**0.46**
2	**0.49**	**0.47**	**0.58**	**0.40**	0.44	**0.48**
7	**0.68**	**0.64**	**0.69**	**0.77**	0.78	**1.20**
7	**0.65**	**0.69**	**0.56**	**0.54**	0.77	**1.02**
7	**0.53**	**0.56**	**0.61**	**0.62**	0.74	**0.95**
14	**0.77**	**0.90**	**0.84**	**0.99**	0.69	**2.08**
14	**0.61**	**1.00**	**0.82**	**0.77**	0.82	**1.64**
14	**0.66**	**0.81**	**0.95**	**0.82**	0.95	**1.77**
21	**0.74**	**1.49**	**1.08**	**1.09**	1.09	**2.12**
21	**0.62**	**1.17**	**1.26**	**1.15**	1.09	**1.75**
21	**0.61**	**1.15**	**1.17**	**1.12**	1.62	**1.95**
28	**0.73**	**2.17**	**1.31**	**1.56**	**2.01**	**2.44**
28	**0.79**	**2.12**	**1.62**	**1.95**	**2.64**	**1.89**
28	**0.73**	**1.51**	**1.83**	**1.99**	**4.74**	**2.27**
35	**0.80**	**2.45**	**1.66**	**1.78**	**8.36**	**3.14**
35	**0.68**	**2.88**	**1.78**	**2.17**	**15.54**	**2.01**
35	**0.66**	**1.38**	**1.89**	**2.20**	**29.75**	**2.28**
42	**1.09**	**3.15**	**1.99**	**2.67**	**23.89**	**3.31**
42	**0.91**	**2.97**	**2.06**	**2.82**	**34.57**	**2.36**
42	**0.99**	**2.87**	**2.50**	**2.53**	**34.17**	**2.91**
49	**0.77**	**3.76**	**2.24**	**5.14**	23.32	**2.95**
49	**0.86**	**3.32**	**2.35**	**2.99**	33.53	**2.01**
49	**1.05**	**3.52**	**3.03**	**2.98**	36.41	**2.80**
56	**1.28**	**6.27**	**4.08**	**6.20**	24.68	**3.71**
56	**0.93**	**4.59**	**4.42**	**3.98**	36.02	**2.57**
56	**1.03**	**3.78**	**4.44**	**4.40**	32.85	**3.08**

Table 2.8/S6. Parameters of linear regressions used to determine rates of microbial CO_2 fixation as presented in Figure 2.3. Regressions were applied to data presented in bold in Tables 2.6/S4 and 2.7/S5 using the LINEST function of Microsoft Excel. The slope of each linear regression is reported as the maximum rate of microbial CO_2 fixation, with error bar lengths corresponding to the standard deviation of that slope. Abbreviations: HK, heat-killed control; Hem., hematite; std dev, standard deviation.

Kötlujökull	HK	CO_2	SO_4^{2-}	Fe(III) (Hem.)	NO_3^-	O_2
slope, m	0.07	0.44	0.44	0.37	2.39	0.52
std dev of slope	0.02	0.05	0.03	0.03	0.36	0.03
intercept, b	0.97	0.42	-0.55	0.49	-24.69	0.79
std dev of intercept	0.58	1.36	0.91	0.93	7.92	0.65
$R^2=SS_R/SS_T$	0.37	0.83	0.92	0.88	0.86	0.96
$s_{y,x}$, std dev of y	1.60	2.52	1.68	1.72	6.24	1.61
Fisher F statistic, $SS_R(n-2)/SS_E$	14.75	79.86	172.26	118.78	43.29	405.38
degrees of freedom, n-2	25	16	16	16	7	19
regression SS (SS_R); explained variation	37.67	508.56	488.77	352.65	1683.49	1056.67
errors SS (SS_E); unexplained variation	63.87	101.90	45.40	47.50	272.24	49.53

Robertson	HK	CO_2	SO_4^{2-}	Fe(III) (Hem.)	NO_3^-	O_2
slope, m	0.01	0.08	0.06	0.08	1.98	0.04
std dev of slope	0.00	0.01	0.00	0.01	0.39	0.00
intercept, b	0.50	-0.06	0.08	-0.15	-52.07	0.86
std dev of intercept	0.04	0.20	0.17	0.23	13.90	0.15
$R^2=SS_R/SS_T$	0.72	0.87	0.85	0.83	0.79	0.77
$s_{y,x}$, std dev of y	0.11	0.55	0.46	0.63	6.72	0.43
Fisher F statistic, $SS_R(n-2)/SS_E$	65.66	161.29	138.12	124.09	25.58	84.88
degrees of freedom, n-2	25	25	25	25	7	25
regression SS (SS_R); explained variation	0.76	49.66	29.32	50.03	1154.70	15.51
errors SS (SS_E); unexplained variation	0.29	7.70	5.31	10.08	316.03	4.57

Table 2.9/S7. Selected parameters of draft genome bins recovered from metagenomes of most probable number assay microcosms as calculated by the 'profile' function of CheckM v.1.0.5.

Glacier	Supplied Oxidant	% Binned Populations	Taxon	RpoB Identity	RpoB Coverage	Estimated Genome Completeness	Estimated Contamination
Kötlujökull	CO_2	92.9	*Glaciimonas* sp. PCH181	91.90%	99.0%	98.95%	0.75%
		3.9	*Cellulomonas* sp. WB94	99.20%	99.0%	95.95%	0.00%
		3.3	*Phycicoccus* sp. Soil748	93.50%	99.0%	98.18%	1.15%
	SO_4^{2-}	88.5	*Glaciimonas* sp. PCH181	92.00%	99.0%	98.56%	0.82%
		3.5	*Phycicoccus* sp. Soil748	93.80%	99.0%	98.18%	1.64%
		4.3	*Cellulomonas* sp. WB94	99.20%	99.0%	80.54%	0.58%
	Hem.*	97.3	*Rhodoferax ferrireducens*	93.70%	99.0%	99.00%	1.40%
		2.7	*Polaromonas* sp. CF318	95.60%	99.0%	99.61%	0.09%
	NO_3^-	100	*Rhodoferax ferrireducens*	93.70%	99.0%	99.59%	0.93%
Robertson	NO_3^-	96.7	*Polaromonas* sp. A23	96.90%	99.0%	99.12%	0.03%
		3.3	*Polaromonas glacialis*	98.10%	99.0%	96.80%	0.93%

Supplementary Figures

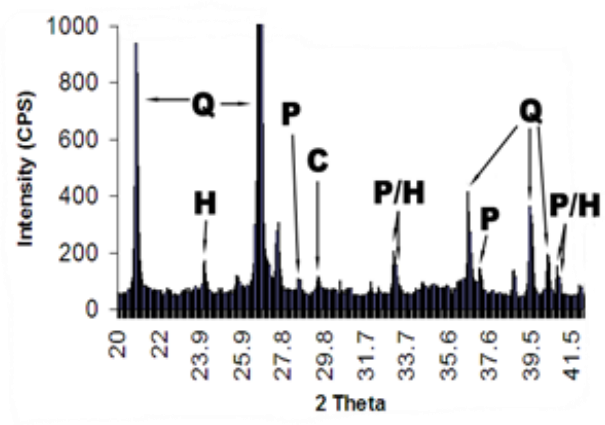

Figure 2.7/S1. XRD analysis of a Robertson Glacier (RG) rock hand sample. The sample was powdered and analyzed via X-ray Diffractometer in the Imaging and Chemical Analysis Laboratory at MSU. Resulting reflection peak patterns indicated the presence of quartz (Q), calcite (C), pyrite (P) and hematite (H).

Supplementary References

44. Mitchell, A.C., et al., *Influence of bedrock mineral composition on microbial diversity in a subglacial environment.* Geology, 2013. **41**(8): p. 855-858.

138. Martin, M., *Cutadapt removes adapter sequences from high-throughput sequencing reads.* EMBnet.journal, 2011. **17**(1): p. 10-12.

139. Mikheenko, A., et al., *Versatile genome assembly evaluation with QUAST-LG.* Bioinformatics, 2018. **34**(13): p. i142-i150.

140. Langmead, B. and S.L. Salzberg, *Fast gapped-read alignment with Bowtie 2.* Nature Methods, 2012. **9**(4): p. 357-359.

141. Kang, D.D., et al., *MetaBAT, an efficient tool for accurately reconstructing single genomes from complex microbial communities.* PeerJ, 2015. **3**: p. e1165.

142. Parks, D.H., et al., *CheckM: assessing the quality of microbial genomes recovered from isolates, single cells, and metagenomes.* Genome Research, 2015. **25**(7): p. 1043-1055.

CHAPTER THREE

INFLUENCE OF FERRIC IRON ON COMMUNITY COMPOSITION IN A BASALTIC GLACIAL CATCHMENT

Contributions of Authors and Co-Authors

Manuscript in Chapter 3

Author: Eric C. Dunham

Contributions: Designed research, performed fieldwork and laboratory research, analyzed data, and co-wrote the manuscript.

Co-Author: K. Rebecca Mitchell

Contributions: Performed fieldwork and laboratory mineralogical research.

Co-Author: Mark L. Skidmore

Contributions: Performed fieldwork and contributed equipment for field- and laboratory-based work.

Author: Eric S. Boyd

Contributions: Designed research, performed fieldwork, analyzed data, and co-wrote the manuscript.

Manuscript Information

Eric C. Dunham, K. Rebecca Mitchell, Mark L. Skidmore, and Eric S. Boyd

Status of Manuscript:
_X_ Prepared for submission to a peer-reviewed journal
____ Officially submitted to a peer-reviewed journal
____ Accepted by a peer-reviewed journal
____ Published in a peer-reviewed journal

Geology, Geological Society of America

Abstract

Microorganisms and their activities accelerate mineral weathering and solute release from glacial catchments. However, little is known of the influence of bedrock mineralogy on microbial communities in glacial environments, in particular those with igneous bedrock. Here, molecular approaches were used to assess the abundance and composition of microbial communities that colonized defined minerals incubated for 12 months in two meltwater streams (termed N and S) emanating from Kaldalónsjökull (Kal), a basalt-hosted glacier in Iceland. The elemental composition of bedrock and proglacial sediment from both outlets was similar. The geochemistry of both meltwaters was also similar, with the exception that the concentration of dissolved (0.22 μm filtered) ferric iron was 6.5 times higher in Kal S than Kal N. Genomic DNA and PCR-amplifiable 16S rRNA genes were not detected in sediment and minerals incubated in Kal N but were detected in Kal S. The amount of recoverable DNA was highest for hematite incubated in Kal S. The composition of 16S rRNA genes recovered from Kal S sediments was also most similar to those recovered from hematite and magnetite incubated in the meltwater stream. This was driven largely by similarities in the relative abundance of phylotypes related to putative iron reducers within the genera *Rhodoferax* and *Methylophilus*. These results suggest that ferric iron exerts a key control on the composition of microbial communities in basalt-hosted glacial habitats. The lack of a microbial community detectable via molecular methods in Kal N meltwaters and sediments has implications for strategies for life detection in basalt-hosted glacial environments on other planetary bodies, such as Mars.

Introduction

Glaciers and ice sheets cover approximately 10% of Earth's land surface [143] and provide unique habitats that support active microbial communities [10, 18, 47, 144]. In subglacial environments or in proglacial sediments shielded from sunlight, microbial communities are largely supported by chemical energy released through microbially mediated redox reactions involving minerals or mineral-sourced (e.g., hydrogen (H_2)) nutrients [15, 44, 145]. As such, microorganisms are catalysts of mineral weathering and solute flux in glacial habitats [19, 20, 41, 48, 75] and influence the cycling of chemicals between the lithosphere, biosphere, hydrosphere, and atmosphere [146].

Pyrite (FeS_2) is a common mineral in glacial catchments underlain by carbonate bedrock [17, 39] and its oxidation is a key source of energy supporting microbial communities in these habitats [15, 19, 20, 48]. Incubation of FeS_2 and other iron-, carbonate-, and silicate-bearing minerals (calcite, quartz, hematite, magnetite, olivine) for seven months in a proglacial meltwater stream draining a carbonate- and shale-hosted glacier showed that the community that colonized FeS_2 was most similar to that associated with proglacial sediments [44]. Further, the amount of DNA (proxy for biomass) that accumulated on FeS_2 following incubation was higher than for silicate minerals or calcite but was lower than hematite and ferrihydrite. This suggests that FeS_2, and its possible oxidation products ferrihydrite and/or hematite, are key controls on the assembly of proglacial communities in carbonate- or shale-hosted glacial systems.

Far less is known of the influence of minerals on sub- and proglacial communities in glacial catchments with igneous bedrock such as granites or basalts. Basalts can be enriched in iron minerals such as pyroxene, olivine, magnetite, and hematite that could be used as electron

donors or acceptors to support microbial metabolism [147]. Indeed, a study of a basalt-hosted glacial system in Iceland revealed the presence of a chemolithoautotrophic H_2-oxidizing and iron-reducing organism affiliated with the genus *Rhodoferax* in enrichment cultures containing proglacial sediments that had been amended with ferrihydrite and hematite [145]. This same study showed that rates of H_2 oxidation and CO_2 fixation in microcosms containing basaltic sediments were stimulated by the addition of ferrihydrite and hematite. In addition to basaltic bedrock, iron-reducing organisms have been identified in glacial sediments from catchments underlain by granitic bedrock [71]. While these data point to ferric iron as a key nutrient supporting microbial populations that inhabit the subglacial and proglacial environments in catchments underlain by igneous bedrock, the extent to which its mineralogy shapes the assembly of endogenous communities in these environment types is not known.

Here, we present cell counts and 16S rRNA gene data from proglacial sediments from two meltwater streams draining Kaldalónsjökull, a glacier in Iceland (**SI Appendix Fig. 3.3/S1**). To characterize the influence of mineralogy on the composition of microbial communities in the proglacial sediments, these data were compared to data collected from defined minerals (hematite, magnetite, pyrite, olivine, and quartz) retained in coupon samplers (**SI Appendix Fig. 3.4/S2**) incubated in the meltwater streams near the outlet of the glacier for 12 months. We suggest that the availability of Fe(III) not only exerts a key control on the assembly of microbial communities in basalt-hosted glacial environments, it may also influence the habitability of these environments. These results provide a potential framework for assessing the habitability of glacial environments on Earth and on other planets where basalts are prevalent, such as Mars.

Materials and Methods

Field Site Description

Kaldalónsjökull is a surge-type glacier draining ice from the southwest flank of Drangajökull, the most northerly icecap in Iceland (**SI Appendix Fig. 3.3/S1**) [148]. Its underlying bedrock consists of Neogene flood basalts interbedded with thin sedimentary layers [148]. At the time of sampling on 15 October 2016, two outlet streams existed at Kaldalónsjökull, which were provisionally called Kaldalónsjökull North (Kal N) and Kaldalónsjökull South (Kal S) (**SI Appendix Figs. 3.5/S3, 3.6/S4**). Kal N (N 66° 07.092', W 22° 17.329') emerges from beneath the glacier at an altitude of 64 m above sea level, while Kal S (N 66° 07.097', W 22° 17.183') emerges at 74 m. Qualitatively, the majority (by volume) of meltwater from Kaldalónsjökull flowed from Kal N.

Sediment Sample Collection and Field-Based Analysis

The sampling methods employed were identical to those previously described [145]. Briefly, saturated sediments were aseptically collected from the banks of both streams after removing the surface layer (1 cm), then frozen on site with dry ice and kept at -20°C during transport and laboratory storage. Geochemical parameters measured in the field included electrical conductivity (EC), pH, dissolved oxygen, and alkalinity. Meltwaters were filtered (0.22 µm) and subjected to colorimetric determination of total sulfide via the methylene blue assay [90] and ferrous and total iron via the ferrozine assay [97]; the concentration of ferric iron was calculated as the difference between ferrous and total iron. Dissolved gasses in meltwaters were determined via bubble stripping and gas chromatography [91, 92]. Meltwater samples for total

organic carbon (TOC) and total dissolved nitrogen (TDN) determinations were collected and analyzed via Shimadzu TOC-V Series TOC analyzer as previously described [149].

Bedrock and Proglacial Sediment X-ray Fluorescence (XRF) and X-ray Diffraction (XRD) Analyses

Bedrock samples 2-3 kg in mass were removed from outcrops near the glacier outlets via hammer. Sediments were collected and dried. Both sets of samples were milled in a tungsten carbide grinding mill. XRF analysis was carried out at Washington State University, as previously described [150]. The major element oxide composition of each sample was determined as weight percent oxide, with total iron determined as FeO, and normalized to 100% without measuring volatile content. XRD analysis of bedrock and sediments was carried out at the Imaging and Chemical Analysis Laboratory (ICAL) at Montana State University using a Scintag X1 Diffractometer with Cu Kα radiation. Mineral phases were identified using Jade 9.0 software.

Recovery and Enumeration of Microbial Cells from Proglacial Sediments

Subsamples of sediments stored at -20°C were thawed at 4°C and subjected to previously described cell separation techniques [151]. Briefly, triplicate aliquots of ~1 g Kal N and Kal S sediments were washed in a solution comprising 300 µL 2.5% (m/v) NaCl, 100 µL cell separation detergent (100 mM EDTA, 100 mM sodium pyrophosphate, 1% (v/v) Tween 80), and 100 µL methanol while shaking at 500 rpm for one hour. Sediment slurries were then carefully layered onto a high-density cushion comprising three layers of Nycodenz (50%, 65%, and 80% m/v). All reagents were filtered to 0.2 µm before use. Samples were centrifuged at 4,500x *g* for one hour, and supernatants, including all Nycodenz layers, were recovered and filtered through

0.2 µm pore size polycarbonate filters. Filters were washed with 2 mL TE buffer and then overlain with 1 mL SYBR Gold solution (4x concentration in TE buffer) and stained for one minute. Cells were enumerated via epifluorescence microscopy using an Evos FL microscope (Life Technologies). Cell counts associated with proglacial sediments were normalized by subtracting out the mean count associated with triplicate reagent blanks.

Mineral Coupon Preparation, Deployment, and Recovery

Mineral samples containing potential microbial electron donors and/or acceptors [pyrite, (Fe(II), S^{-}), hematite (Fe(III)), magnetite (Fe(II), Fe(III)), and olivine (Fe(II)) (90% forsterite + 10% fayalite; $Fo_{90}Fa_{10} = Mg_{1.8}Fe_{0.2}SiO_4$; Fe^{2+} = 75,000 ± 1425 ppm)] or providing only a physical substrate without apparent metabolic potential [quartz (SiO_2)] were crushed and sieved to ~2 mm diameter. Coupon samplers (capped 25.4 x 1.27 cm stainless steel mesh cylinders) were loaded with ~5 g of each sample substrate separated by glass wool to retain and compartmentalize different minerals during incubation (**SI Appendix Fig. 3.4/S2**) [152]. Mineral-containing coupon samplers were autoclave-sterilized (dry cycle) before transport to the field, where they were deployed at Kal N ~100 m from the glacier terminus and Kal S ~3 m from the terminus. Coupons were attached via zip-tie to galvanized steel corner bead posts that were hammered into outlet stream sediments such that coupons were fully submerged in meltwater. Posts were further secured by tethering to nearby boulders with nylon paracord. After incubation for 12 months, coupons were rinsed in meltwater to remove glacial sediments and were then frozen on dry ice for transport back to the laboratory, where they were stored at -80°C.

Mineral-Associated DNA Extraction, 16S rRNA Gene Amplification, and Sequencing

Coupons were thawed at 4°C overnight and minerals were removed from the coupon and placed in sterile petri dishes containing molecular grade water to further remove residual glacial flour associated with individual mineral grains (**SI Appendix Fig. 3.5/S4**). Cleaned minerals were collected and triplicate subsamples of 500 mg of each incubated mineral and of native Kal N and Kal S sediments were subjected to DNA extraction using the FastDNA Spin Kit for Soil (MP Biomedicals, Santa Ana, CA). Triplicate extracts were quantified via the Qubit dsDNA HS Assay kit and fluorometer (Molecular Probes, Eugene, OR), then equal volumes were pooled and the pooled volume (120 µL) was vacuum concentrated to 20 µL.

PCR amplification of 16S rRNA genes was performed in triplicate for each pooled DNA extract using universal primers 515F Modified (5'- GTG**Y**CAGCMGCCGCGGTAA-3') and 806R Modified (5'- GGACTAC**N**VGGGTWTCTAAT') and previously described methods [153]. Amplification was verified via gel electrophoresis and triplicate PCR products for each extract were pooled. Sequencing adapters were added using 5 µL pooled product as template with 8 cycles of PCR and an annealing temperature of 50°C. Amplicons were subjected to paired-end sequencing (2 × 300 bp) on the MiSeq platform at the Genomics Core Facility at the University of Wisconsin. Post sequence processing was performed with Mothur (ver. 1.43.0) [154] using a previously described pipeline [155]. Briefly, forward and reverse reads were combined into contigs that were then trimmed to 350 bp. Unique contigs were aligned to v132 of the SILVA database [156]. After pre-clustering and chimeric sequence removal, operational taxonomic units (OTUs) were assigned at a sequence similarity of 97%. Sample libraries were randomly subsampled to retrieve 69,463 sequences each (the size of the smallest sample set) and

sequences specific for each OTU were classified using the Bayesian classifier of Mothur [157] and the RDP database (training set 18), with manual verification using BLASTn. Raw reads, quality scores, and mapping files for 16S rRNA gene libraries have been deposited in the NCBI Sequence Read Archive under BioProject accession number PRJNA732716.

Community Dissimilarity Calculations

Bray-Curtis dissimilarity indices for each pair of specified mineral substrate- or sediment-associated microbial communities were calculated using Mothur's dist.shared command. The tree.shared command was then used to construct a dendrogram of community composition differences using the unweighted pair group method with arithmetic mean (UPGMA), classical clustering, and Bray-Curtis dissimilarity indices.

Results and Discussion

Availability of Nutrients at Kaldalónsjökull

Bedrock from the Kal N and Kal S outlets contained abundant iron as determined by XRF (**Table 3.1**), with visually distinguishable samples designated A and B based on different degrees of weathering. The B bedrock sample contained 16% more iron oxide as a percentage of dry weight than A bedrock sample. The proglacial outcrops visible near the Kal N meltwater outlet comprised predominantly A type bedrock, while those near the Kal S outlet were predominantly of B type bedrock, but the relative influence of each type on the meltwater chemistry of the two outlets could not be determined conclusively because their distribution beneath the glacier is unknown. XRD analysis indicates differences in the mineralogical composition of the bedrock samples, with the A type comprising labradorite (58.6% by weight)

and augite (41.4%) and the B type comprising augite (33.0%), clinochlore (30.9%), mordenite (17.2%), anorthite (14.4%), and heulandite (3.8%) (**SI Appendix Figs. 3.7/S5, 3.8/S6**). Proglacial sediment samples from Kal N and Kal S had similar iron content (**Table 3.1**) and XRD analysis revealed labradorite (60.7% by weight), augite (24.4%), and diopside (14.8%) in Kal N sediments and labradorite (63.3%) and augite (36.7%) in Kal S (**SI Appendix Figs. 3.9/S7, 3.10/S8**).

At the time of coupon deployment (15 Oct 2016), meltwaters from both Kal N and Kal S contained soluble (<0.22 μm) Fe(II) and Fe(III), with Fe(III) being more abundant than Fe(II) in both meltwaters (**Table 3.1**). At the time of coupon recovery (2 Oct 2017), soluble Fe(II) was not detected in meltwaters from either Kal N or Kal S, while soluble Fe(III) was detected at both sites. The concentration of soluble Fe(III) was six times higher at Kal S than at Kal N on both sampling dates. Sulfide was detected in both meltwater streams at the time of coupon recovery but was not detected at the time of coupon deployment. Dissolved H_2, a possible reductant for microbial metabolism, was present at both sampling times, although it was 41-390 times more abundant at the time coupons were deployed than when they were recovered. The variation in available electron donors and acceptors point to annual variability in the geological/geochemical processes that source the meltwaters with these solutes. Importantly, Fe(III) has been shown to support microbial respiration in several subglacial systems [71], including a basaltic system in Iceland where it was shown to be coupled to H_2 oxidation [145]. Given these observations, we hypothesized that Fe(III) may represent a key control on sediment-associated microbial community composition at Kaldalónsjökull by supporting Fe(III)-reducing microbial populations.

Sediment- and Mineral-Associated Biomass

DNA was recovered from Kal S proglacial sediments at 4.17 ± 2.97 (mean ± standard deviation) ng per gram dry weight sediment (gdws) and from all minerals incubated in that meltwater stream, with the exception of olivine (**Fig. 3.1**). While recoverable DNA from olivine incubated in Kal S was below the limit of detection of our assay (0.005 ng μL^{-1} extract), 16S rRNA genes were able to be PCR amplified from this extract. Hematite incubated in Kal S yielded the highest amount of quantifiable DNA, followed by magnetite and quartz (equal amounts), and then pyrite. The higher DNA yields recovered from hematite, and to a lesser extent magnetite, support the hypothesis that Fe(III) is a key control on the assembly of microbial communities.

In contrast to Kal S, attempts to extract genomic DNA from subglacial sediments collected from Kal N and from minerals incubated in the Kal N outlet failed to yield quantifiable amounts. This remained true regardless of the chemical and/or physical lysis techniques that were used, including a technique specifically designed for basaltic sediments [112]. Standard additions of *Escherichia coli* K12 cells to sediment prior to extraction resulted in quantitative recovery of DNA that was PCR-amplifiable (data not shown), indicating that the sediments themselves were not influencing DNA recovery or downstream PCR. Furthermore, application of PCR to DNA extracts from Kal N failed to produce amplicons from any of these extracts, even after a multiple displacement amplification reaction (data not shown). In an effort to discern whether substantial differences in microbial abundance exist between Kal N and Kal S sediments, subsamples were subjected to cell separation and enumeration using techniques optimized for life detection in sedimentary habitats [151]. Cell counts revealed extremely low

biomass in proglacial sediments collected from both outlets, with $5.22 \times 10^4 \pm 4.43 \times 10^4$ (mean ± standard deviation) cells $gdws^{-1}$ recovered from Kal N sediments and $3.69 \times 10^5 \pm 1.2 \times 10^5$ cells $gdws^{-1}$ at Kal S. The one order of magnitude lesser cellular abundance in Kal N sediments may account at least partially for the difficulty in recovering quantifiable DNA from that environment.

The extremely low biomass and lack of extractable DNA from Kal N proglacial sediments and incubated minerals is reminiscent of proglacial sediments from Kötlujökull, where PCR-amplifiable DNA could not be generated but where cultivation-based enrichment of Fe(III) reducers was possible. Our limited geochemical analyses suggest the most salient difference between Kal N and Kal S is the availability of soluble Fe(III). Notably, the soluble Fe(III) concentrations of both Kal N and Kötlujökull were lower (1.11 and 1.56 mg L^{-1}, respectively) than the lowest concentration detected at Kal S (1.91 mg L^{-1}), suggesting a threshold soluble Fe(III) concentration of 1.6-1.9 mg L^{-1} may limit application of molecular approaches to detect life in basalt-hosted glacial systems.

Taxonomic Affiliation of Kal S Sediment Microbial Communities

To further investigate the extent to which Fe(III) influences the assembly of microbial communities in Kaldalónsjökull meltwaters, we sequenced 16S rRNA gene amplicons from DNA extracted from the sediments and the mineral samples incubated in Kal S. Hierarchical clustering of a matrix describing the dissimilatory in the composition of 16S rRNA gene OTUs among communities showed that those colonizing hematite and magnetite were more similar in composition to the Kal S sediments when compared to those that colonized olivine, pyrite, and

quartz (**Fig. 3.2**). This further points to the role of Fe(III) as a control on the composition of the Kal S sediment community.

To evaluate whether the observed similarity in composition of the Kal S proglacial sediment community to those that colonized hematite and magnetite is due to the potential use of Fe(III) as an electron acceptor by populations comprising those communities, 16S rRNA gene OTUs were compared to characterized organisms. Taxonomically, the communities associated with native Kal S sediments and defined minerals were all dominated (>46% of recovered reads) by OTUs closely affiliated with members of the Burkholderiales (order Proteobacteria) (**Fig. 3.2**), which is in agreement with the results of an earlier survey of 16S rRNA gene sequences derived from Kaldalónsjökull [158]. However, the most abundant Burkholderiales-affiliated OTUs differed among Kal S sediments and incubated minerals (**Table 3.2**). The most abundant OTU (14% of total reads) in the Kal S sediment community was most closely related to *Rhodoferax*. *Rhodoferax* is a physiologically diverse genus, with many isolated strains having the ability to reduce Fe(III) [134]. Notably, of the incubated mineral samples, only hematite and magnetite (i.e., those minerals with the highest Fe(III) content) yielded communities enriched (~19% relative abundance) in *Rhodoferax* sequences relative to the Kal S sediments and all sequences recovered belonged to the same OTU.

The *Rhodoferax*-associated OTU detected in Kal S sediments and on hematite and magnetite incubated in Kal S meltwaters was previously detected in proglacial sediments from Kötlujökull, another basalt-based glacier Iceland [145]. In that study, Kötlujökull proglacial sediments amended with hematite and H_2 produced a culture dominated (97% of recovered reads) by *Rhodoferax*. Further, the 16S rRNA gene encoded by the *Rhodoferax*-associated

metagenome assembled genome (MAG) recovered from Kötlujökull sediment enrichments differs from that amplified from Kal S sediments by only 0.8%, and thereby represents the same OTU (**SI Appendix Fig. 3.11/S9**). The prevalence of *Rhodoferax*-affiliated 16S rRNA genes in the proglacial sediment, hematite, and magnetite communities incubated at Kal S, when combined with the near identical 16S rRNA gene from a demonstrated H_2-oxidizing and Fe(III)-reducing *Rhodoferax* strain from a nearby basalt-hosted glacier in Iceland [145], provides additional evidence indicating that Fe(III) is a key control on the composition of microbial communities in basalt-hosted glacial environments.

In addition to *Rhodoferax*, abundant OTUs in communities that colonized hematite and magnetite were related to the aerobic methylotrophs *Methylophilus* (31% of hematite community, 35% of magnetite community) and *Methylibium* (15% of hematite community, 22% of magnetite community). Bacterial methanotrophs have been identified in numerous environments that fluctuate between oxic to hypoxic conditions [159], suggesting the potential for alternative electron acceptors to support their energy metabolisms. Indeed, a recent study demonstrated that a *Methylophilus* strain could reduce iron oxides [160]. This points to the possibility that *Methylophilus*, and possibly *Methylibium*, catalyze Fe(III) reduction in Kal S, potentially explaining the enrichment of these OTUs in communities that colonized the iron oxides hematite and magnetite.

The communities that colonized quartz and olivine grains were similar to each other but distinct from the other minerals and were dominated (63-82% of recovered reads, respectively) by an OTU related to *Ralstonia*. The dominance of this OTU on quartz and its low relative abundance in Kal S sediments (3% of recovered reads) provides further support for the

importance of redox active minerals (e.g., iron oxides) in controlling microbial community composition in proglacial sediments at Kal S. The FeS_2-associated community's most abundant OTU (38% of reads) was closely related to *Actimicrobium antarcticum*, an aerobe isolated from Antarctic seawater [161]. It is unclear if this taxon can oxidize FeS_2 or its oxidation products (e.g., thiosulfate). That this OTU only comprised 5% of reads in Kal S sediments is consistent with the lack of detectable FeS_2 in those sediments (**SI Appendix Fig. 3.8/S6**).

Conclusions

The microbial community compositions of two outlets of the same basalt-based glacier are shown to differ markedly. Sediments collected from Kal S hosted an order of magnitude more microbial cells than those collected at Kal N, and sterilized minerals incubated in each outlet were colonized only in the meltwaters of Kal S. Sediments and sterilized minerals incubated in Kal N were indicated to be devoid of life using the molecular approaches described herein, but traditional microscopy-based methods detected sparse microbial cells in Kal N sediments. Kal S sediments and the Fe(III)-bearing minerals hematite and magnetite were colonized by a population closely affiliated with the known Fe(III) reducer *Rhodoferax*. A closely related strain (same 16S rRNA gene OTU) enriched from proglacial sediments from Kötlujökull, a nearby basalt-hosted glacier, was previously demonstrated to couple H_2 oxidation to Fe(III) reduction to fuel autotrophic growth [145]. The detection of the *Rhodoferax* OTU at both Kaldalónsjökull and Kötlujökull suggests it to be a ubiquitous member of sediment communities in basalt-hosted glaciers in Iceland, and perhaps other basalt-hosted glaciers globally.

The inability to detect PCR amplifiable DNA in proglacial sediments from Kötlujökull and Kal N, both of which had lower Fe(III) contents than Kal S, may point to the abundance and bioavailability of Fe(III) as a key control on the development of robust communities founded on dissimilatory Fe(III)-based metabolism. Incubation of fresh Fe(III) oxides in Kal S meltwaters likely selects for Fe(III) reducing organisms that inhabit proglacial sediments; these organisms may be supported by soluble or particulate (<0.22 μm) Fe(III) *in situ*, which may help explain why extractable DNA (proxy for biomass) was so low in Kal N and Kötlujökull. It is possible that the low natural abundances of Fe(III) reducing cells in Kal N resulted in an inability to substantially enrich for such organisms on Fe(III) oxide minerals over the 12 month incubation period. These observations have implications for the ability to detect molecular biosignatures of microbial life in glacial environments on other planets where basalts and solid phase or soluble Fe(III) compounds are prevalent, such as Mars, and may indicate that cultivation- or geochemical-based approaches are more appropriate techniques to apply to detect life in those environments.

Acknowledgements

This work was supported by a grant (NNX16AJ64G) from the National Aeronautics and Space Administration Exobiology and Evolutionary Biology program to M.L.S. and E.S.B. E.C.D. was supported by an NSF Graduate Research Fellowship.

References

10. Skidmore, M.L., J.M. Foght, and M.J. Sharp, *Microbial Life beneath a High Arctic Glacier.* Applied and Environmental Microbiology, 2000. **66**(8): p. 3214-3220.

15. Boyd, E.S., et al., *Chemolithotrophic primary production in a subglacial ecosystem.* Applied and Environmental Microbiology, 2014. **80**(19): p. 6146-53.

17. Bottrell, S.H. and M. Tranter, *Sulphide oxidation under partially anoxic conditions at the bed of the Haut Glacier d'Arolla, Switzerland.* Hydrological Processes, 2002. **16**(12): p. 2363-2368.

18. Hamilton, T.L., et al., *Molecular evidence for an active endogenous microbiome beneath glacial ice.* The ISME Journal, 2013. **7**(7): p. 1402-12.

19. Montross, S.N., et al., *A microbial driver of chemical weathering in glaciated systems.* Geology, 2013. **41**(2): p. 215-218.

20. Skidmore, M., et al., *Comparison of Microbial Community Compositions of Two Subglacial Environments Reveals a Possible Role for Microbes in Chemical Weathering Processes.* Applied and Environmental Microbiology, 2005. **71**(11): p. 6986-6997.

39. Tranter, M., et al., *Geochemical weathering at the bed of Haut Glacier d'Arolla, Switzerland—a new model.* Hydrological Processes, 2002. **16**(5): p. 959-993.

41. Wynn, P.M., et al., *Nitrate production beneath a High Arctic glacier, Svalbard.* Chemical Geology, 2007. **244**(1): p. 88-102.

44. Mitchell, A.C., et al., *Influence of bedrock mineral composition on microbial diversity in a subglacial environment.* Geology, 2013. **41**(8): p. 855-858.

47. Christner, B.C., et al., *A microbial ecosystem beneath the West Antarctic ice sheet.* Nature, 2014. **512**(7514): p. 310-313.

48. Harrold, Z.R., et al., *Aerobic and Anaerobic Thiosulfate Oxidation by a Cold-Adapted, Subglacial Chemoautotroph.* Applied and Environmental Microbiology, 2016. **82**(5): p. 1486-1495.

71. Nixon, S.L., et al., *Viable cold-tolerant iron-reducing microorganisms in geographically diverse subglacial environments.* Biogeosciences, 2017. **14**(6): p. 1445-1455.

75. Boyd, E.S., et al., *Diversity, Abundance, and Potential Activity of Nitrifying and Nitrate-Reducing Microbial Assemblages in a Subglacial Ecosystem.* Applied and Environmental Microbiology, 2011. **77**(14): p. 4778-4787.

90. Fogo, J.K. and M. Popowsky, *Spectrophotometric Determination of Hydrogen Sulfide - Methylene Blue Method.* Analytical Chemistry, 1949. **21**(6): p. 732-734.

91. Chapelle, F.H., et al., *Practical Considerations for Measuring Hydrogen Concentrations in Groundwater.* Environmental Science & Technology, 1997. **31**(10): p. 2873-2877.

92. Lindsay, M.R., et al., *Subsurface processes influence oxidant availability and chemoautotrophic hydrogen metabolism in Yellowstone hot springs.* Geobiology, 2018. **16**(6): p. 674-692.

97. Viollier, E., et al., *The ferrozine method revisited: Fe(II)/Fe(III) determination in natural waters.* Applied Geochemistry, 2000. **15**(6): p. 785-790.

112. Wang, H. and K.J. Edwards, *Bacterial and Archaeal DNA Extracted from Inoculated Experiments: Implication for the Optimization of DNA Extraction from Deep-Sea Basalts.* Geomicrobiology Journal, 2009. **26**(7): p. 463-469.

134. Finneran, K.T., C.V. Johnsen, and D.R. Lovley, *Rhodoferax ferrireducens sp. nov., a psychrotolerant, facultatively anaerobic bacterium that oxidizes acetate with the reduction of Fe(III).* International Journal of Systematic and Evolutionary Microbiology, 2003. **53**(3): p. 669-673.

143. Liu, H., et al., *Annual dynamics of global land cover and its long-term changes from 1982 to 2015.* Earth System Science Data, 2020. **12**(2): p. 1217-1243.

144. Marteinsson, V.T., et al., *Microbial communities in the subglacial waters of the Vatnajökull ice cap, Iceland.* The ISME Journal, 2013. **7**(2): p. 427-37.

145. Dunham, E.C., et al., *Lithogenic hydrogen supports microbial primary production in subglacial and proglacial environments.* Proceedings of the National Academy of Sciences of the United States of America, 2021. **118**(2).

146. Lafrenière, M.J. and M.J. Sharp, *A comparison of solute fluxes and sources from glacial and non-glacial catchments over contrasting melt seasons.* Hydrological Processes, 2005. **19**(15): p. 2991-3012.

147. Stefánsson, A., *Dissolution of primary minerals of basalt in natural waters: I. Calculation of mineral solubilities from 0°C to 350°C.* Chemical Geology, 2001. **172**(3): p. 225-250.

148. Brynjólfsson, S., A. Schomacker, and Ó. Ingólfsson, *Geomorphology and the Little Ice Age extent of the Drangajökull ice cap, NW Iceland, with focus on its three surge-type outlets.* Geomorphology, 2014. **213**: p. 292-304.

149. Vick-Majors, T.J., et al., *Biogeochemical Connectivity Between Freshwater Ecosystems beneath the West Antarctic Ice Sheet and the Sub-Ice Marine Environment.* Global Biogeochemical Cycles, 2020. **34**(3): p. e2019GB006446.

150. Johnson, D.M., P.R. Hooper, and R.M. Conrey, *XRF Analysis of Rocks and Minerals for Major and Trace Elements on a Single Low Dilution Li-tetraborate Fused Bead.* Advances in X-Ray Analysis, 1999. **2**: p. 25.

151. Morono, Y., et al., *An improved cell separation technique for marine subsurface sediments: applications for high-throughput analysis using flow cytometry and cell sorting.* Environmental Microbiology, 2013. **15**(10): p. 2841-2849.

152. Boyd, E.S., D.E. Cummings, and G.G. Geesey, *Mineralogy influences structure and diversity of bacterial communities associated with geological substrata in a pristine aquifer.* Microbial Ecology, 2007. **54**(1): p. 170-82.

153. Colman, D.R., et al., *Seasonal hydrologic and geologic forcing drive hot spring geochemistry and microbial biodiversity.* Environmental Microbiology, 2021.

154. Schloss, P.D., et al., *Introducing mothur: Open-Source, Platform-Independent, Community-Supported Software for Describing and Comparing Microbial Communities.* Applied and Environmental Microbiology, 2009. **75**(23): p. 7537-7541.

155. Kozich, J.J., et al., *Development of a Dual-Index Sequencing Strategy and Curation Pipeline for Analyzing Amplicon Sequence Data on the MiSeq Illumina Sequencing Platform.* Applied and Environmental Microbiology, 2013. **79**(17): p. 5112-5120.

156. Glöckner, F.O., et al., *25 years of serving the community with ribosomal RNA gene reference databases and tools.* Journal of Biotechnology, 2017. **261**: p. 169-176.

157. Wang, Q., et al., *Naïve Bayesian Classifier for Rapid Assignment of rRNA Sequences into the New Bacterial Taxonomy.* Applied and Environmental Microbiology, 2007. **73**(16): p. 5261-5267.

158. Kohler, T.J., et al., *Patterns in microbial assemblages exported from the meltwater of Arctic and Sub-Arctic glaciers.* Frontiers in Microbiology, 2020. **11**: p. 669.

159. Oshkin, I.Y., et al., *Methane-fed microbial microcosms show differential community dynamics and pinpoint taxa involved in communal response.* The ISME Journal, 2015. **9**(5): p. 1119-1129.

160. Yang, Y., et al., *Extracellular electron transfer of Methylophilus methylotrophs.* Process Biochemistry, 2020. **94**: p. 313-318.

161. Kim, E.H., et al., *Actimicrobium antarcticum gen. nov., sp. nov., of the Family Oxalobacteraceae, Isolated from Antarctic Coastal Seawater.* Current Microbiology, 2011. **63**(2): p. 213-217.

Tables

Table 3.1. Major element oxide composition of bedrock and sediment samples from Kaldalónsjökull North (Kal N) and Kaldalónsjökull South (Kal S) as determined by x-ray fluorescence analysis. Measured physical and geochemical parameters in meltwaters from Kal N and Kal S during deployment (15 Oct 2016) and recovery (2 Oct 2017) of coupons. Bedrock samples were collected at the time of coupon deployment. Values are expressed as weight percent oxide, with total iron determined as FeO, and normalized to 100% ignoring volatile content.

			Major element oxide composition of bedrock and sediments										
Date	Sample Type	Sample ID	SiO_2	TiO_2	Al_2O_3	FeO	MnO	MgO	CaO	Na_2O	K_2O	P_2O_5	Total
10/15/16	Bedrock	A	49.60	1.92	14.70	12.24	0.21	7.24	11.72	2.04	0.18	0.16	100.00
		B	50.37	2.09	14.64	14.15	0.29	8.10	8.62	1.23	0.33	0.18	100.00
10/15/16	Sediment	Kal N	48.38	2.03	14.23	13.58	0.22	8.13	11.35	1.82	0.18	0.10	100.00
		Kal S	49.45	2.12	13.37	13.81	0.22	7.96	10.86	1.82	0.30	0.09	100.00

			Physical and chemical characterization of meltwaters											
Date	Sample	Site	pH	EC	DO	Fe^{2+}	Fe^{3+}	HS^-	H_2	CH_4	CO_2	Alk	DOC	TDN
				µS cm^{-1}	nM	nM	nM	µM	nM	nM	µM	mg L^{-1}	mg L^{-1}	mg L^{-1}
10/15/16	Meltwater	Kal N	6.6	15.5	407.5	1.8 (2.5)	5.2 (4.3)	0.0	273.8 (3.9)	0.0 (0.0)	28.7 (44.0)	1.4	0.15 (0.03)	0.02 (0.00)
		Kal S	6.5	15.3	ND	0.9 (0.5)	34.2 (4.5)	0.0	266.3 (10.6)	0.0 (0.0)	10.5 (9.2)	1.1	0.07 (0.01)	0.02 (0.00)
10/02/17	Meltwater	Kal N	ND	ND	ND	0.0 (0.0)	19.9 (5.2)	2.6 (0.5)	0.7 (1.2)	0.0 (0.0)	11.4 (10.6)	ND	ND	ND
		Kal S	ND	ND	ND	0.0 (1.1)	125.2 (39.9)	1.6 (0.9)	6.4 (9.1)	0.0 (0.0)	2.0 (3.5)	ND	ND	ND

Standard deviations of triplicate analyses are denoted in parentheses, where available. Abbreviations: EC, electrical conductivity; DO, dissolved oxygen; Alk, carbonate alkalinity; DOC, dissolved organic carbon; TDN, total dissolved nitrogen; ND, not determined.

Table 3.2. Phylogenetic affiliation of bacterial 16S rRNA genes recovered from native sediments and minerals incubated at Kaldalónsjökull South. Only operational taxonomic units (OTUs) comprising >5% of at least one sample community are shown.

			% Reads					
Taxon	% Identity	Accession	Sediment	Hematite	Magnetite	Pyrite	Olivine	Quartz
Rhodoferax sp. GR-4	99.2%	KC759436.2	14.2%	18.9%	18.8%	3.7%	1.8%	7.3%
Ralstonia solanacearum SL3022	99.2%	CP023016.1	3.2%	5.8%	3.0%	1.6%	81.6%	62.9%
Methylophilus medardicus MMS-M-37	97.6%	CP040947.1	11.5%	31.2%	34.5%	3.0%	1.1%	2.3%
Methylibium Eza7	98.8%	JQ977655.1	8.0%	15.2%	22.1%	4.3%	0.8%	2.0%
Actimicrobium antarcticum KOPRI 25157	99.2%	NR_118029.1	5.3%	0.1%	0.5%	37.6%	0.3%	0.1%
Methylotenera mobilis	95.7%	AB698738.1	3.0%	6.3%	8.1%	0.4%	0.4%	0.6%
Pseudomonas yamanorum 5XgY1B_A	99.6%	MT605320.1	0.0%	0.0%	0.0%	15.3%	3.0%	0.2%
Alpha proteobacterium BAC11	95.7%	EU180508.1	10.2%	2.9%	1.7%	0.4%	0.3%	0.8%
Candidatus Nitrotoga arctica clone 6680	98.8%	DQ839562.1	1.2%	0.4%	0.2%	7.9%	0.1%	0.1%
Pseudomonas lurida MAIDO-R16b-4	100.0%	MW631975.1	0.0%	0.0%	0.0%	8.4%	0.2%	0.0%
Undibacterium terreum UCF-10-6	99.2%	MK443061	0.1%	1.3%	0.1%	0.4%	1.5%	6.1%

Figures

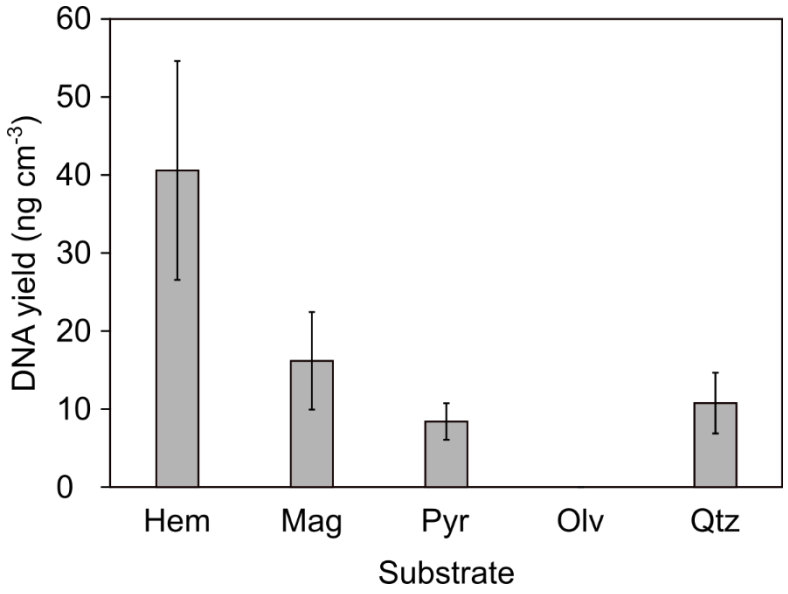

Figure 3.1. Total DNA (proxy for biomass) recovered from specified minerals retained in stainless steel coupon samplers and incubated for 12 months in the Kaldalónsjökull South meltwater stream three meters from the glacial terminus. Error bars represent the standard deviations associated with triplicate DNA extractions performed on each sediment or mineral substrate. No detectable DNA was recovered from any substrate incubated at Kaldalónsjökull North. Abbreviations: Hem, hematite; Mag, magnetite; Pyr, pyrite; Olv, olivine; Qtz, quartz.

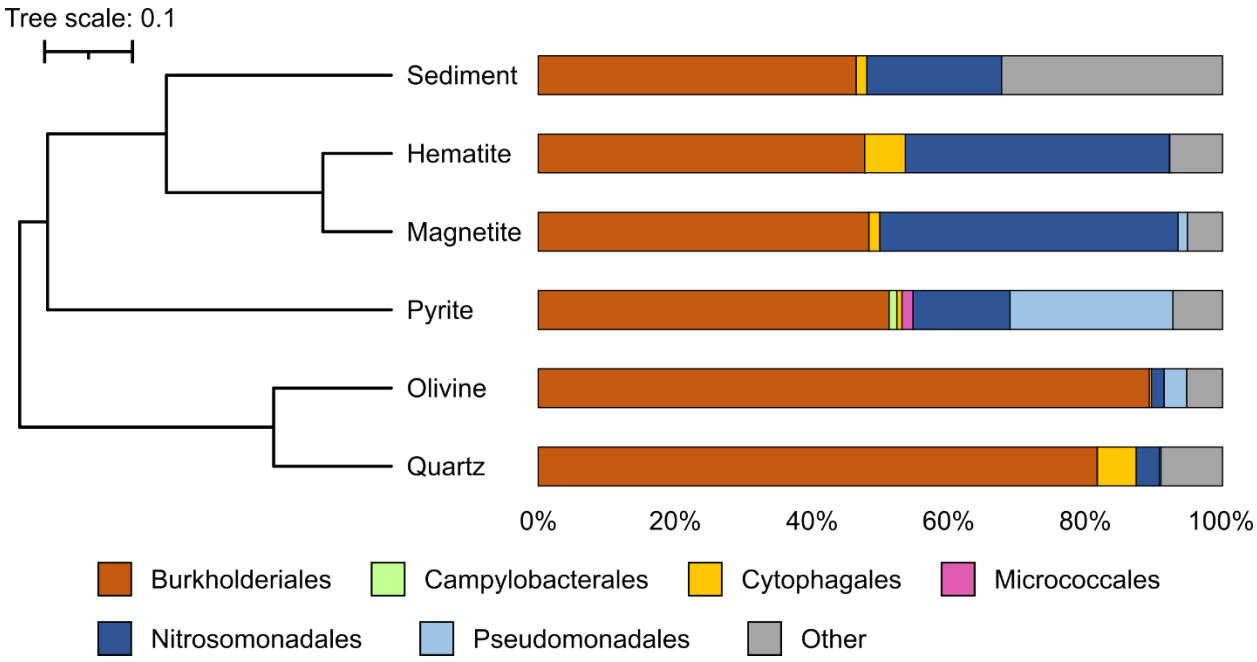

Figure 3.2. 16S rRNA gene composition of microbial communities recovered from native Kaldalónsjökull South sediments or specified minerals retained in stainless steel coupon samplers and incubated for 12 months in the meltwater stream three meters from the glacial terminus. Representative operational taxonomic units (OTUs) representing ≥0.5% of total sequences recovered from each substrate were binned at the order level. OTUs representing <0.5% of the total sequences from each assemblage were pooled and depicted as "other." A dendrogram of community composition dissimilarity was constructed using the unweighted pair group method with arithmetic mean (UPGMA) and Bray-Curtis dissimilarity indices (top left).

Supplementary Materials and Methods

Recovery of 16S rRNA Gene Sequence from a Metagenome Assembled Genome (MAG)

A *Rhodoferax*-associated MAG was generated from an enrichment culture of proglacial sediments from Kötlujökull, Iceland, amended with H_2 and hematite in a previous study [145]. To compare the *Rhodoferax*-associated 16S rRNA gene operational taxonomic unit (OTU) recovered from minerals and sediments incubated in the Kaldalónsjökull South (Kal S) meltwater stream with the MAG recovered from Kötlujökull, 16S rRNA gene sequences were extracted from the MAG using the CheckM ssu_finder script [142]. A pairwise alignment of the 253 bp 16S rRNA gene sequences recovered from the Kötlujökull MAG and that of the Kal S OTU was created using BLASTn.

Supplementary Results and Discussion

Comparison of 16S rRNA Gene Sequences Recovered from Kal S and Kötlujökull

The 16S rRNA gene sequence recovered from the Kötlujökull MAG differed from those recovered from minerals and sediments incubated at Kal S by only two nucleotides (**Fig. 3.7/S5**). The two sequences were thus 99.2% identical, with an associated pairwise e-value of $6e^{-132}$. Applying the 97.0% identity cutoff used to define OTUs in this study, these sequences therefore comprise the same OTU.

Supplementary Figures

Figure 3.3/S1. View of Kaldalónsjökull (Kal) from the southwest. The points of emergence of the Kal N and Kal S meltwater streams (*) and the sites of coupon deployment (↓) are indicated.

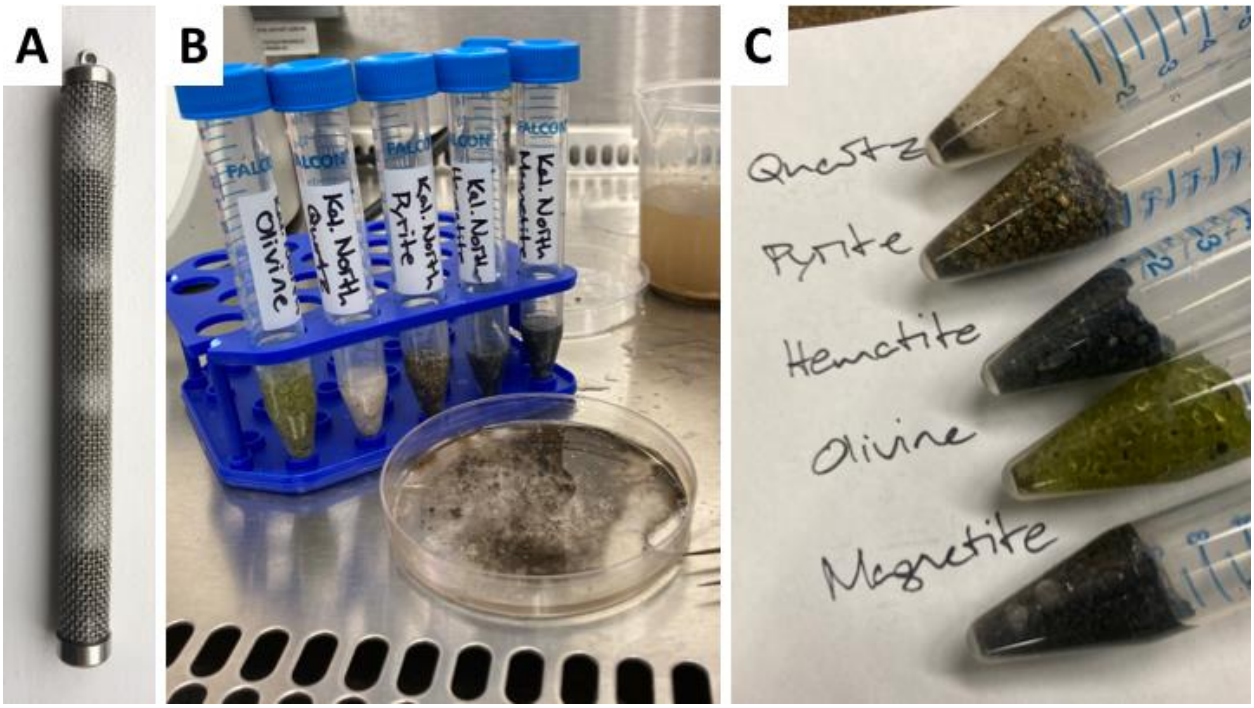

Figure 3.4/S2. Minerals deployed and recovered from coupon samplers. (A) Coupon sampler loaded with minerals prior to deployment. Note mineral grains (dark) separated by glass wool (light). (B) Washing of minerals in molecular grade H_2O and sorting after coupon recovery. (C) Washed and sorted mineral grains prior to DNA extraction.

Figure 3.5/S3. Site of coupon deployment in the Kal N meltwater stream, taken upon coupon recovery on 18 August 2018. (A) View upstream from coupon deployment site toward the glacier terminus. (B) Site of coupon deployment as viewed from stream bank. (C) Coupon anchored in place by corner bead post and nylon paracord. (D) Coupon secured to corner bead post by zip ties.

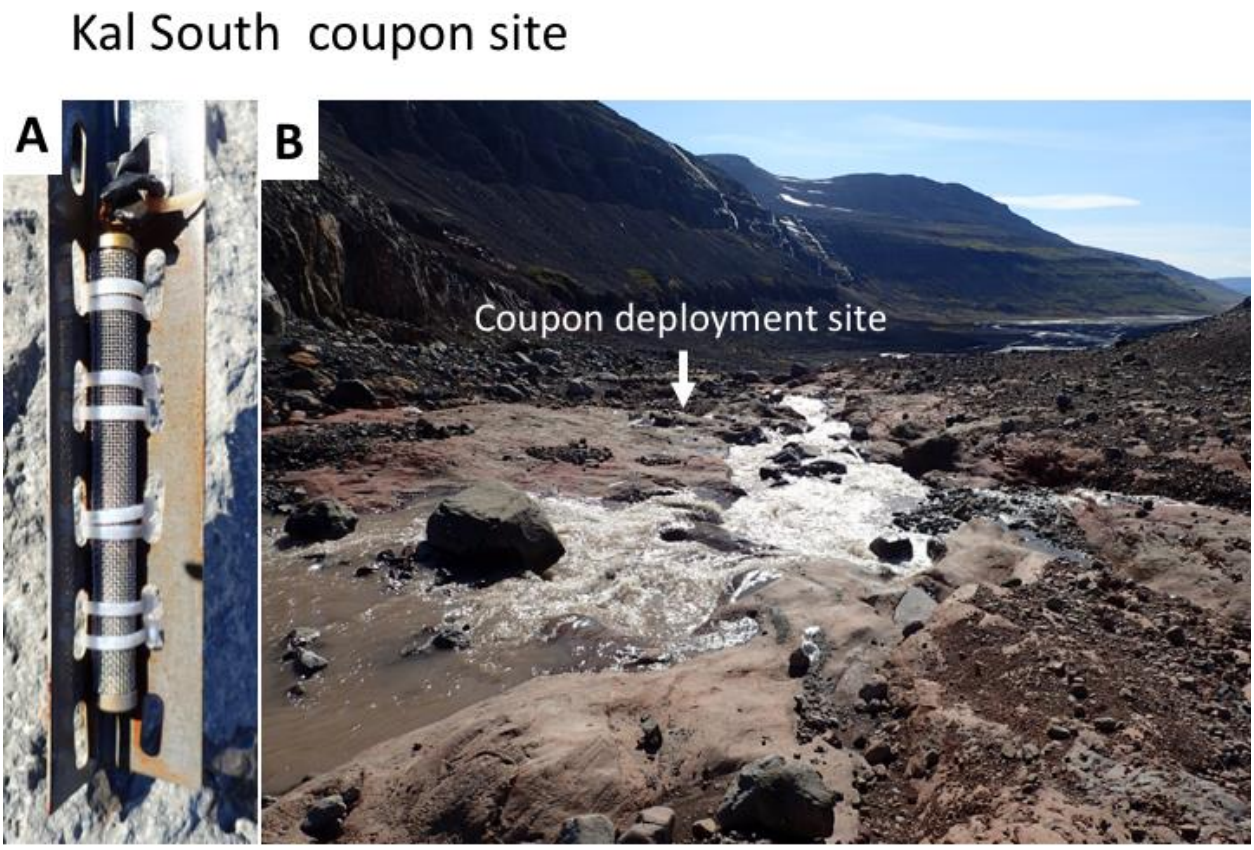

Figure 3.6/S4. Site of coupon deployment in the Kal S meltwater stream, taken upon coupon recovery on 18 August 2018. (A) Coupon secured to corner bead post by zip ties. (B) View downstream toward coupon deployment site taken from the glacier terminus.

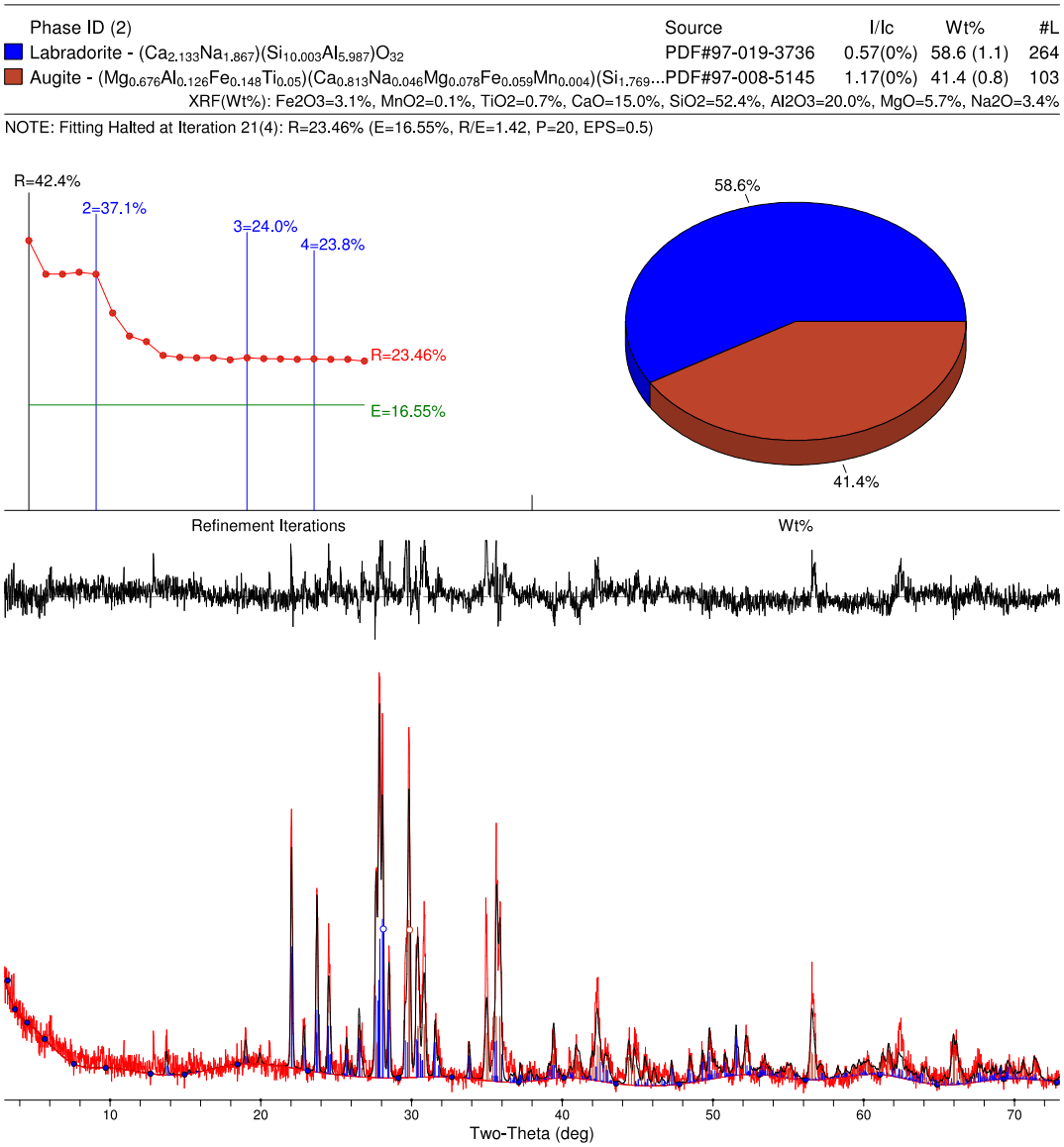

Figure 3.7/S5. Powder X-ray diffraction (XRD) analysis of the A type bedrock sample performed using Jade 9 software.

Phase ID (5)	Source	I/Ic	Wt%	#L
Augite - $(Mg_{0.81}Fe_{0.15}Al_{0.03}Ti_{0.01})(Ca_{0.76}Na_{0.02}Mg_{0.04}Fe_{0.17}Mn_{0.01})(Si_{1.92}Al_{0.08}O_6)$	PDF#97-005-6923	1.16(0%)	33.7 (1.2)	103
Clinochlore (IIb - $(Mg_{11.126}Fe_{0.874})((Si_{5.116}Al_{2.884})O_{20}(OH)_{16})$	PDF#97-016-4237	0.82(0%)	30.9 (1.9)	266
Mordenite - $Na_{5.33}(Al_{5.55}Si_{42.45}O_{96})(H_2O)_{32}$	PDF#97-009-7847	1.20(0%)	17.2 (1.2)	248
Anorthite - $(Na_{0.45}Ca_{0.55})(Al_{1.55}Si_{2.45}O_8)$	PDF#97-006-1329	0.60(0%)	14.4 (0.9)	270
Heulandite - $(Na_{0.26}K_{0.89}Ca_{3.37}Sr_{0.24}Ba_{0.034})H_{1.03}(Al_{9.48}Si_{26.61}O_{72})(H_2O)_{24.84}$	PDF#97-003-1278	0.40(0%)	3.8 (0.9)	440

XRF(Wt%): BaO=0.0%, SrO=0.0%, Fe2O3=5.8%, MnO2=0.1%, TiO2=0.1%, CaO=8.3%, K2O=0.1%, SiO2=48.4%, Al2O3=11.1%, MgO=17.6%, Na2O=1.7%

NOTE: Fitting Halted at Iteration 29(4): R=22.3% (E=15.16%, R/E=1.47, P=39, EPS=0.5)

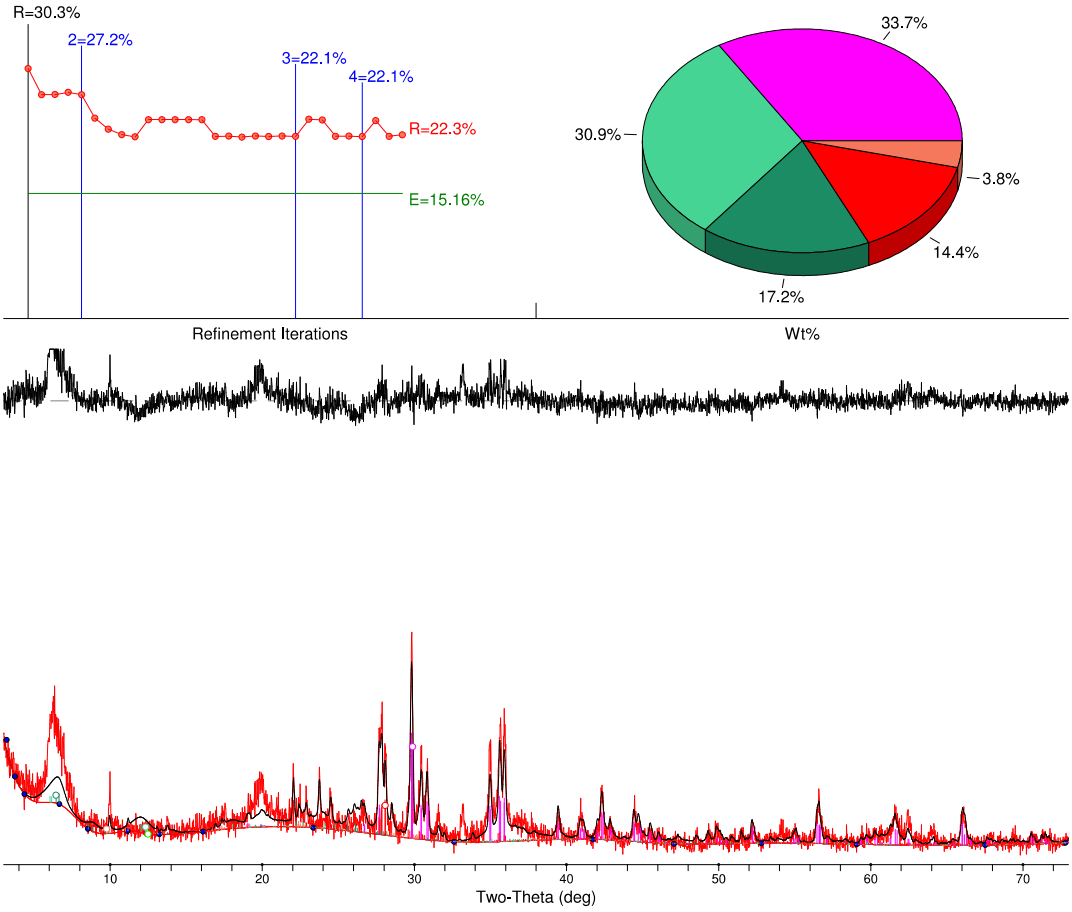

Figure 3.8/S6. Powder X-ray diffraction (XRD) analysis of the B type bedrock sample performed using Jade 9 software.

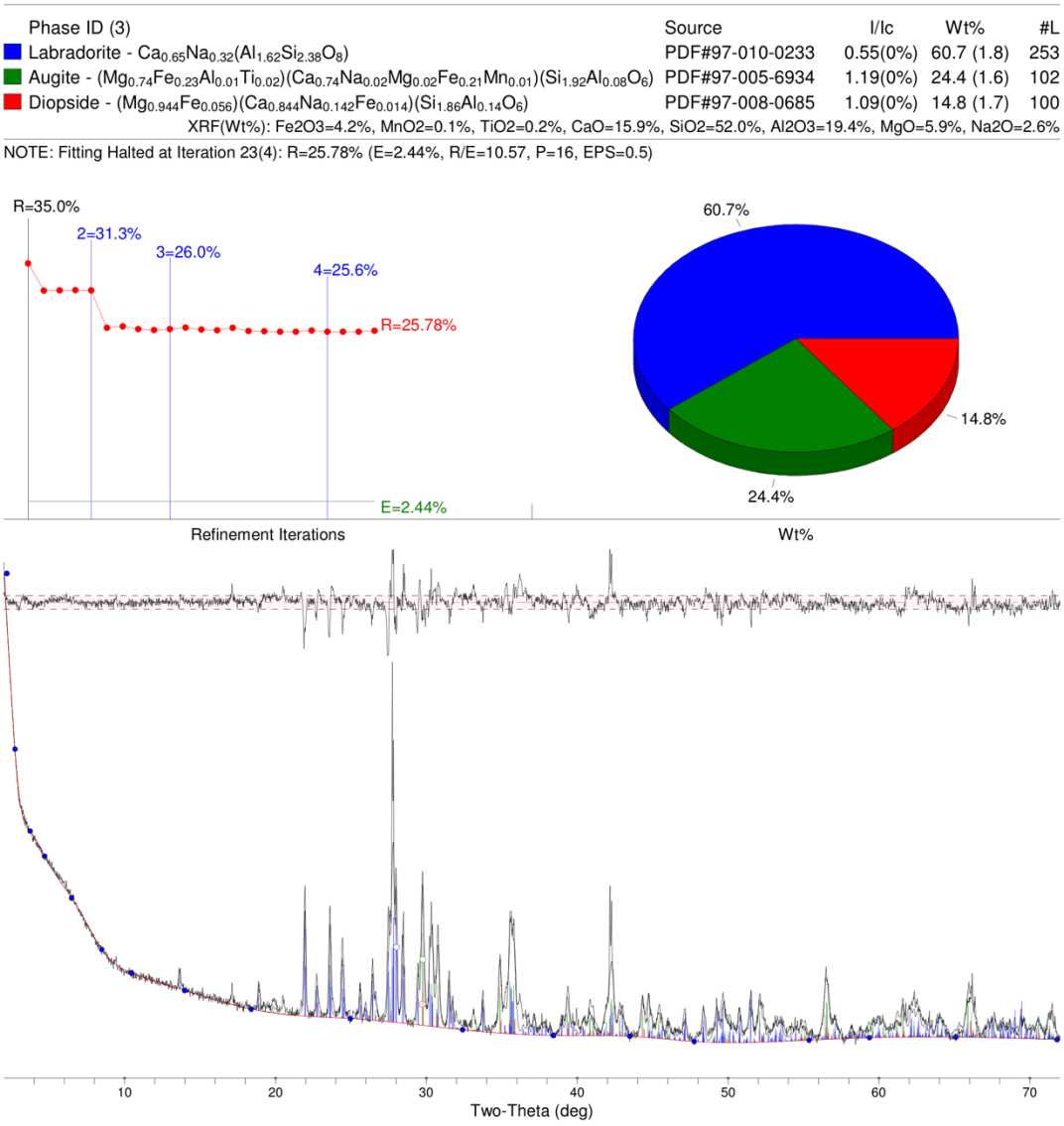

Figure 3.9/S7. Powder X-ray diffraction (XRD) analysis of Kal N proglacial sediment performed using Jade 9 software.

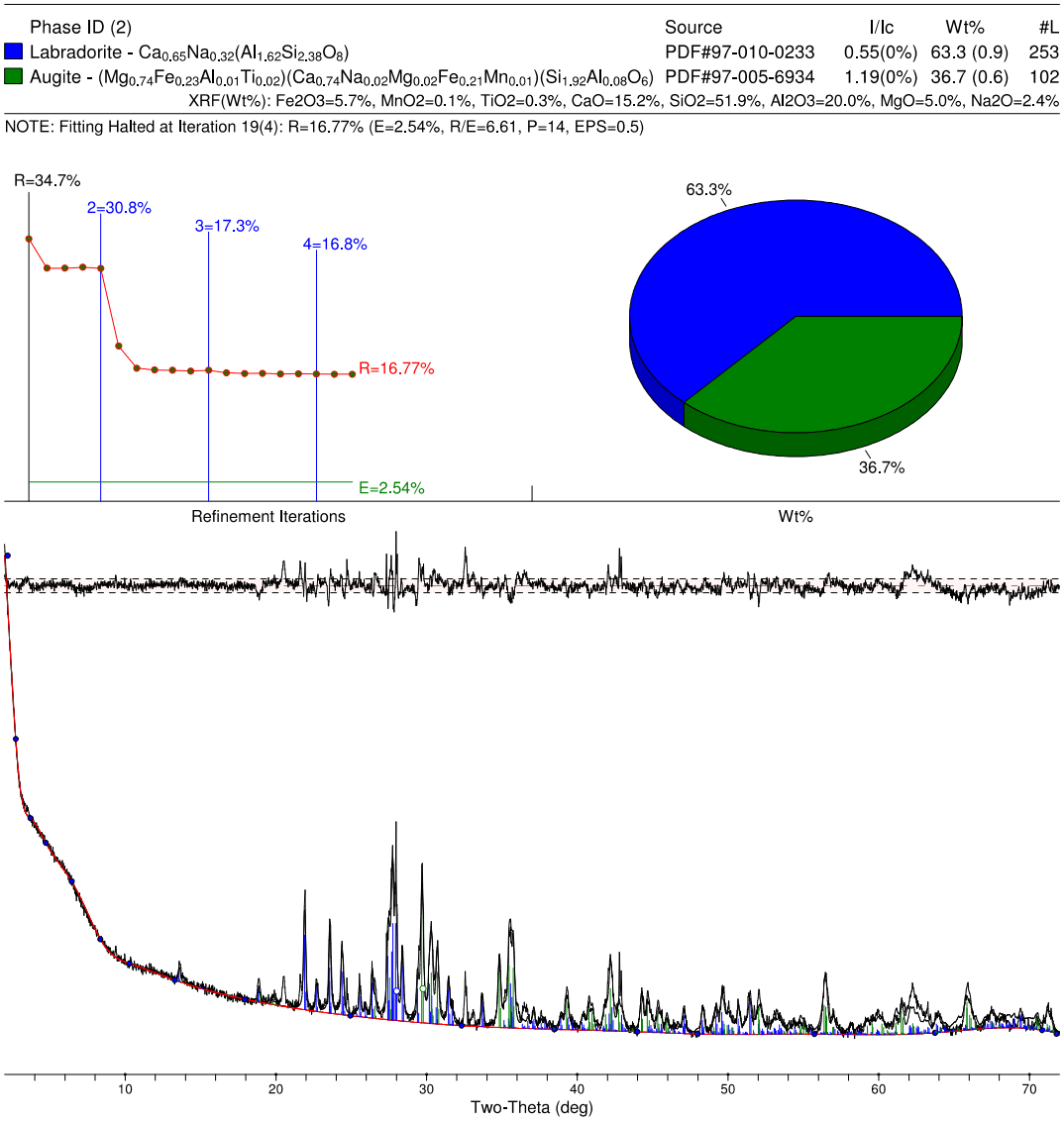

Figure 3.10/S8. Powder X-ray diffraction (XRD) analysis of Kal S proglacial sediment performed using Jade 9 software.

```
Query: M04026_507_000000000-JH26P_1_1101_10223_5426 Query ID: lcl|Query_61105 Length:
253

>NODE_74_length_11445_cov_27.830714
Sequence ID: Query_61107 Length: 11445
Range 1: 968 to 1220

Score:457 bits (247), Expect:6e-132,
Identities:251/253(99%), Gaps:0/253(0%), Strand: Plus/Plus

Query  1     TACGTAGGGTGCGAGCGTTAATCGGAATTACTGGGCGTAAAGCGTGCGCAGGCGGTTATA  60
             ||||||||||||||||||||||||||||||||||||||||||||||||||||||||||||
Sbjct  968   TACGTAGGGTGCGAGCGTTAATCGGAATTACTGGGCGTAAAGCGTGCGCAGGCGGTTATA  1027

Query  61    TAAGACAGATGTGAAATCCCCGGGCTCAACCTGGAACCTGCATCTGTGACTGTATAGCTA  120
             |||||||||||||||||||||||||||||| |||||||| ||||||||||||||||
Sbjct  1028  TAAGACAGATGTGAAATCCCCGGGCTCAACCTGGGACCTGCATTTGTGACTGTATAGCTA  1087

Query  121   GAGTACGGTAGAGGGGGATGGAATTCCGCGTGTAGCAGTGAAATGCGTAGATATGCGGAG  180
             ||||||||||||||||||||||||||||||||||||||||||||||||||||||||||||
Sbjct  1088  GAGTACGGTAGAGGGGGATGGAATTCCGCGTGTAGCAGTGAAATGCGTAGATATGCGGAG  1147

Query  181   GAACACCGATGGCGAAGGCAATCCCCTGGACCTGTACTGACGCTCATGCACGAAAGCGTG  240
             ||||||||||||||||||||||||||||||||||||||||||||||||||||||||||||
Sbjct  1148  GAACACCGATGGCGAAGGCAATCCCCTGGACCTGTACTGACGCTCATGCACGAAAGCGTG  1207

Query  241   GGGAGCAAACAGG  253
             |||||||||||||
Sbjct  1208  GGGAGCAAACAGG  1220
```

Figure 3.11/S9. Pairwise sequence alignment generated from BLASTn of 16S rRNA gene sequences amplified from mineral grain and sediment DNA. Representative sequences of a *Rhodoferax*-affiliated 16S rRNA gene operational taxonomic unit recovered from Kal S mineral and proglacial sediment communities (Query) and a 16S rRNA gene recovered from a metagenome amplified genome (MAG) of a *Rhodoferax*-associated autotrophic H_2-dependent Fe(III) reducer (Sbjct) enriched from Kötlujökull, Iceland sediments [145].

Supplementary References

142. Parks, D.H., et al., *CheckM: assessing the quality of microbial genomes recovered from isolates, single cells, and metagenomes.* Genome Research, 2015. **25**(7): p. 1043-1055.

145. Dunham, E.C., et al., *Lithogenic hydrogen supports microbial primary production in subglacial and proglacial environments.* Proceedings of the National Academy of Sciences of the United States of America, 2021. **118**(2).

CHAPTER FOUR

CONCLUSIONS AND FUTURE DIRECTIONS

Conclusions

With this work, I sought to improve our understanding of the determinants controlling the distribution, composition, and activity of microbial communities that inhabit silicate-based glaciated catchments. While prior work had outlined the potential for glacial comminution of bedrock to regenerate the mineral surfaces that provide lithogenic redox-active substrates for chemolithotrophic microbial metabolism, most scientific attention had been focused on sedimentary catchments and the influence of FeS_2. My efforts contributed important findings on the availability of energy and its sources in silicate-based catchments.

In Chapter 2, I examined this relationship through the lens of lithogenic H_2 production. Comparing dissolved H_2 concentrations in the meltwaters of Kötlujökull and Robertson Glacier provided an opportunity to examine the relationship between bedrock composition and the availability of lithogenic sources of energy for sediment-associated microbial communities. Using a combination of modern molecular microbiology techniques and traditional culture-based approaches, I showed that the microbial populations at Kötlujökull sediments exhibit adaptations that allow them to more efficiently utilize H_2, including shorter lag times and higher maximum rates of oxidation. I further connected H_2 metabolism in the Kötlujökull community to primary production, showing that geologically derived oxidants that stimulated H_2 oxidation also stimulated H_2-dependent carbon dioxide fixation. These results indicate the potential for the subglacial ecosystem of Kötlujökull to subsist largely in the absence of surface-derived organic

carbon, whether derived from organic sediments buried by glacial advance or from supraglacial meltwaters bearing surface runoff.

While Chapter 2 describes the influence of bedrock composition on lithogenic reductant availability, lithotrophic microbial populations often utilize lithogenic oxidants as well. In Chapter 3, I investigated the influence of Fe(III) on the abundance and composition of sediment-associated microbial communities at Kaldalónsjökull. Sterilized minerals were incubated in Kaldalónsjökull meltwaters for one year, providing an opportunity for them to be colonized by microbial populations in meltwater streams draining the subglacial environment. Comparing the quantifiable DNA extracted from the incubated minerals and from the sediments of the meltwater streams allowed me to estimate the amount of biomass supported by each substrate. I found that the Fe(III)-bearing mineral hematite supported more biomass than any of the other substrates, including redox active compounds such as olivine and non-redox active compounds such as quartz and calcite. Next, I compared the compositions of each community by sequencing PCR-amplified 16S rRNA genes from each DNA extract. Comparison of the composition of those communities in proglacial sediments to those of incubated minerals showed that the proglacial sediment community was most similar to those recovered from the two minerals containing Fe(III), hematite and magnetite. Further, all three of these communities were dominated by operational taxonomic units (OTUs) affiliated with iron-reducing taxa.

In an unexpected result that nonetheless further emphasizes the importance of lithogenic energy substrates in structuring subglacial communities, I discovered that the basaltic sediments of Kötlujökull and Kaldalónsjökull share an important community member: an autotrophic, H_2-dependent iron reducing population affiliated with the genus *Rhodoferax*. The ability to fix CO_2

using H_2-dependent Fe(III) reduction is not in itself novel, but this metabolism had been previously documented only in environments of high temperature (>65°C) or low pH (<3.5). It is perhaps not surprising to find the two Icelandic catchments studied here sharing an important community member given their geographic proximity and similarity in bedrock composition. Nonetheless, the abundance of this population at both sites unifies the themes of Chapters 2 and 3, namely the influence of bedrock composition on the supplies of lithogenic reductants and oxidants, respectively, and further reinforces the hypothesis that subglacial communities in basaltic catchments can sustain themselves independent of photosynthetically fixed organic carbon.

The potential for subglacial communities to exist in environments devoid of sunlight and independent of photosynthetic carbon fixation has important implications for the maintenance of the metabolic potential of the biosphere as a whole through Snowball Earth states and also for the potential for microbial communities to exist on extraterrestrial bodies. While photosynthetic life might persist on the surface of a Snowball Earth [16], the dramatic slowing of the biogeochemical cycles supplying important nutrients such as phosphorous, iron, and sulfur to the ice surface during such periods would severely limit the accumulation of biomass. However, the continuation of biogeochemical cycling beneath the ice by chemolithotrophic microbial populations would not only increase the diversity of mineral nutrients available to the biosphere through microbially accelerated chemical weathering processes, but would also represent a mechanism to conserve the genes that encode key metabolic processes associated with these important biogeochemical functions. Beyond Earth itself, scientific observation of the icy moons Enceladus [74] and Europa [73] in our own solar system suggest they might host environments

remarkably similar in their geochemistry to those found beneath the ice of basalt-based glaciers on Earth. If chemolithotrophic primary production supported by H_2 oxidation coupled to Fe(III) reduction occurs in cold, dark environments on our planet and can support diverse and potentially robust microbial biospheres, then the conditions necessary to support such biospheres quite possibly exist on multiple extraterrestrial bodies. This makes these moons exciting potential targets in the search for extraterrestrial life, emphasizing the need to further develop remote life detection strategies in analog environments on Earth.

Future Directions

An intriguing result obtained in the studies describe in Chapter 3 is the difficulty in detecting microbial life in the sediments of the Kaldalónsjökull North (Kal N) outlet and Kötlujökull using molecular techniques. A recent study was able to recover community DNA from an unspecified outlet of Kaldalónsjökull by filtering large volumes of meltwater and performing DNA extractions on the filters used [158]. This suggests the potential for Kal N sediments to be colonized by microbial populations suspended in meltwater. In a forthcoming study, I will report the results of a reciprocal transfer experiment in which A type bedrock samples collected near the Kal N outlet were crushed and loaded into sampler coupons to be incubated for one year in the Kaldalónsjökull South (Kal S) outlet. In parallel, B type bedrock collected at Kal S was likewise crushed and incubated in the meltwaters of Kal N. The sampler coupons incubated at each site also contained crushed bedrock samples taken from the outlets of two other Icelandic glaciers, Sólheimajökull and Leirufjarðarjökull. Extracting DNA from the colonized bedrock surfaces and subjecting this DNA to 16S rRNA gene amplification as described in Chapter 3 will provide information on the extent to which bedrock composition

and/or meltwater geochemistry determine the habitability of the Kal N and Kal S outlet streams, which can be extended to understand controls on the habitability of Kötlujökull.

Additionally, traditional microbiological techniques such as spread plating have shown that at least four morphologically distinct populations of aerobic heterotrophs inhabit Kal N sediments (E.C. Dunham, unpublished data). Propagating the colonies isolated on these spread plates in liquid culture media would provide a platform for assessing the characteristics of the Kal N community without relying on extraction of community DNA from sediments themselves. Simple growth experiments conducted at different temperatures could determine whether the isolated populations are adapted to growth at cold temperatures and therefore likely endemic to the subglacial sediments of Kaldalónsjökull. Growth in defined media would also provide a simple platform for determining the metabolic capabilities of these populations by testing for autotrophic growth or the utilization of lithogenic energy sources like those utilized in Chapters 2 and 3 of the current work.

Finally, in order to better understand the factors allowing chemolithotrophic carbon fixation to support diverse microbial communities in subglacial environments, future studies might use techniques such as stable isotope probing (SIP) combined with metabolomic or molecular genetic approaches to track the incorporation of inorganic carbon into populations of primary producers and its subsequent distribution throughout the community. This research might start with metabolomic characterization of the autotrophic *Rhodoferax* population isolated from Kötlujökull sediments. A profile of the waste products generated by this culture when grown autotrophically could be used to design SIP experiments in which enrichment cultures inoculated with subglacial sediments were amended with ^{13}C-labelled versions of these waste

products. DNA would then be extracted from these enrichment cultures and separated by ultracentrifugation. Sequencing of the heavier ^{13}C-labelled fraction would reveal the populations supported by primary production at least partly attributable to *Rhodoferax* and begin to reveal the structure of the subglacial trophic web. Taken together, the experiments described in Chapters 2 and 3 and those proposed here would constitute a dramatic expansion of current knowledge on the biogeochemical interactions that sustain subglacial life in basaltic catchments and would provide a robust framework for predicting whether and where such life might be found on worlds beyond our own.

References

16. Corsetti, F.A., A.N. Olcott, and C. Bakermans, *The biotic response to Neoproterozoic snowball Earth.* Palaeogeography, Palaeoclimatology, Palaeoecology, 2006. **232**(2): p. 114-130.

73. Vance, S.D., K.P. Hand, and R.T. Pappalardo, *Geophysical controls of chemical disequilibria in Europa.* Geophysical Research Letters, 2016. **43**(10): p. 4871-4879.

74. Hsu, H.-W., et al., *Ongoing hydrothermal activities within Enceladus.* Nature, 2015. **519**(7542): p. 207-210.

158. Kohler, T.J., et al., *Patterns in microbial assemblages exported from the meltwater of Arctic and Sub-Arctic glaciers.* Frontiers in Microbiology, 2020. **11**: p. 669.

CUMULATIVE REFERENCES

1. Hoffman, P.F., et al., *A Neoproterozoic Snowball Earth.* Science, 1998. **281**(5381): p. 1342-1346.

2. Hoffman, P.F. and D.P. Schrag, *The snowball Earth hypothesis: testing the limits of global change.* Terra Nova, 2002. **14**(3): p. 129-155.

3. Kasting, J.F. and S. Ono, *Palaeoclimates: the first two billion years.* Philosophical Transactions of the Royal Society B: Biological Sciences, 2006. **361**(1470): p. 917-929.

4. Tang, H. and Y. Chen, *Global glaciations and atmospheric change at ca. 2.3 Ga.* Geoscience Frontiers, 2013. **4**(5): p. 583-596.

5. Young, G.M., et al., *Earth's Oldest Reported Glaciation: Physical and Chemical Evidence From the Archean Mozaan Group (~2.9 Ga) of South Africa.* The Journal of Geology, 1998. **106**(5): p. 523-538.

6. Sagan, C. and G. Mullen, *Earth and Mars: Evolution of Atmospheres and Surface Temperatures.* Science, 1972. **177**(4043): p. 52-56.

7. Berner, R.A., A.C. Lasaga, and R.M. Garrels, *The carbonate-silicate geochemical cycle and its effect on atmospheric carbon dioxide over the past 100 million years.* American Journal of Science, 1983. **283:7**.

8. Des Marais, D.J., *When did photosynthesis emerge on Earth?* Science, 2000. **289**(5485): p. 1703-1705.

9. Sharp, M., et al., *Widespread bacterial populations at glacier beds and their relationship to rock weathering and carbon cycling.* Geology, 1999. **27**(2): p. 107-110.

10. Skidmore, M.L., J.M. Foght, and M.J. Sharp, *Microbial Life beneath a High Arctic Glacier.* Applied and Environmental Microbiology, 2000. **66**(8): p. 3214-3220.

11. Foght, J., et al., *Culturable Bacteria in Subglacial Sediments and Ice from Two Southern Hemisphere Glaciers.* Microbial Ecology, 2004. **47**(4): p. 329-340.

12. Abyzov, S.S., *Microorganisms in the Antarctic ice.* Antarctic Microbiology, 1993. **1**(1): p. 265-296.

13. Priscu, J.C., et al., *Geomicrobiology of Subglacial Ice Above Lake Vostok, Antarctica.* Science, 1999. **286**(5447): p. 2141-2144.

14. Abyzov, S.S., et al. *Long-term conservation of viable microorganisms in the ice sheet of Central Antarctica*. in *Instruments, Methods, and Missions for Astrobiology*. 1998. International Society for Optics and Photonics.

15. Boyd, E.S., et al., *Chemolithotrophic primary production in a subglacial ecosystem.* Applied and Environmental Microbiology, 2014. **80**(19): p. 6146-53.

16. Corsetti, F.A., A.N. Olcott, and C. Bakermans, *The biotic response to Neoproterozoic snowball Earth.* Palaeogeography, Palaeoclimatology, Palaeoecology, 2006. **232**(2): p. 114-130.

17. Bottrell, S.H. and M. Tranter, *Sulphide oxidation under partially anoxic conditions at the bed of the Haut Glacier d'Arolla, Switzerland.* Hydrological Processes, 2002. **16**(12): p. 2363-2368.

18. Hamilton, T.L., et al., *Molecular evidence for an active endogenous microbiome beneath glacial ice.* The ISME Journal, 2013. **7**(7): p. 1402-12.

19. Montross, S.N., et al., *A microbial driver of chemical weathering in glaciated systems.* Geology, 2013. **41**(2): p. 215-218.

20. Skidmore, M., et al., *Comparison of Microbial Community Compositions of Two Subglacial Environments Reveals a Possible Role for Microbes in Chemical Weathering Processes.* Applied and Environmental Microbiology, 2005. **71**(11): p. 6986-6997.

21. Wadham, J.L., et al., *Potential methane reservoirs beneath Antarctica.* Nature, 2012. **488**(7413): p. 633-637.

22. Stibal, M., et al., *Methanogenic potential of Arctic and Antarctic subglacial environments with contrasting organic carbon sources.* Global Change Biology, 2012. **18**(11): p. 3332-3345.

23. Boyd, E.S., et al., *Methanogenesis in subglacial sediments.* Environmental Microbiology Reports, 2010. **2**(5): p. 685-692.

24. Christner, B.C., G.G. Montross, and J.C. Priscu, *Dissolved gases in frozen basal water from the NGRIP borehole: implications for biogeochemical processes beneath the Greenland Ice Sheet.* Polar Biology, 2012. **35**(11): p. 1735-1741.

25. Michaud, A.B., et al., *Microbial oxidation as a methane sink beneath the West Antarctic Ice Sheet.* Nature Geoscience, 2017. **10**(8): p. 582-586.

26. Wadham, J.L., et al., *Subglacial methanogenesis: A potential climatic amplifier?* Global Biogeochemical Cycles, 2008. **22**(2).

27. Bennett, P.C., et al., *Silicates, Silicate Weathering, and Microbial Ecology.* Geomicrobiology Journal, 2001. **18**(1): p. 3-19.

28. McLean, A.L., *Bacteria of Ice and Snow in Antarctica.* Nature, 1918. **102**(2550): p. 35-39.

29. Darling, C.A. and P.A. Siple, *Bacteria of Antarctica.* Journal of Bacteriology, 1941. **42**(1): p. 83-98.

30. Abyzov, S., N. Bobin, and B. Dudriashov, *Quantitative registration of microorganisms at microbiological studies of the Antarctic glaciers.* Izvestiya Akademii nauk SSSR. Seriya Biologicheskaya, 1982.

31. Karl, D.M., et al., *Microorganisms in the Accreted Ice of Lake Vostok, Antarctica.* Science, 1999. **286**(5447): p. 2144-2147.

32. Dancer, S., P. Shears, and D. Platt, *Isolation and characterization of coliforms from glacial ice and water in Canada's High Arctic.* Journal of Applied Microbiology, 1997. **82**(5): p. 597-609.

33. Christner, B.C., et al., *Recovery and Identification of Viable Bacteria Immured in Glacial Ice.* Icarus, 2000. **144**(2): p. 479-485.

34. Sheridan, P.P., V.I. Miteva, and J.E. Brenchley, *Phylogenetic Analysis of Anaerobic Psychrophilic Enrichment Cultures Obtained from a Greenland Glacier Ice Core.* Applied and Environmental Microbiology, 2003. **69**(4): p. 2153-2160.

35. Miteva, V.I., P.P. Sheridan, and J.E. Brenchley, *Phylogenetic and Physiological Diversity of Microorganisms Isolated from a Deep Greenland Glacier Ice Core.* Applied and Environmental Microbiology, 2004. **70**(1): p. 202-213.

36. Wadham, J.L., et al., *Stable isotope evidence for microbial sulphate reduction at the bed of a polythermal high Arctic glacier.* Earth and Planetary Science Letters, 2004. **219**(3): p. 341-355.

37. Mikucki, J.A., et al., *Geomicrobiology of Blood Falls: An Iron-Rich Saline Discharge at the Terminus of the Taylor Glacier, Antarctica.* Aquatic Geochemistry, 2004. **10**(3): p. 199-220.

38. Dieser, M., et al., *Molecular and biogeochemical evidence for methane cycling beneath the western margin of the Greenland Ice Sheet.* The ISME Journal, 2014. **8**(11): p. 2305-2316.

39. Tranter, M., et al., *Geochemical weathering at the bed of Haut Glacier d'Arolla, Switzerland—a new model.* Hydrological Processes, 2002. **16**(5): p. 959-993.

40. Wynn, P.M., A. Hodson, and T. Heaton, *Chemical and Isotopic Switching within the Subglacial Environment of a High Arctic Glacier.* Biogeochemistry, 2006. **78**(2): p. 173-193.

41. Wynn, P.M., et al., *Nitrate production beneath a High Arctic glacier, Svalbard.* Chemical Geology, 2007. **244**(1): p. 88-102.

42. Wadham, J.L., et al., *Hydro-biogeochemical coupling beneath a large polythermal Arctic glacier: Implications for subice sheet biogeochemistry.* Journal of Geophysical Research: Earth Surface, 2010. **115**(F4).

43. Hodson, A., et al., *Chemical weathering and solute export by meltwater in a maritime Antarctic glacier basin.* Biogeochemistry, 2010. **98**(1-3): p. 9-27.

44. Mitchell, A.C., et al., *Influence of bedrock mineral composition on microbial diversity in a subglacial environment.* Geology, 2013. **41**(8): p. 855-858.

45. Irvine-Fynn, T.D., et al., *Polythermal glacier hydrology: a review.* Reviews of Geophysics, 2011. **49**(4).

46. Stibal, M., et al., *Prokaryotic diversity in sediments beneath two polar glaciers with contrasting organic carbon substrates.* Extremophiles, 2012. **16**(2): p. 255-265.

47. Christner, B.C., et al., *A microbial ecosystem beneath the West Antarctic ice sheet.* Nature, 2014. **512**(7514): p. 310-313.

48. Harrold, Z.R., et al., *Aerobic and Anaerobic Thiosulfate Oxidation by a Cold-Adapted, Subglacial Chemoautotroph.* Applied and Environmental Microbiology, 2016. **82**(5): p. 1486-1495.

49. Tranter, M., M. Skidmore, and J. Wadham, *Hydrological controls on microbial communities in subglacial environments.* Hydrological Processes, 2005. **19**(4): p. 995-998.

50. Yde, J.C., et al., *Basal ice microbiology at the margin of the Greenland ice sheet.* Annals of Glaciology, 2010. **51**(56): p. 71-79.

51. Sheik, C.S., et al., *Microbial communities of the Lemon Creek Glacier show subtle structural variation yet stable phylogenetic composition over space and time.* Frontiers in Microbiology, 2015. **6**.

52. Frey, B., et al., *Weathering-Associated Bacteria from the Damma Glacier Forefield: Physiological Capabilities and Impact on Granite Dissolution.* Applied and Environmental Microbiology, 2010. **76**(14): p. 4788-4796.

53. Cottle, J.M. and A.F. Cooper, *Geology, geochemistry, and geochronology of an A-type granite in the Mulock Glacier area, southern Victoria Land, Antarctica.* New Zealand Journal of Geology and Geophysics, 2006. **49**(2): p. 191-202.

54. Wongfun, N., et al., *Weathering of Granite from the Damma Glacier Area: The Contribution of Cyanogenic Bacteria.* Geomicrobiology Journal, 2014. **31**(2): p. 93-100.

55. Lapanje, A., et al., *Pattern of elemental release during the granite dissolution can be changed by aerobic heterotrophic bacterial strains isolated from Damma Glacier (central Alps) deglaciated granite sand.* Microbial Ecology, 2012. **63**(4): p. 865-882.

56. Telling, J., et al., *Rock comminution as a source of hydrogen for subglacial ecosystems.* Nature Geoscience, 2015. **8**(12).

57. Macdonald, M.L., et al., *Glacial Erosion Liberates Lithologic Energy Sources for Microbes and Acidity for Chemical Weathering Beneath Glaciers and Ice Sheets.* Frontiers in Earth Science, 2018. **6**.

58. Spear, J.R., et al., *Hydrogen and bioenergetics in the Yellowstone geothermal ecosystem.* Proceedings of the National Academy of Sciences of the United States of America, 2005. **102**(7): p. 2555-2560.

59. Lin, L.-H., et al., *Radiolytic H_2 in continental crust: Nuclear power for deep subsurface microbial communities.* Geochemistry, Geophysics, Geosystems, 2005. **6**(7).

60. Martin, W.F., *Hydrogen, metals, bifurcating electrons, and proton gradients: the early evolution of biological energy conservation.* FEBS Letters, 2012. **586**(5): p. 485-493.

61. Wächtershäuser, G., *Evolution of the first metabolic cycles.* Proceedings of the National Academy of Sciences of the United States of America, 1990. **87**(1): p. 200-204.

62. Peters, J.W., et al., *[FeFe]- and [NiFe]-hydrogenase diversity, mechanism, and maturation.* Biochimica et Biophysica Acta (BBA) - Molecular Cell Research, 2015. **1853**(6): p. 1350-1369.

63. Lindsay, M.R., et al., *Probing the geological source and biological fate of hydrogen in Yellowstone hot springs.* Environmental Microbiology, 2019. **21**(10): p. 3816-3830.

64. Nealson, K.H., F. Inagaki, and K. Takai, *Hydrogen-driven subsurface lithoautotrophic microbial ecosystems (SLiMEs): do they exist and why should we care?* Trends in Microbiology, 2005. **13**(9): p. 405-410.

65. Stevens, T.O. and J.P. McKinley, *Abiotic controls on H_2 production from basalt-water reactions and implications for aquifer biogeochemistry.* Environmental Science & Technology, 2000. **34**(5): p. 826-831.

66. Kita, I., S. Matsuo, and H. Wakita, *H_2 generation by reaction between H_2O and crushed rock: An experimental study on H_2 degassing from the active fault zone.* Journal of Geophysical Research: Solid Earth, 1982. **87**(B13): p. 10789-10795.

67. Christner, B.C., et al., *Limnological conditions in subglacial Lake Vostok, Antarctica.* Limnology and Oceanography, 2006. **51**(6): p. 2485-2501.

68. Lanoil, B., et al., *Bacteria beneath the West Antarctic Ice Sheet.* Environmental Microbiology, 2009. **11**(3): p. 609-615.

69. Bhatia, M., M. Sharp, and J. Foght, *Distinct bacterial communities exist beneath a high Arctic polythermal glacier.* Applied and Environmental Microbiology, 2006. **72**(9): p. 5838-5845.

70. Cheng, S.M. and J.M. Foght, *Cultivation-independent and -dependent characterization of Bacteria resident beneath John Evans Glacier.* FEMS Microbiology Ecology, 2007. **59**(2): p. 318-330.

71. Nixon, S.L., et al., *Viable cold-tolerant iron-reducing microorganisms in geographically diverse subglacial environments.* Biogeosciences, 2017. **14**(6): p. 1445-1455.

72. Hoffman, P.F., et al., *Snowball Earth climate dynamics and Cryogenian geology-geobiology.* Science Advances, 2017. **3**(11): p. e1600983.

73. Vance, S.D., K.P. Hand, and R.T. Pappalardo, *Geophysical controls of chemical disequilibria in Europa.* Geophysical Research Letters, 2016. **43**(10): p. 4871-4879.

74. Hsu, H.-W., et al., *Ongoing hydrothermal activities within Enceladus.* Nature, 2015. **519**(7542): p. 207-210.

75. Boyd, E.S., et al., *Diversity, Abundance, and Potential Activity of Nitrifying and Nitrate-Reducing Microbial Assemblages in a Subglacial Ecosystem.* Applied and Environmental Microbiology, 2011. **77**(14): p. 4778-4787.

76. Cameron, K.A., et al., *Meltwater export of prokaryotic cells from the Greenland ice sheet.* Environmental Microbiology, 2017. **19**(2): p. 524-534.

77. Hindshaw, R.S., et al., *Influence of glaciation on mechanisms of mineral weathering in two high Arctic catchments.* Chem. Geol., 2016. **420**: p. 37-50.

78. Kelley, D.S., et al., *A Serpentinite-Hosted Ecosystem: The Lost City Hydrothermal Field.* Science, 2005. **307**(5714): p. 1428.

79. Boyd, E.S., et al., *[FeFe]-hydrogenase in Yellowstone National Park: evidence for dispersal limitation and phylogenetic niche conservatism.* The ISME Journal, 2010. **4**(12): p. 1485.

80. Parkes, R.J., et al., *Rock-crushing derived hydrogen directly supports a methanogenic community: significance for the deep biosphere.* Environmental Microbiology Reports, 2019. **11**(2): p. 165-172.

81. Ma, H., et al., *Ex Situ Culturing Experiments Revealed Psychrophilic Hydrogentrophic Methanogenesis Being the Potential Dominant Methane-Producing Pathway in Subglacial Sediment in Larsemann Hills, Antarctic.* Frontiers in Microbiology, 2018. **9**.

82. Yang, Z., et al., *H_2 Metabolism revealed by metagenomic analysis of subglacial sediment from East Antarctica.* Journal of Microbiology, 2019. **57**(12): p. 1095-1104.

83. Gale, A., et al., *The mean composition of ocean ridge basalts.* Geochemistry, Geophysics, Geosystems, 2013. **14**(3): p. 489-518.

84. Kruger, J., *Development of minor outwash fans at Kötlujökull, Iceland.* Quaternary Science Reviews, 1997. **16**(7): p. 649-659.

85. Jóhannesson, H., *Geological Map of Iceland. Bedrock Geology*. 2014, Icelandic Institute of Natural History: Reykjavík.

86. Lacasse, C., et al., *Bimodal volcanism at the Katla subglacial caldera, Iceland: insight into the geochemistry and petrogenesis of rhyolitic magmas.* Bulletin of Volcanology, 2006. **69**(4): p. 373.

87. McMechan, M.E., *Geology of Peter Lougheed Provincial Park, Rocky Mountain Front Ranges, Alberta*. 1988: Geological Survey of Canada.

88. Sharp, M., R.A. Creaser, and M. Skidmore, *Strontium isotope composition of runoff from a glaciated carbonate terrain.* Geochimica et Cosmochimica Acta, 2002. **66**(4): p. 595-614.

89. Griggs, R.K., *Characterization of Subglaical Till from Robertson Glacier, Alberta, Canada: Implications for Biogeochemical Weathering*, in *Department of Earth Sciences*. 2013, Montana State University: Bozeman, Montana.

90. Fogo, J.K. and M. Popowsky, *Spectrophotometric Determination of Hydrogen Sulfide - Methylene Blue Method.* Analytical Chemistry, 1949. **21**(6): p. 732-734.

91. Chapelle, F.H., et al., *Practical Considerations for Measuring Hydrogen Concentrations in Groundwater.* Environmental Science & Technology, 1997. **31**(10): p. 2873-2877.

92. Lindsay, M.R., et al., *Subsurface processes influence oxidant availability and chemoautotrophic hydrogen metabolism in Yellowstone hot springs.* Geobiology, 2018. **16**(6): p. 674-692.

93. Atlas, R.M., in *Handbook of Microbiological Media*. 2004, ASM Press: Washington, D.C. p. 981.

94. Straub, K.L., A. Kappler, and B. Schink, *Enrichment and isolation of ferric-iron- and humic-acid-reducing bacteria.* Methods in Enzymology, 2005. **397**: p. 58-77.

95. Mitchell, K.R. and C.D. Takacs-Vesbach, *A comparison of methods for total community DNA preservation and extraction from various thermal environments.* Journal of Industrial Microbiology and Biotechnology, 2008. **35**(10): p. 1139-47.

96. Blodgett, R. *Appendix 2: Most Probable Number from Serial Dilutions*. Bacterial Analytical Manual 2010 [cited 2017 14 July]; 8th:[Available from: https://www.fda.gov/food/foodscienceresearch/laboratorymethods/ucm109656.htm.

97. Viollier, E., et al., *The ferrozine method revisited: Fe(II)/Fe(III) determination in natural waters.* Applied Geochemistry, 2000. **15**(6): p. 785-790.

98. Strickland, J.D.H. and T.R. Parsons, *A Practical Handbook of Seawater Analysis*, J.C. Stevenson, Editor. 1972, Fisheries Research Board of Canada: Ottawa. p. 77-80.

99. Payne, D., et al., *Geologic legacy spanning >90 years explains unique Yellowstone hot spring geochemistry and biodiversity.* Environmental Microbiology, 2019. **21**(11): p. 4180-4195.

100. Schut, G.J., et al., *The role of geochemistry and energetics in the evolution of modern respiratory complexes from a proton-reducing ancestor.* Biochimica et Biophysica Acta (BBA) - Bioenergetics, 2016. **1857**(7): p. 958-970.

101. Søndergaard, D., C.N.S. Pedersen, and C. Greening, *HydDB: A web tool for hydrogenase classification and analysis.* Scientific Reports, 2016. **6**(1): p. 34212.

102. Jones, M.T., et al., *Monitoring of jökulhlaups and element fluxes in proglacial Icelandic rivers using osmotic samplers.* Journal of Volcanology and Geothermal Research, 2015. **291**: p. 112-124.

103. Canovas, P.A., *Energy Transfer Between the Geosphere and Biosphere*. 2016, Arizona State University: United States -- Arizona. p. 433.

104. Amenabar, M.J., M.R. Urschel, and E.S. Boyd, *Metabolic and taxonomic diversification in continental magmatic hydrothermal systems.* Microbial Evolution Under Extreme Conditions. Berlin: De Gruyter, 2015.

105. Klein, F., N.G. Grozeva, and J.S. Seewald, *Abiotic methane synthesis and serpentinization in olivine-hosted fluid inclusions.* Proceedings of the National Academy of Sciences of the United States of America, 2019. **116**(36): p. 17666-17672.

106. Bas, M.J.L. and A.L. Streckeisen, *The IUGS systematics of igneous rocks.* Journal of the Geological Society, 1991. **148**(5): p. 825-833.

107. Novelli, P.C., et al., *Molecular hydrogen in the troposphere: Global distribution and budget.* Journal of Geophysical Research. Atmospheres, 1999. **104**(D23): p. 30427-30444.

108. Greening, C., et al., *Persistence of the dominant soil phylum Acidobacteria by trace gas scavenging.* Proceedings of the National Academy of Sciences of the United States of America, 2015. **112**(33): p. 10497-10502.

109. Tranter, M., *Sediment and Solute Transport in Glacial Meltwater Streams*, in *Encyclopedia of Hydrological Sciences*. 2006.

110. Wiggins, B.A., S.H. Jones, and M. Alexander, *Explanations for the acclimation period preceding the mineralization of organic chemicals in aquatic environments.* Applied and Environmental Microbiology, 1987. **53**(4): p. 791-796.

111. Aamand, J., et al., *Microbial adaptation to degradation of hydrocarbons in polluted and unpolluted groundwater.* Journal of Contaminant Hydrology, 1989. **4**(4): p. 299-312.

112. Wang, H. and K.J. Edwards, *Bacterial and Archaeal DNA Extracted from Inoculated Experiments: Implication for the Optimization of DNA Extraction from Deep-Sea Basalts.* Geomicrobiology Journal, 2009. **26**(7): p. 463-469.

113. Ji, M., et al., *Atmospheric trace gases support primary production in Antarctic desert surface soil.* Nature, 2017. **552**(7685): p. 400.

114. Urschel, M.R., et al., *Substrate preference, uptake kinetics and bioenergetics in a facultatively autotrophic, thermoacidophilic crenarchaeote.* FEMS Microbiology Ecology, 2016. **92**(5).

115. Amenabar, M.J., et al., *Electron acceptor availability alters carbon and energy metabolism in a thermoacidophile.* Environmental Microbiology, 2018. **20**(7): p. 2523-2537.

116. Carere, C.R., et al., *Mixotrophy drives niche expansion of verrucomicrobial methanotrophs.* The ISME Journal, 2017. **11**(11): p. 2599-2610.

117. Beller, H.R., et al., *The Genome Sequence of the Obligately Chemolithoautotrophic, Facultatively Anaerobic Bacterium Thiobacillus denitrificans.* Journal of Bacteriology, 2006. **188**(4): p. 1473-1488.

118. Jónasson, K., *Silicic volcanism in Iceland: Composition and distribution within the active volcanic zones.* Journal of Geodynamics, 2007. **43**(1): p. 101-117.

119. Robson, G.R., *The volcanic geology of Vestur–Skaftarfellssýsla Iceland*. 1956, Durham University.

120. Hansel, C.M., et al., *Dominance of sulfur-fueled iron oxide reduction in low-sulfate freshwater sediments.* The ISME Journal, 2015. **9**(11): p. 2400-2412.

121. Kashefi, K., et al., *Geoglobus ahangari gen. nov., sp. nov., a novel hyperthermophilic archaeon capable of oxidizing organic acids and growing autotrophically on hydrogen with Fe(III) serving as the sole electron acceptor.* International Journal of Systematic and Evolutionary Microbiology,, 2002. **52**(3): p. 719-728.

122. Kashefi, K., et al., *Use of Fe(III) as an Electron Acceptor To Recover Previously Uncultured Hyperthermophiles: Isolation and Characterization of Geothermobacterium ferrireducens gen. nov., sp. nov.* Applied and Environmental Microbiology, 2002. **68**(4): p. 1735-1742.

123. Norris, P.R., et al., *Acidithiobacillus ferrianus sp. nov.: an ancestral extremely acidophilic and facultatively anaerobic chemolithoautotroph.* Extremophiles, 2020. **24**(2): p. 329-337.

124. Margesin, R., et al., *Glaciimonas frigoris sp. nov., a psychrophilic bacterium isolated from ancient Siberian permafrost sediment, and emended description of the genus Glaciimonas.* International Journal of Systematic and Evolutionary Microbiology, 2016. **66**(2): p. 744-748.

125. Frasson, D., et al., *Glaciimonas alpina sp. nov. isolated from alpine glaciers and reclassification of Glaciimonas immobilis Cr9-12 as the type strain of Glaciimonas alpina sp. nov.* International Journal of Systematic and Evolutionary Microbiology, 2015. **65**(Pt 6): p. 1779-1785.

126. Zhang, D.-C., et al., *Glaciimonas immobilis gen. nov., sp. nov., a member of the family Oxalobacteraceae isolated from alpine glacier cryoconite.* International Journal of Systematic and Evolutionary Microbiology, 2011. **61**(9): p. 2186-2190.

127. Lenz, O., et al., *The hydrogen-sensing apparatus in Ralstonia eutropha.* Journal of Molecular Microbiology and Biotechnology, 2002. **4**(3): p. 255-262.

128. Darcy, J.L., et al., *Global Distribution of Polaromonas Phylotypes - Evidence for a Highly Successful Dispersal Capacity.* PLOS ONE, 2011. **6**(8): p. e23742.

129. Hiraishi, A. and J.F. Imhoff, *Rhodoferax,* in *Bergey's Manual of Systematics of Archaea and Bacteria*. 2015. p. 1-11.

130. Liu, Y., et al., *A trans-outer membrane porin-cytochrome protein complex for extracellular electron transfer by Geobacter sulfurreducens PCA.* Environmental Microbiology Reports, 2014. **6**(6): p. 776-785.

131. Shi, L., J.K. Fredrickson, and J.M. Zachara, *Genomic analyses of bacterial porin-cytochrome gene clusters.* Frontiers in Microbiology, 2014. **5**.

132. Shi, L., et al., *Mtr extracellular electron-transfer pathways in Fe(III)-reducing or Fe(II)-oxidizing bacteria: a genomic perspective.* Biochemical Society Transactions, 2012. **40**(6): p. 1261-1267.

133. White, G.F., et al., *Rapid electron exchange between surface-exposed bacterial cytochromes and Fe(III) minerals.* Proceedings of the National Academy of Sciences of the United States of America, 2013. **110**(16): p. 6346-6351.

134. Finneran, K.T., C.V. Johnsen, and D.R. Lovley, *Rhodoferax ferrireducens sp. nov., a psychrotolerant, facultatively anaerobic bacterium that oxidizes acetate with the reduction of Fe(III).* International Journal of Systematic and Evolutionary Microbiology, 2003. **53**(3): p. 669-673.

135. Hotaling, S., E. Hood, and T.L. Hamilton, *Microbial ecology of mountain glacier ecosystems: biodiversity, ecological connections and implications of a warming climate: Microbial ecology of mountain glaciers.* Environmental Microbiology, 2017. **19**(8): p. 2935-2948.

136. Garcia-Lopez, E. and C. Cid, *Glaciers and Ice Sheets As Analog Environments of Potentially Habitable Icy Worlds.* Frontiers in Microbiology, 2017. **8**.

137. Waite, J.H., et al., *Cassini finds molecular hydrogen in the Enceladus plume: Evidence for hydrothermal processes.* Science, 2017. **356**(6334): p. 155-159.

138. Martin, M., *Cutadapt removes adapter sequences from high-throughput sequencing reads.* EMBnet.journal, 2011. **17**(1): p. 10-12.

139. Mikheenko, A., et al., *Versatile genome assembly evaluation with QUAST-LG.* Bioinformatics, 2018. **34**(13): p. i142-i150.

140. Langmead, B. and S.L. Salzberg, *Fast gapped-read alignment with Bowtie 2.* Nature Methods, 2012. **9**(4): p. 357-359.

141. Kang, D.D., et al., *MetaBAT, an efficient tool for accurately reconstructing single genomes from complex microbial communities.* PeerJ, 2015. **3**: p. e1165.

142. Parks, D.H., et al., *CheckM: assessing the quality of microbial genomes recovered from isolates, single cells, and metagenomes.* Genome Research, 2015. **25**(7): p. 1043-1055.

143. Liu, H., et al., *Annual dynamics of global land cover and its long-term changes from 1982 to 2015.* Earth System Science Data, 2020. **12**(2): p. 1217-1243.

144. Marteinsson, V.T., et al., *Microbial communities in the subglacial waters of the Vatnajökull ice cap, Iceland.* The ISME Journal, 2013. **7**(2): p. 427-37.

145. Dunham, E.C., et al., *Lithogenic hydrogen supports microbial primary production in subglacial and proglacial environments.* Proceedings of the National Academy of Sciences of the United States of America, 2021. **118**(2).

146. Lafrenière, M.J. and M.J. Sharp, *A comparison of solute fluxes and sources from glacial and non-glacial catchments over contrasting melt seasons.* Hydrological Processes, 2005. **19**(15): p. 2991-3012.

147. Stefánsson, A., *Dissolution of primary minerals of basalt in natural waters: I. Calculation of mineral solubilities from 0°C to 350°C.* Chemical Geology, 2001. **172**(3): p. 225-250.

148. Brynjólfsson, S., A. Schomacker, and Ó. Ingólfsson, *Geomorphology and the Little Ice Age extent of the Drangajökull ice cap, NW Iceland, with focus on its three surge-type outlets.* Geomorphology, 2014. **213**: p. 292-304.

149. Vick-Majors, T.J., et al., *Biogeochemical Connectivity Between Freshwater Ecosystems beneath the West Antarctic Ice Sheet and the Sub-Ice Marine Environment.* Global Biogeochemical Cycles, 2020. **34**(3): p. e2019GB006446.

150. Johnson, D.M., P.R. Hooper, and R.M. Conrey, *XRF Analysis of Rocks and Minerals for Major and Trace Elements on a Single Low Dilution Li-tetraborate Fused Bead.* Advances in X-Ray Analysis, 1999. **2**: p. 25.

151. Morono, Y., et al., *An improved cell separation technique for marine subsurface sediments: applications for high-throughput analysis using flow cytometry and cell sorting.* Environmental Microbiology, 2013. **15**(10): p. 2841-2849.

152. Boyd, E.S., D.E. Cummings, and G.G. Geesey, *Mineralogy influences structure and diversity of bacterial communities associated with geological substrata in a pristine aquifer.* Microbial Ecology, 2007. **54**(1): p. 170-82.

153. Colman, D.R., et al., *Seasonal hydrologic and geologic forcing drive hot spring geochemistry and microbial biodiversity.* Environmental Microbiology, 2021.

154. Schloss, P.D., et al., *Introducing mothur: Open-Source, Platform-Independent, Community-Supported Software for Describing and Comparing Microbial Communities.* Applied and Environmental Microbiology, 2009. **75**(23): p. 7537-7541.

155. Kozich, J.J., et al., *Development of a Dual-Index Sequencing Strategy and Curation Pipeline for Analyzing Amplicon Sequence Data on the MiSeq Illumina Sequencing Platform.* Applied and Environmental Microbiology, 2013. **79**(17): p. 5112-5120.

156. Glöckner, F.O., et al., *25 years of serving the community with ribosomal RNA gene reference databases and tools.* Journal of Biotechnology, 2017. **261**: p. 169-176.

157. Wang, Q., et al., *Naïve Bayesian Classifier for Rapid Assignment of rRNA Sequences into the New Bacterial Taxonomy.* Applied and Environmental Microbiology, 2007. **73**(16): p. 5261-5267.

158. Kohler, T.J., et al., *Patterns in microbial assemblages exported from the meltwater of Arctic and Sub-Arctic glaciers.* Frontiers in Microbiology, 2020. **11**: p. 669.

159. Oshkin, I.Y., et al., *Methane-fed microbial microcosms show differential community dynamics and pinpoint taxa involved in communal response.* The ISME Journal, 2015. **9**(5): p. 1119-1129.

160. Yang, Y., et al., *Extracellular electron transfer of Methylophilus methylotrophs.* Process Biochemistry, 2020. **94**: p. 313-318.

161. Kim, E.H., et al., *Actimicrobium antarcticum gen. nov., sp. nov., of the Family Oxalobacteraceae, Isolated from Antarctic Coastal Seawater*. Current Microbiology, 2011. **63**(2): p. 213-217.